Rheology and Hydraulics of Oil-well Drilling Fluids

API RECOMMENDED PRACTICE 13D
FIFTH EDITION, JUNE 2006

Rheology and Hydraulics of Oil-well Drilling Fluids

Upstream Segment

API RECOMMENDED PRACTICE 13D
FIFTH EDITION, JUNE 2006

SPECIAL NOTES

API publications necessarily address problems of a general nature. With respect to particular circumstances, local, state, and federal laws and regulations should be reviewed.

Neither API nor any of API's employees, subcontractors, consultants, committees, or other assignees make any warranty or representation, either express or implied, with respect to the accuracy, completeness, or usefulness of the information contained herein, or assume any liability or responsibility for any use, or the results of such use, of any information or process disclosed in this publication. Neither API nor any of API's employees, subcontractors, consultants, or other assignees represent that use of this publication would not infringe upon privately owned rights.

API publications may be used by anyone desiring to do so. Every effort has been made by the Institute to assure the accuracy and reliability of the data contained in them; however, the Institute makes no representation, warranty, or guarantee in connection with this publication and hereby expressly disclaims any liability or responsibility for loss or damage resulting from its use or for the violation of any authorities having jurisdiction with which this publication may conflict.

API publications are published to facilitate the broad availability of proven, sound engineering and operating practices. These publications are not intended to obviate the need for applying sound engineering judgment regarding when and where these publications should be utilized. The formulation and publication of API publications is not intended in any way to inhibit anyone from using any other practices.

Any manufacturer marking equipment or materials in conformance with the marking requirements of an API standard is solely responsible for complying with all the applicable requirements of that standard. API does not represent, warrant, or guarantee that such products do in fact conform to the applicable API standard.

FOREWORD

Nothing contained in any API publication is to be construed as granting any right, by implication or otherwise, for the manufacture, sale, or use of any method, apparatus, or product covered by letters patent. Neither should anything contained in the publication be construed as insuring anyone against liability for infringement of letters patent.

This document was produced under API standardization procedures that ensure appropriate notification and participation in the developmental process and is designated as an API standard. Questions concerning the interpretation of the content of this publication or comments and questions concerning the procedures under which this publication was developed should be directed in writing to the Director of Standards, American Petroleum Institute, 1220 L Street, N.W., Washington, D.C. 20005. Requests for permission to reproduce or translate all or any part of the material published herein should also be addressed to the director.

Generally, API standards are reviewed and revised, reaffirmed, or withdrawn at least every five years. A one-time extension of up to two years may be added to this review cycle. Status of the publication can be ascertained from the API Standards Department, telephone (202) 682-8000. A catalog of API publications and materials is published annually and updated quarterly by API, 1220 L Street, N.W., Washington, D.C. 20005.

Suggested revisions are invited and should be submitted to the Standards and Publications Department, API, 1220 L Street, NW, Washington, DC 20005, standards@api.org.

Contents

API Recommended Practice 13D — Rheology and hydraulics of oil-well drilling fluids

1 Scope

1.1 The objective of this Recommended Practice (RP) is to provide a basic understanding of and guidance about drilling fluid rheology and hydraulics, and their application to drilling operations.

1.2 The target audience for this RP covers both the office and wellsite engineer. The complexity of the equations used is such that a competent engineer can use a simple spreadsheet program to conduct the analyses. Given that the equations used herein are constrained by the spreadsheet limitation, more advanced numerical solutions containing multiple subroutines and macros are not offered. This limitation does not mean that only the results given by the spreadsheet methods are valid engineering solutions.

1.3 Rheology is the study of the deformation and flow of matter. Drilling fluid hydraulics pertains to both laminar and turbulent flow regimes. The methods for the calculations used herein take into account the effects of temperature and pressure on the rheology and density of the drilling fluid.

1.4 For this RP, rheology is the study of flow characteristics of a drilling fluid and how these characteristics affect movement of the fluid. Specific measurements are made on a fluid to determine rheological parameters under a variety of conditions. From this information the circulating system can be designed or evaluated regarding how it will accomplish certain desired objectives.

1.5 The purpose for updating the existing Recommended Practice, last published in May 2003, is to make the work more applicable to the complex wells that are now commonly drilled. These include: High-Temperature/High-Pressure (HTHP), Extended-Reach Drilling (ERD), and High-Angle Wells (HAW). Drilling fluid rheology is important in the following determinations:

a) calculating frictional pressure losses in pipes and annuli

b) determining equivalent circulating density of the drilling fluid under downhole conditions

c) determining flow regimes in the annulus

d) estimating hole-cleaning efficiency

e) estimating swab/surge pressures

f) optimizing the drilling fluid circulating system for improved drilling efficiency

1.6 The discussion of rheology in this RP is limited to single-phase liquid flow. Some commonly used concepts pertinent to rheology and flow are presented. Mathematical models relating shear stress to shear rate and formulas for estimating pressure losses, equivalent circulating densities and hole cleaning are included.

1.7 The conventional U.S. Customary (USC) unit system is used in this Recommended Practice.

1.8 Conversion factors and examples are included for all calculations so that USC units can be readily converted to SI units.

Where units are not specified, as in the development of equations, any consistent system of units may be used.

1.9 The concepts of viscosity, shear stress, and shear rate are very important in understanding the flow characteristics of a fluid. The measurement of these properties allows a mathematical description of circulating fluid flow. The rheological properties of a drilling fluid directly affect its flow characteristics and all hydraulic calculations. They must be controlled for the fluid to perform its various functions.

1.10 This revised document includes some example calculations to illustrate how the equations contained within the document can be used to model a hypothetical well. Due to space constraints, it has not been possible to include a step-by-step procedure for every case. However, the final results should serve as a benchmark if the user wishes to replicate the given cases.

2   Normative references

API RP 13B-1/ISO 10414-1, *Recommended Practice Standard Procedure for Field Testing Water-Based Drilling Fluids*

API RP 13B-2/ISO 10414-2, *Recommended Practice Standard Procedure for Field Testing Oil-Based Drilling Fluids*

API RP 13D:2003, *Recommended Practice on the Rheology and Hydraulics of Oil-well Drilling Fluids*

RP 13M/ISO 13503-1, *Recommended Practice for the Measurement of Viscous Properties of Completion Fluids*

3   Terms, definitions, symbols and abbreviations

Table 1 – Symbols, definitions, units, and conversion factors

Symbol	Definition	Standard Units	Multiplier	SI Units
a	Numerator in Blasius form of friction-factor equation	dimensionless	-	dimensionless
A	Surface area	in^2	6.4516E+02	Mm^2
a_1	Density correction coefficient for pressure	lb_m/gal	1.1983E+02	kg/m^3
a_2	Density correction coefficient for temperature	$lb_m/gal/ºF$	2.1569E+02	$kg/m^3/ºC$
A_b	Bit cross-sectional area	in^2	6.4516E+02	Mm^2
a_p	Pipe acceleration	ft/s^2	3.048E-01	m/s^2
b	Exponent in Blasius form of friction-factor equation	dimensionless	-	dimensionless
b_1	Density correction coefficient for pressure	$lb_m/gal/psi$	1.7379E-02	$kg/m^3/(Pa)$
b_2	Density correction coefficient for temperature	$lb_m/gal/psi/ºF$	3.1283E-02	$kg/m^3/(Pa)/ºC$
B	Expansibility of the conduit			
B_a	Well geometry correction factor	dimensionless	-	dimensionless
B_x	Viscometer geometry correction factor	dimensionless	-	dimensionless
c_1	Density correction coefficient for pressure	$lb_m/gal/psi^2$	2.5206E-06	$kg/m^3/(Pa)^2$
c_2	Density correction coefficient for temperature	$lb_m/gal/psi^2/ºF$	4.5370E-06	$kg/m^3/(Pa)^2/ºC$
c_a	In-situ cuttings volume concentration	decimal fraction	-	decimal fraction
$CaCl_2$	$CaCl_2$ concentration	wt%	-	wt%
CCI	Carrying Capacity Index	-	-	-
C_{dt}	Proportionality constant for downhole tool pressure loss	-	-	-

2

Symbol	Definition	Standard Units	Multiplier	SI Units
C_f	Fluid compressibility	$(lb_f/in^2)^{-1}$	6.894757E+03	$(Pa)^{-1}$
C_g	Drilling fluid clinging factor on pipe for surge / swab	-	-	-
C_{sc}	Proportionality constant for surface-connection pressure l	-	-	-
C_v	Jet nozzle discharge coefficient	dimensionless	-	Dimensionless
d	Diameter	in.	2.54E+01	Mm
d_b	Bit diameter	in.	2.54E+01	Mm
d_c	Cuttings diameter	in.	2.54E+01	Mm
d_h	Hole diameter or casing inside diameter	in.	2.54E+01	Mm
d_{hyd}	Hydraulic diameter	in.	2.54E+01	Mm
d_i	Pipe internal diameter	in.	2.54E+01	Mm
d_n	Bit nozzle diameter	1/32 in.	7.9375E-01	Mm
d_{ni}	Diameter of ith bit nozzle	1/32 in.	7.9375E-01	Mm
d_p	Pipe outside diameter	in.	2.54E+01	Mm
D_{td}	Total depth (measured)	ft	3.048E-01	M
D_{tvd}	True vertical depth	ft	3.048E-01	M
D_w	Water depth	ft	3.048E-01	M
e	Eccentricity	dimensionless	-	Dimensionless
ECD	Equivalent Circulating Density	lb_m/gal	1.198264E+02	kg/m^3
EMW	Equivalent Mud Weight	lb_m/gal	1.198264E+02	kg/m^3
Err	Error	%	-	%
ESD_D	Equivalent Static Density at depth D	lb_m/gal	1.198264E+02	kg/m^3
ESD_{D+L}	Equivalent Static Density at depth D + length L	lb_m/gal	1.198264E+02	kg/m^3
ESD	Equivalent Static Density	lb_m/gal	1.198264E+02	kg/m^3
ESD_a	Equivalent Static Density in annulus	lb_m/gal	1.198264E+02	kg/m^3
ESD_f	Final Equivalent Static Density	lb_m/gal	1.198264E+02	kg/m^3
ESD_i	Initial Equivalent Static Density	lb_m/gal	1.198264E+02	kg/m^3
ESD_p	Equivalent Static Density in pipe (drillstring)	lb_m/gal	1.198264E+02	kg/m^3
f	Fanning friction factor	dimensionless	-	Dimensionless
F	Force	lb_f	4.448222E+00	N
f_{lam}	Friction factor (laminar)	dimensionless	-	Dimensionless
F_{po}	Pump-off force	lb_f	4.448222E+00	N
f_{trans}	Friction factor (transitional)	dimensionless	-	Dimensionless
f_{tt}	Intermediate friction factor (transitional and turbulent)	dimensionless	-	Dimensionless
f_{turb}	Friction factor (turbulent)	dimensionless	-	Dimensionless
g	Acceleration of gravity	32.152 ft/s^2	3.048E-01	m/s^2
G	Geometry shear-rate correction (Herschel-Bulkley fluids)	dimensionless	-	Dimensionless
G_{10m}	Gel strength (10 min)	$lb_f/100\ ft^2$	4.788026E-01	Pa
G_{10s}	Gel strength (10 s)	$lb_f/100\ ft^2$	4.788026E-01	Pa
G_p	Geometry shear-rate correction (power-law fluids)	dimensionless	-	Dimensionless
h	Cuttings thickness	in.	2.54E+01	Mm
HHP	Hydraulic horsepower	hhp	7.46043E-01	Kw

Symbol	Definition	Standard Units	Multiplier	SI Units
HHP_{max}	Maximum hydraulic horsepower	hhp	7.46043E-01	kw
HPO	Hydraulic pump-off force	lb_f	4.448222E+00	N
HSI	Specific hydraulic horsepower	hhp/in^2	1.15637E-03	kw/mm^2
IF	Jet impact force	lb_f	4.448222E+00	N
I_x	System pressure-loss intercept	$lb_f/in^2/(gal/min)^u$	6.894757E+00	$kPa/(dm^3/s)^u$
J	Intermediate parameter used for critical velocity	-	-	-
k	Consistency factor (Herschel-Bulkley fluids)	$lb_f{\cdot}s^n/100\ ft^2$	4.78803E-01	$Pa{\cdot}s^n$
K	Parasitic pressure loss coefficient	psi/gpm^u	-	-
k_1	Power law viscosity at 1 s^{-1}	cP	1.0E-03	$Pa{\cdot}s$
k_p	Consistency factor (power-law fluids)	$lb_f{\cdot}s^n/100\ ft^2$	4.78803E-01	$Pa{\cdot}s^n$
L	Length of drillstring or annular segment	ft	3.048E-01	m
n	Flow behavior index (Herschel-Bulkley fluids)	dimensionless	-	dimensionless
N	Viscometer rotary speed	rpm	-	rpm
n_p	Flow behavior index (power-law fluids)	dimensionless	-	dimensionless
N_{Re}	Reynolds number	dimensionless	-	dimensionless
N_{ReG}	Generalized Reynolds number	dimensionless	-	dimensionless
N_{Rep}	Particle Reynolds number	dimensionless	-	dimensionless
P	Pressure	lb_f/in^2	6.894757E+00	kPa
P_a	Annular pressure loss	lb_f/in^2	6.894757E+00	kPa
P_b	Bit pressure loss	lb_f/in^2	6.894757E+00	kPa
P_{bh}	Bottomhole pressure	lb_f/in^2	6.894757E+00	kPa
P_{bopt}	Optimum pressure loss across bit	lb_f/in^2	6.894757E+00	kPa
P_c	Casing (back) pressure	lb_f/in^2	6.894757E+00	kPa
P_{cl}	Choke line pressure loss	lb_f/in^2	6.894757E+00	kPa
P_{ds}	Drillstring pressure loss	lb_f/in^2	6.894757E+00	kPa
P_{dt}	Downhole tools pressure loss	lb_f/in^2	6.894757E+00	kPa
P_f	Formation pressure	lb_f/in^2	6.894757E+00	kPa
P_{ha}	Annular hydrostatic pressure	lb_f/in^2	6.894757E+00	kPa
P_{hd}	Drillstring hydrostatic pressure	lb_f/in^2	6.894757E+00	kPa
P_{max}	Maximum pump (standpipe) pressure	lb_f/in^2	6.894757E+00	kPa
P_p	Pump (standpipe) pressure	lb_f/in^2	6.894757E+00	kPa
Δp	Inertial surge pressure	lb_f/in^2	6.894757E+00	kPa
P_{sc}	Surface-connections pressure loss	lb_f/in^2	6.894757E+00	kPa
PV	Plastic Viscosity	cP	1.0E-03	$Pa{\cdot}s$
P_x	Parasitic pressure losses (P_p excluding P_b)	lb_f/in^2	6.894757E+00	kPa
psi	Pressure, pounds per square inch, is measured by gauge and is psig (unless otherwise noted)			
Q	Flow rate	gal/min	6.309.20E-02	dm^3/s
Q_c	Critical flow rate	gal/min	6.309.20E-02	dm^3/s
Q_{opt}	Optimum flow rate	gal/min	6.309.20E-02	dm^3/s

Symbol	Definition	Standard Units	Multiplier	SI Units
Q_x	Flow rate at maximum pump pressure and available horsepower	gal/min	6.309.20E-02	dm^3/s
R	Ratio yield stress / yield point (τ_y / YP)	dimensionless	-	Dimensionless
R_{100}	Viscometer reading at 100 rpm	° deflection	-	° deflection
R_{200}	Viscometer reading at 200 rpm	° deflection	-	° deflection
R_3	Viscometer reading at 3 rpm	° deflection	-	° deflection
R_{300}	Viscometer reading at 300 rpm	° deflection	-	° deflection
R_6	Viscometer reading at 6 rpm	° deflection	-	° deflection
R_{600}	Viscometer reading at 600 rpm	° deflection	-	° deflection
RF	Rheology Factor	-	-	-
R_{lam}	Eccentric annulus laminar pressure ratio	dimensionless	-	Dimensionless
ROP	Rate of Penetration	ft/h	3.048E-01	m/h
RT	Transport Ratio	dimensionless	-	Dimensionless
R_{turb}	Eccentric annulus turbulent pressure ratio	dimensionless	-	Dimensionless
SICP	Shut-in Casing Pressure	lb_f/in^2	6.894757E+00	kPa
SPP_{max}	Maximum standpipe (pump) pressure	lb_f/in^2	6.894757E+00	kPa
T	Temperature	°F	(°F-32)/1.8	°C
T_0	Surface temperature at 50 ft depth	°F	(°F-32)/1.8	°C
T_{bhc}	Bottomhole circulating temperature	°F	(°F-32)/1.8	°C
T_{bhs}	Bottomhole static temperature	°F	(°F-32)/1.8	°C
TFA	Total Fluid Area	in^2	6.4516E+02	mm^2
T_{fl}	Flowline temperature	°F	(°F-32)/1.8	°C
t_g	Geothermal gradient	°F/100 ft	(°F-32)/1.8	°C/30.48 m
t_{gw}	Geothermal gradient adjusted for water depth	°F/100 ft	(°F-32)/1.8	°C/30.48 m
TI	Transport Index	-	-	-
T_{ml}	Temperature at mud line	°F	(°F-32)/1.8	°C
T_s	Temperature at surface	°F	(°F-32)/1.8	°C
u	Slope of logarithmic parasitic system pressure loss	dimensionless	-	Dimensionless
v	Jet velocity	ft/s	3.048E-01	m/s
V	Velocity	ft/min	5.08E-03	m/s
V_a	Fluid velocity in annulus	ft/min	5.08E-03	m/s
V_c	Critical velocity	ft/min	5.08E-03	m/s
V_{cb}	Critical velocity (Bingham plastic fluids)	ft/min	5.08E-03	m/s
V_{cp}	Critical velocity (power-law fluids)	ft/min	5.08E-03	m/s
V_d	Velocity component due to string displacement	ft/min	5.08E-03	m/s
V_{ds}	Drillstring (pipe) velocity	ft/min	5.08E-03	m/s
Vol_{base}	Volume fraction of base fluid	vol%	-	vol%
Vol_{brine}	Volume fraction of brine	vol%	-	vol%
Vol_{ds}	Volume fraction of drilled solids	vol%	-	vol%
Vol_{salt}	Volume fraction of salt	vol%	-	vol%
Vol_{solids}	Volume fraction of solids	vol%	-	vol%

Symbol	Definition	Standard Units	Multiplier	SI Units
Vol_{total}	Volume fraction of all components	vol%	-	vol%
Vol_{water}	Volume fraction of water	vol%	-	vol%
Vol_{wb}	Volume of wellbore	bbl	1.589873E-01	m^3
V_p	Fluid velocity inside pipe	ft/min	5.08E-03	m/s
V_s	Cuttings slip velocity	ft/min	5.08E-03	m/s
V_u	Cuttings net upward velocity	ft/min	5.08E-03	m/s
V_w	Velocity component due to relative drillstring motion	ft/min	5.08E-03	m/s
V_{wave}	Propagation velocity	ft/min	5.08E-03	m/s
x	Viscometer ratio (sleeve radius / bob radius)	dimensionless	-	dimensionless
X_c	Conduit expansibility	$(lb_f/in^2)^{-1}$	6.894757E+03	$(Pa)^{-1}$
YP	Yield point	$lb_f/100\ ft^2$	4.788026E-01	Pa
α	Geometry factor	dimensionless	-	dimensionless
γ	Shear rate	s^{-1}	-	s^{-1}
γ_i	Iterative shear rate used in curve-fit method	s^{-1}	-	s^{-1}
γ_s	Particle (cutting) shear rate	s^{-1}	-	s^{-1}
γ_w	Shear rate at the wall	s^{-1}	-	s^{-1}
ΔP_{ss}	Surge / swab pressure change	lb_f/in^2	6.894757E+00	kPa
μ	Viscosity	cP	1.0E-03	Pa•s
μ_e	Apparent viscosity around particle (cutting)	cP	1.0E-03	Pa•s
ρ	Fluid density	lb_m/gal	1.198264E+02	kg/m^3
ρ_a	Fluid density in annulus (local)	lb_m/gal	1.198264E+02	kg/m^3
ρ_b	Fluid density through bit nozzles	lb_m/gal	1.198264E+02	kg/m^3
ρ_{base}	Base fluid density	g/cm^3	1.00E-03	kg/m^3
ρ_{brine}	Brine density	g/cm^3	1.00E-03	kg/m^3.
ρ_c	Particle (cutting) density	g/cm^3	1.00E-03	kg/m^3
ρ_{dt}	Reference drilling fluid density used for empirical pressure loss	lb_m/gal	1.198264E+02	kg/m^3
ρ_i	Dynamic local drilling fluid density	lb_m/gal	1.198264E+02	kg/m^3
ρ_p	Drilling fluid density in drillstring (local)	lb_m/gal	1.198264E+02	kg/m^3
ρ_s	Drilling fluid density at surface	lb_m/gal	1.198264E+02	kg/m^3
ρ_{solids}	Density of solids	g/cm^3	1.00E-03	kg/m^3
ρ_{total}	Total density	g/cm^3	1.00E-03	kg/m^3
ρ_i	Local density in i^{th} cell	g/cm^3	1.00E-03	kg/m^3
τ	Shear stress	$lb_f/100\ ft^2$	4.788026E-01	Pa
τ_b	Shear stress at viscometer bob	° deflection	-	° deflection
τ_i	Iterative shear stress in curve-fit method	$lb_f/100\ ft^2$	4.788026E-01	Pa
τ_s	Shear stress due to particle (cuttings) slip	$lb_f/100\ ft^2$	4.788026E-01	Pa
τ_w	Shear stress at the wall	$lb_f/100\ ft^2$	4.788026E-01	Pa
τ_y	Yield stress	$lb_f/100\ ft^2$	4.788026E-01	Pa

4 Fundamentals and fluid models

4.1 Flow regime principle

4.1.1 The behavior of a fluid is determined by the flow regime, which in turn has a direct effect on the ability of that fluid to perform its basic functions. The flow can be either laminar or turbulent, depending on the fluid velocity, size and shape of the flow channel, fluid density, and viscosity. Between laminar and turbulent flow, the fluid will pass through a transition region where the movement of the fluid has both laminar and turbulent characteristics. It is important to know which of the flow regimes is present in a particular situation to evaluate the performance of a fluid. If the flow occurs in an annulus, like in a drilling situation, the rotation of the inner surface (the drillpipe) can create turbulent instabilities for all flow rates.

4.1.2 In axial laminar flow, the fluid moves parallel to the walls of the flow channel in smooth lines. Flow tends to be laminar when moving slowly or when the fluid is viscous. In laminar flow, the pressure required to move the fluid increases with increases in the velocity and viscosity.

4.1.3 In turbulent flow, the fluid is swirling and eddying as it moves along the flow channel, even though the bulk of the fluid moves forward. These velocity fluctuations arise spontaneously. Wall roughness or changes in flow direction will increase the amount of turbulence. Flow tends to be turbulent with higher velocities or when the fluid has low viscosity. In turbulent flow, the pressure required to move the fluid increases linearly with density and approximately with the square of the velocity. This means more pump pressure is required to move a fluid in turbulent flow than in laminar flow.

4.1.4 The transition from axial laminar and turbulent flow is controlled by the relative importance of viscous forces and inertial forces in the flow. In laminar flow, the viscous forces dominate, while in turbulent flow the inertial forces are more important. For Newtonian fluids, viscous forces vary linearly with the flow rate, while the inertial forces vary as the square of the flow rate.

4.1.5 The ratio of inertial forces to viscous forces is the *Reynolds number*. If consistent units are chosen, this ratio is dimensionless and the Reynolds number (N_{Re}) in a pipe is defined by:

$$N_{Re} = \frac{dV\rho}{\mu} \qquad\qquad (1)$$

where

    d is the diameter of the flow channel

    V is the average flow velocity

    ρ is the fluid density

    μ is the fluid viscosity

NOTE: If the flow occurs in an annulus, the flow channel diameter should be exchanged with $d_{hyd} = d_h - d_p$, as the difference between the outer diameter of the drillpipe and inner diameter of casing or open hole (see Subclause 7.4.4.).

4.1.6 The flow of a liquid in a particular flow channel can be laminar, transitional, or turbulent. The transition from laminar to transitional flow occurs at a critical velocity. For typical drilling fluids, this normally occurs over a range of velocities corresponding to Reynolds number between 2,000 and 4,000 (see Clause 7 for further details).

4.2   Viscosity

4.2.1   *Viscosity* is defined as the ratio of shear stress to shear rate. The traditional units of viscosity are dyne-s/cm^2, which is termed Poise (P). Since 1 P represents a relatively high viscosity for most fluids, the term centiPoise (cP) is normally used. A centiPoise is equal to one-hundredth of poise or one millipascal-second.

$$\mu = \frac{\tau}{\gamma} \tag{2}$$

where

      μ is the viscosity

      τ is the shear stress

      γ is the shear rate.

4.2.2   Viscosity is not a constant value for most drilling fluids. It varies with shear rate. To check for rate dependent effects, shear stress measurements are made at a number of shear rates. From these measured data, rheological parameters can be calculated or can be plotted as viscosity versus shear rate.

4.2.3   The term *effective viscosity* is used to describe the viscosity either measured or calculated at the shear rate corresponding to existing flow conditions in the wellbore or drillpipe. This special term is used to differentiate the viscosity as discussed in this clause from other viscosity terms. To be meaningful, a viscosity measurement must always specify the shear rate.

4.3   Shear stress

4.3.1   *Shear stress* is the force required to sustain a particular rate of fluid flow and is measured as a force per unit area. Suppose, in the parallel-plate example (see Figure 1), that a force of 1.0 dyne is applied to each square centimeter of the top plate to keep it moving. Then the shear stress would be 1.0 dyne/cm^2. The same force in the opposite direction is needed on the bottom plate to keep it from moving. The same shear stress of 1.0 dyne/cm^2 is found at any level in the fluid.
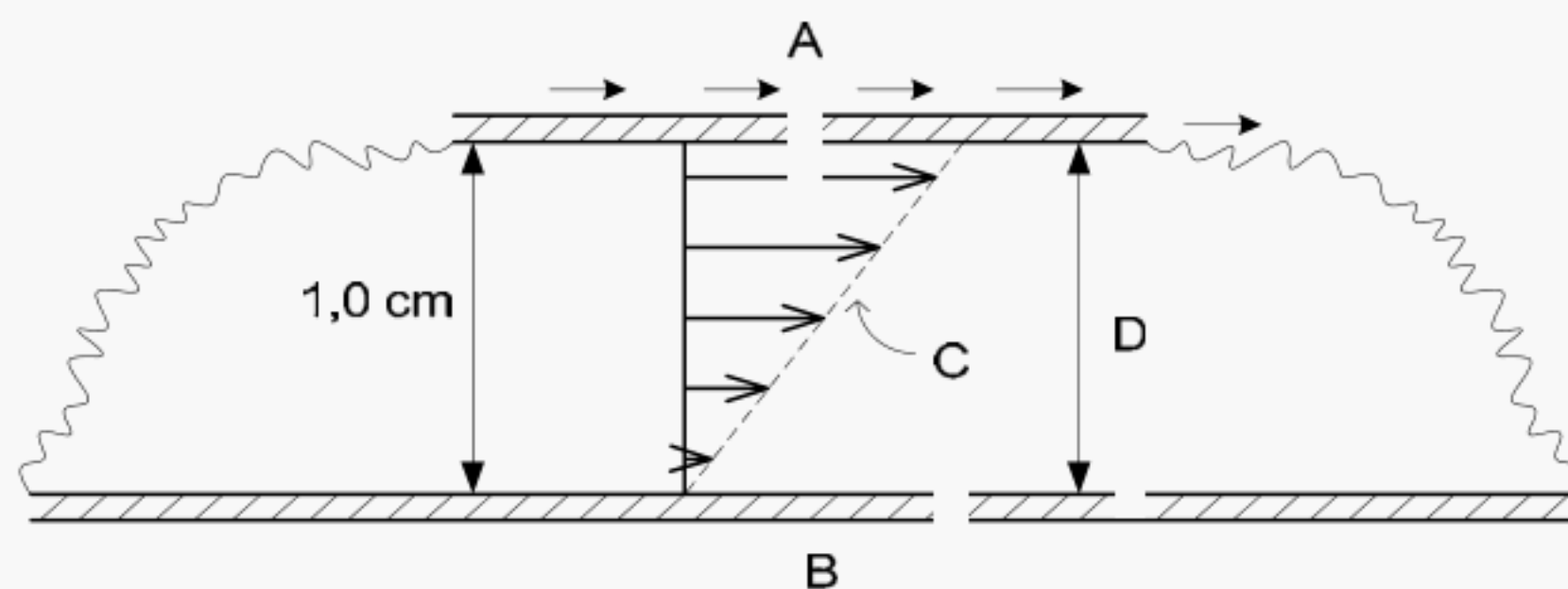
KEY

      A   is the moving plate with a velocity of 1.0 cm/s

      B   is the stationary plate

      C   is the velocity profile

D   is the velocity gradient, velocity divided by height, $\Delta V / h$, 1.0 cm/s / 1 cm = 1 s^{-1}

Figure 1 – Parallel plates showing shear rate in fluid-filled gap as one plate slides past another

4.3.2   Shear stress τ is expressed mathematically as:

$$\tau = \frac{F}{A} \tag{3}$$

where

F   is the force

A   is the surface area subjected to stress

4.3.3   In a pipe, the force pushing a column of liquid through the pipe is expressed as the pressure on the end of the liquid column times the area of the end of the column:

$$F = P\frac{\pi d^2}{4} \tag{4}$$

where

d   is the diameter of pipe

P   is the pressure on end of liquid column

4.3.4   The area of the fluid surface in contact with the pipe wall over the length is given by:

$$A = \pi dL \tag{5}$$

where

A   is the surface area of the fluid

L   is the length.

4.3.5   Thus, the shear stress at the pipe wall is expressed as:

$$\tau_w = \frac{F}{A} = \frac{dP}{4L} \tag{6}$$

4.3.6   In an annulus with inner and outer diameters known, the shear stress is expressed in the same manner:

$$F = \frac{P\pi d_h^2}{4} - \frac{P\pi d_p^2}{4} = P\pi\frac{d_h^2 - d_p^2}{4} \tag{7}$$

where

d_p is the outer diameter of pipe

d_h is the diameter of hole

and

$$A = \pi d_h L + \pi d_p L = \pi L (d_h + d_p) \tag{8}$$

so that

$$\tau_w = \frac{F}{A} = \frac{P \frac{\pi}{4} (d_h - d_p)(d_h + d_p)}{\pi L (d_h + d_p)} = \frac{P(d_h - d_p)}{4L} \tag{9}$$

4.4   Shear rate

4.4.1   *Shear rate* is a velocity gradient measured across the diameter of a pipe or annulus. It is the rate at which one layer of fluid is moving past another layer. As an example, consider two large flat plates parallel to each other and one centimeter (cm) apart. The space between the plates is filled with fluid. If the bottom plate is fixed while the top plate slides parallel to it at a constant velocity of 1 cm/s, the velocities indicated in Figure 1 are found within the fluid. The fluid layer near the bottom plate is motionless while the fluid layer near the top plate is moving at almost 1 cm/s. Halfway between the plates the fluid velocity is the average 0.5 cm/s.

4.4.2   The *velocity gradient* is the rate of change of velocity ΔV with distance from the wall h. For the simple case of Figure 1, the shear rate is dV/h and will have units of 1/time. The reciprocal second, or often called the inverse second, ($1/s$ or s^{-1}) is the standard unit of shear rate.

4.4.3   This reference example is unusual in that the shear rate is constant throughout the fluid. This situation is not the case with a circulating fluid. In laminar flow inside a pipe, for example, the shear rate is highest next to the pipe wall. An average shear rate may be used for calculations, but the shear rate itself is not constant across the flow channel.

4.4.4   It is important to express the above concept mathematically so that models and calculations can be developed. Shear rate (γ) is defined as:

$$\gamma = \frac{\Delta V}{\Delta r} \tag{10}$$

where

ΔV is the velocity change between fluid layers

Δr is the distance between fluid layers

4.4.5   In a pipe the shear rate at the pipe wall (γ_{wp}) for a Newtonian fluid can be expressed as a function of the average velocity (V) and the diameter of the pipe (d).

$$\gamma_{wp} = f(V, d) = \frac{8V_p}{d} \tag{11}$$

in which

$$V_P = \frac{Q}{A} = \frac{4Q}{\pi d^2} \tag{12}$$

where

γ_{wp} is the shear rate at pipe wall for a Newtonian fluid

Q is the volumetric flow rate

A is the surface area of cross section

d is the pipe diameter

V is the velocity

V_p is the average velocity in pipe

4.4.6   In an annulus of outside diameter (d_h) and inside diameter (d_p), the wall shear rate for a Newtonian fluid can be shown to be:

$$\gamma_{wa} = f(V, d_p, d_h) = \frac{12V_a}{d_h - d_p} \tag{13}$$

in which

$$V_a = \frac{4Q}{\pi\left(d_h^2 - d_p^2\right)} \tag{14}$$

where

γ_{wa} is the shear rate at annulus wall for a Newtonian fluid

V is the velocity

Q is the volumetric flow rate

d_p is the outer diameter of pipe

d_h is the diameter of hole

V_a is the average velocity in annulus

4.4.7 Equations which correct the pipe and annulus shear rates for non-Newtonian behavior are given in Clause 5 and Clause 7.

4.5   Relationship of shear stress and shear rate

4.5.1   In summary, the *shear stress* is the force per unit area required to sustain fluid flow. *Shear rate* is the rate at which the fluid velocity changes with respect to the distance from the wall. *Viscosity* is the ratio of the shear stress to shear rate. The mathematical relationship between shear rate and shear stress is the *rheological model* of the fluid.

4.5.2   When a drill cutting particle settles in a drilling fluid, the fluid immediately surrounding the particle is subjected to a shear rate defined as settling shear rate γ_s:

$$\gamma_s = \frac{12V_s}{d_c} \tag{15}$$

where

V_s is the average settling velocity (ft/s)

d_c is the equivalent particle diameter (in.)

11

The settling shear rate is used to calculate the viscosity of fluid experienced by the settling particle.

4.6 Fluid characterization

4.6.1 Fluids can be classified by their rheological behavior. Fluids whose viscosity remains constant with changing shear rate are known as *Newtonian* fluids. *Non-Newtonian* fluids are those fluids whose viscosity varies with changing shear rate.

4.6.2 Temperature and pressure affect the viscosity of a fluid. Therefore, to properly describe the drilling fluid flow, the test temperature and pressure must be specified.

4.6.3 Some mathematical models used for hydraulic calculations are shown in this subclause.

4.7 Newtonian fluids

4.7.1 Fluids for which shear stress is directly proportional to shear rate are called Newtonian. Water, glycerin, and light oil are examples of Newtonian fluids.

4.7.2 A single viscosity measurement characterizes a Newtonian fluid at a specified temperature and pressure.

4.8 Non-Newtonian fluids

4.8.1 Fluids for which shear stress is not directly proportional to shear rate are called non-Newtonian. Most drilling fluids are non Newtonian.

4.8.1.1 Drilling fluids are shear thinning when they exhibit less viscosity at higher shear rates than at lower shear rates.

4.8.1.2 There are some non-Newtonian fluids which exhibit dilatant behavior. The viscosity of these fluids increases with increasing shear rate. Dilatant behavior rarely occurs in drilling fluids.

4.8.2 The distinction between Newtonian and non-Newtonian fluids can be illustrated by using the API standard concentric-cylinder viscometer. If the 600-rpm dial reading is twice the 300-rpm reading, the fluid exhibits Newtonian flow behavior. If the 600-rpm reading is less than twice the 300-rpm reading, the fluid is non-Newtonian and shear thinning.

4.8.3 One type of shear thinning fluid will begin to flow as soon as any shearing force or pressure, regardless of how slight, is applied. Such fluids are termed *pseudoplastic*. Increased shear rate causes a progressive decrease in viscosity.

4.8.4 Another type of shear thinning fluid will not flow until a given shear stress is applied. The shear stress required to initiate flow is called the *yield stress*. These fluids are referred to as *viscoplastic*.

4.8.5 Fluids can also exhibit time-dependent effects. Under constant shear rate, the viscosity changes with time until equilibrium is established. *Thixotropic* fluids experience a decrease in viscosity with time, while *rheopectic* fluids experience an increase in viscosity with time.

4.8.6 Thixotropic fluids can also exhibit a behavior described as *gelation* or *gel strength* development. The time-dependent forces cause an increase in viscosity as the fluid remains static. Sufficient force must be exerted on the fluid to overcome the gel strength to initiate flow.

4.8.7 The range of rheological characteristics of drilling fluids can vary from an elastic, gelled solid at one extreme, to a purely viscous, Newtonian fluid at the other. Circulating fluids have a very complex flow behavior, yet it is still common practice to express the flow properties in simple rheological terms.

4.8.8   General statements regarding drilling fluids are usually subject to exceptions because of the extraordinary complexity of these fluids.

4.9   Rheological models

4.9.1   Rheological models are intended to provide assistance in characterizing fluid flow. No single, commonly-used model completely describes rheological characteristics of drilling fluids over their entire shear-rate range. Knowledge of rheological models combined with practical experience is necessary to fully understand fluid performance. A plot of shear stress versus shear rate (*rheogram*) is often used to graphically depict a rheological model.

4.9.2   *Bingham Plastic Model*: This model describes fluids in which the shear stress/shear rate ratio is linear once a specific shear stress has been exceeded. Two parameters, *plastic viscosity* and *yield point*, are used to describe this model. Because these parameters are determined from shear rates of 511 s^{-1} and 1022 s^{-1}, this model characterizes fluids in the higher shear-rate range. A rheogram of the Bingham plastic model on rectilinear coordinates is a straight line that intersects the zero shear-rate axis at a shear stress greater than zero (*yield point*).

4.9.3   *Power Law*: The Power Law is used to describe the flow of shear thinning or pseudoplastic drilling fluids. This model describes fluids in which the rheogram is a straight line when plotted on a log-log graph. Such a line has no intercept, so a true power law fluid does not exhibit a yield stress. The two required power law constants, *n* and *K*, from this model are typically determined from data taken at shear rates of 511 s^{-1} and 1022 s^{-1}. However, the *generalized power law* applies if several shear-rate pairs are defined along the shear-rate range of interest. This approach has been used in the recent versions of API RP 13D.

4.9.4   *Herschel-Bulkley Model*: Also called the "modified" power law and yield-psuedoplastic model, the Herschel-Bulkley model is used to describe the flow of pseudoplastic drilling fluids which require a yield stress to initiate flow. A rheogram of shear stress minus yield stress versus shear rate is a straight line on log-log coordinates. This model is widely used because it (a) describes the flow behavior of most drilling fluids, (b) includes a yield stress value important for several hydraulics issues, and (c) includes the Bingham plastic model and power law as special cases.

4.9.5   The rheological parameters recorded in an API Drilling Fluid Report are plastic viscosity and yield point from the Bingham plastic model. These two terms can be used to calculate key parameters for other rheological models.

4.9.6   The mathematical treatment of Herschel-Bulkley, Bingham plastic and power law fluids is described in Clause 5.

4.9.7   The flow characteristics of a drilling fluid are controlled by: the viscosity of the base fluid (the continuous phase); and any solid particles, oil, or gases within the fluid (the discontinuous phases); the flow channel characteristics; and the volumetric flow rate. Any interactions among the continuous and discontinuous phases, either chemical or physical, have a marked effect on the rheological parameters of a drilling fluid. The parameters calculated by use of Bingham plastic, power law and other models are indicators that are commonly used to guide fluid conditioning to obtain the desired rheological properties.

5   Determination of drilling fluid rheological parameters

5.1 Measurement of rheological parameters

The determination of drilling fluid rheological parameters is important in the calculation of circulating hydraulics, hole cleaning efficiency, and prediction of barite sag in oil wells.

5.1.1   Orifice viscometer—Marsh funnel

a)   Description

The Marsh funnel is widely used as a field measuring instrument. The measurement is referred to as the *funnel viscosity* and is a timed rate of flow, usually recorded in seconds per quart. It consists of a conical funnel that holds 1.5 liters of drilling fluid with an orifice at the bottom of the cone. The instrument is designed so that by following standard procedures the outflow time of one quart of fresh water at 70 °F ± 5 °F (21 °C ± 2°C) is 26 s ± 0.5 s.

b)   Uses

Funnel viscosity is a rapid, simple test that is made routinely on all liquid drilling fluid systems. It is most useful to alert personnel to changes in the drilling fluid properties or conditions. When a change in funnel viscosity is observed, rheological testing using a concentric-cylinder viscometer will identify the change in fluid properties. It is, however, a one-point measurement and therefore does not give any information as to why the viscosity may be high or low. No single funnel viscosity measurement can be taken to represent a consistent value for all drilling fluids of the same type or of the same density.

c)   Operating procedures

Refer to API Recommended Practice 13B-1/ISO 10414-1, Recommended Practice Standard Procedure for Field Testing Water-Based Drilling Fluids, or Recommended Practice 13B-2/ ISO 10414-2, Recommended Practice Standard Procedure for "Field Testing Oil-Based Drilling Fluids", Clauses entitled "Marsh Funnel".

5.1.2   Concentric-cylinder viscometer

5.1.2.1   Low-temperature, non-pressurized instruments

a)   Description

Concentric-cylinder (Couette) viscometers are rotational instruments powered by an electric motor or a hand-crank. Fluid is contained in the annular space between two cylinders. The outer sleeve (rotor) is driven at a constant rotational velocity. The rotation of the rotor in the fluid produces a torque on the inner cylinder or bob. The torque on the inner cylinder is usually measured with a torsion spring that retains the movement. This mechanism is illustrated in Figure 2. In most cases, a dial attached to the bob indicates deflection of the bob in degrees. Instrument constants are such that plastic viscosity and yield point are directly obtained by readings from rotor speeds of 300 and 600 rpm.

b)   Selection of instruments

Low-temperature, atmospheric concentric-cylinder viscometers are commonly used in testing drilling fluids. They differ in drive, available speeds, methods of readouts and measuring angles. All permit rapid calculation of plastic viscosity and yield point from readings at 300 rpm and 600 rpm. Table 2 shows two models and their operating limits.

Table 2 — Low-temperature, non-pressurized concentric-cylinder viscometers

Model	Drive	Power	Readout	Rotor Speed rpm	Max. Temperature °F
Model A	Motor	115 v, 60 Hz	Dial	1,2,3,6,10,20,30,60,100,200,300,600	200
Model B	Motor	12 V DC 115 v, 60 Hz 220 v, 50 Hz	Dial	0.10, 0.20, 0.30, 0.60, 1,2,3,6,10,20,30,60,100,200,300,600	200

c)   Operating procedures

Operating procedures for several models of concentric-cylinder viscometers are detailed in API Recommended Practice 13B-1/ISO 10414-1 or API Recommended Practice 13B-2/ISO-10414-2. Specific operating procedures for those instruments not included in the Recommended Practice 13B-1 or 13B-2 can be obtained from the manufacturers.
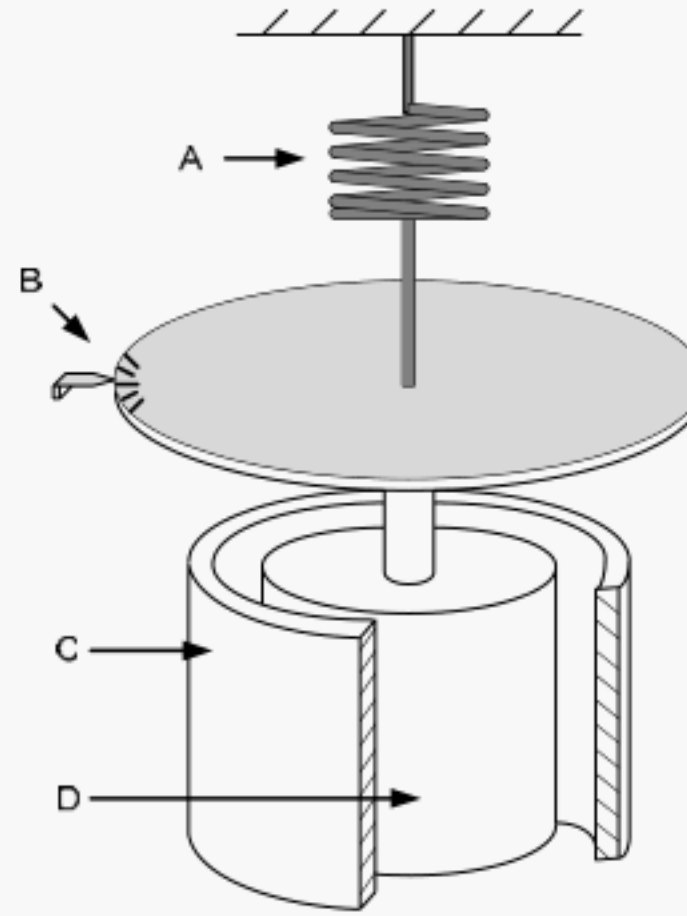
KEY

A   spring

B   dial

C   rotor

D   bob

Figure 2- Concentric-cylinder viscometer

5.1.2.2   High-temperature, pressurized instruments

a) Description

High-pressure, high-temperature, concentric-cylinder viscometers are used to measure flow properties of drilling fluids at elevated temperatures and pressures. Each instrument has differences in temperature and pressure limitations, and design variation. Specific operating procedures for these instruments can be obtained from the manufacturer.

b) High-temperature, low-pressure instrument

A high-temperature, low-pressure instrument is designed in the same fashion as non-pressurized viscometers. The upper operating limits are 2,000 psig and 500 °F. The pressurizing medium for this viscometer is nitrogen gas. Fluid is contained in the annular space between two cylinders with the outer sleeve being driven at a controlled rotational velocity. Torque is exerted on the inner cylinder or bob by the rotation of the outer sleeve in the fluid. This torque is then measured to determine flow properties. This instrument has variable rotor speeds from 1 rpm to 600 rpm with a viscosity range of 1 to 300,000 cP. The temperature range of 0 °F to 500 °F is programmable. A personal computer interface provides real-time graphic display and data storage.

c) High-temperature, high-pressure instrument

A high-temperature, high-pressure instrument has upper operation limits of 40,000 psig and 600°F. The pressurizing medium is mineral oil. It is a concentric-cylinder viscometer that uses the same geometry as the atmospheric viscometers. Rotor speeds are variable to 600 rpm. The rotor has external flights to induce circulation. Temperature, pressure, rotor speed, and shear stress are displayed through digital readouts. The digital temperature control has ramp and soak capacities. A computer provides control and digital display of parameters.

5.2 Rheological models

5.2.1 Principle

The determination of drilling fluid rheological parameters is important in the calculation of circulating hydraulics, hole cleaning efficiency, and prediction of barite sag in oil wells. In this subclause, the rheological model recommended for field and office use is the Herschel-Bulkley (H-B) rheological model. Originally developed in 1926, the model consistently provides good simulation of measured rheological data for both water-based and non-aqueous drilling fluids. It has become the drilling industry's *de facto* rheological model for advanced engineering calculations.

5.2.2 Instrumentation configuration

In this subclause, the use of a concentric-cylinder viscometer is assumed. A rotating outer cylinder shears fluid between its inner wall and a bob lying within. A diagram of the viscometer cylinder and bob is shown in Figure 2,. The gap between the rotating cylinder and the bob is carefully controlled to ensure uniform shear rate development across the gap during shear. In the oilfield, this configuration is commonly given as the R1B1 configuration. With a rotor inner diameter fixed at 3.683 cm and a bob diameter fixed at 3.449 cm, the diameter ratio is maintained at 1.0678, a value which meets international DIN standards.

5.2.3 Herschel-Bulkley rheological model

The H-B model requires three parameters as shown in the following equation:

$$\tau = \tau_y + k\gamma^n \tag{16}$$

where

    n is the flow index (dimensionless)

    k is the consistency index (force/area times time)

    τ_y is the fluid yield stress (force/area)

It should be noted that the H-B governing equation reduces to more commonly-known rheological models under certain conditions. When the yield stress τ_y equals the yield point, the flow index n =1 and the H-B equation reduces to the Bingham plastic model. When fluid τ_y = 0 (*e.g.*, a drilling fluid with no yield stress), the H-B model reduces to the power law. Consequently the H-B model can be considered the unifying model that fits Bingham plastic fluids, power law fluids, and everything else in between.

In the H-B model, the consistency parameter k can be considered equivalent to the *PV* or plastic viscosity term in the Bingham plastic rheological model, but will nearly always have significantly different numerical value. Similarly, the τ_y parameter describes the suspension characteristics of a drilling fluid and can be considered equivalent to the Bingham plastic model yield point, but will also nearly always have lower numerical value. The true yield stress τ_y can be approximated using measurements from field viscometers or using numerical techniques. Both procedures are outlined in this clause.

5.2.4 Conversion factors

In the mathematics of fluid rheology as measured using a standard oilfield viscometer, there are instrument conversion factors[6] that need to be applied in the calculations.

a)   Shear stress (lb_f/100 ft^2) is determined by multiplying the dial reading (° deflection) by 1.066. This correction is sometimes ignored in doing simple calculations.

b)   Shear rate (s^{-1}) is determined by multiplying the rotor speed (rpm) by 1.703.

5.2.5   Solution methods for drilling fluid H-B parameters

Solving for drilling fluid H-B parameters using the measurement method[9] involves the following steps:

5.2.5.1   Approximate the fluid yield stress, commonly known as the low-shear-rate yield point, by the following equation. The τ_y value should be between zero and the Bingham yield point:

$$\tau_y = 2\theta_3 - \theta_6 \tag{18}$$

a)   Determine the fluid flow index value by:

$$n = 3{,}32 \log_{10}\left(\frac{(\theta_{600} - \tau_y)}{(\theta_{300} - \tau_y)}\right) \tag{19}$$

b)   Determine the fluid consistency index by:

$$k = \frac{(\theta_{300} - \tau_y)}{511^n} \tag{20}$$

5.2.5.2   For water-based drilling fluids containing large amounts of viscous polymers and hence have high θ_{600} values, the yield stress calculation in 5.2.5.1 above can overstate values for τ_y.

5.2.6   Solving for the H-B parameters using numerical techniques[7] involves the following steps:

a)   The solution involves a curve fit of the measured viscometer data using a minimum of 3 shear stress/shear rate data pairs N. The following numerical solution method can be programmed in a spreadsheet:

b)   Convert the shear stress dial readings to τ_i (units of lb_f/100 ft^2)

c)   Guess a value of n_1. It is recommended to start at $n = 1$. For each of the N data sets, calculate:

   1)   the corrected shear rates γ_i (not needed for guess of n=1).

   2)   the following data summations: $\Sigma \tau_i$, $\Sigma \gamma_i^n$, $\Sigma \gamma_i^{2n}$, $\Sigma \tau_i \gamma_i^n$

   3)   the value for τ_y and k by:

$$\tau_y = \left(\frac{\Sigma\tau_i \times \Sigma\gamma_i^{2n} - \Sigma\tau_i\gamma_i^n \times \Sigma\gamma_i^n}{N \times \Sigma\gamma_i^{2n} - \left(\Sigma\gamma_i^n\right)^2}\right) \tag{21}$$

$$k = \left(\frac{N \times \Sigma\tau_i\gamma_i^n - \Sigma\gamma_i^n \times \Sigma\tau_i}{N \times \Sigma\gamma_i^{2n} - \left(\Sigma\gamma_i^n\right)^2}\right) \tag{22}$$

   4)   the error in curve fitting by:

a. calculating the following

$$\left(\Sigma\gamma_i^n \times \ln(\gamma_i)\right)\left(\Sigma\gamma_i^{2n} \times \ln(\gamma_i)\right)\left(\Sigma\tau_i \times \gamma_i^n \times \ln(\gamma_i)\right) \tag{23}$$

b. calculating the error *Err* by:

$$\mathrm{Err} = \tau_y \times \left(\Sigma\gamma_i^n \times \ln(\gamma_i)\right) + k \times \left(\Sigma\gamma_i^{2n} \times \ln(\gamma_i)\right) - \left(\Sigma\tau_i \times \ln(\gamma_i)\right) \tag{24}$$

d) Guess a second value of n. Repeat calculations in steps 5.2.6a to 5.2.6d. If the value of *Err* is less than an arbitrary acceptable error (0.05 recommended), then stop the calculations. Use the values for n, k, and τ_y calculated in the last set. If the value of *Err* is greater than an arbitrary acceptable error, then determine a new value of n_3 using a common convergence routine.

e) When the calculated values of τ_y are less than 0, this indicates the numerical procedure had trouble in fitting the data. When this happens, the user can choose either of the following courses of action:

1) Use another rheological model (Bingham plastic or power law) in the calculations, or

2) Reset the value of τ_y to 0 or to a very small positive value such as 0.001 lb_f/100 ft^2.

5.2.7 Checking for H-B parameter accuracy

5.2.7.1 As a normal course of action, the values of n, k, and τ_y should be checked for their accuracy in predicting the measured dial readings regardless of whether the measurement or numerical method of calculation is used.

5.2.7.2 To do this, the following procedure is recommended:

a) Using the corrected shear rates for each of the viscometer measurements (γ_i) and the calculated values of the three H-B parameters, calculate values of τ on the viscometer bob using the H-B model:

$$\tau = \tau_y + k\,\gamma^n \tag{16}$$

b) Convert the predicted values of τ into dial reading units (° deflection) by dividing by 1.066.

c) Apply statistical methods to evaluate the degree of fit between the measured and predicted data.

5.2.8 Applying the H-B parameters

Assuming a high degree of fit between the measured and predicted dial readings, the calculated values of the H-B parameters can be applied with confidence in hydraulics and hole-cleaning equations to calculate pressure losses and Equivalent Circulating Density (ECD).

5.2.9 Other rheological models used

5.2.9.1 In some calculations used in this Bulletin, parameters from the Bingham plastic and power law rheological models are needed. The calculation methods for these parameters remain as published in the API Recommended Practice 13D (1995)[10].

5.2.9.2 *Bingham plastic rheological model*. This model uses the θ_{600} and θ_{300} viscometer dial reading to calculate two parameters:

Plastic viscosity (PV), in cP = θ_{600} - θ_{300} (25)

Yield point (YP), in lb_f/100 ft^2 = θ_{300} − PV (26)

5.2.9.3 ***Power law***. As used in the recent version of this Bulletin, this model uses two sets of viscometer dial readings to calculate flow index n and consistency index k for pipe flow and annular flow. The conventional power law only uses the data set from the higher shear rates, so that $n_a = n_p$ and $k_a = k_p$. The values obtained using the calculation methods given below will produce values of n and k that are usually significantly different from those calculated using the Herschel-Bulkley rheological model.

1. Pipe flow

$$n_p = 3.32 \; \log_{10}\left(\frac{\theta_{600}}{\theta_{300}}\right) \tag{27}$$

$$k_p = \frac{(\theta_{300})}{511^{n_p}} \tag{28}$$

2. Annular flow

$$n_a = 0.657 \; \log_{10}\left(\frac{\theta_{100}}{\theta_3}\right) \tag{29}$$

$$k_a = \frac{(\theta_{100})}{170.3^{n_a}} \tag{30}$$

6   Prediction of downhole behavior of drilling fluids

6.1   Principle

The downhole behavior of fluid properties should be taken into account to accurately calculate the hydraulics of oil-well drilling fluids. This is especially important when oil-based and synthetic-based drilling fluids are being used. The downhole behavior of drilling fluids should be predicted in three principal areas:

—static and dynamic temperatures
—drilling fluid rheological properties
—drilling fluid density

Each of these areas is discussed in this subclause.

6.2   Circulating temperature predictions in oil-well drilling

6.2.1   While drilling oil-wells, the prediction of bottom hole circulating temperature T_{bhc} is necessary for use in hydraulic and drilling fluid density modeling, especially when invert emulsion and all-oil drilling fluids are used. The prediction of circulating temperatures in a wellbore can be a very complex task, as many operational and physical parameters are required. A simplified calculation procedure is presented that requires a minimum of input parameters and is generally sufficiently accurate to predict circulating temperatures. This model[11,12] which can be easily programmed in a spreadsheet program, gives good results within the following ranges for the bottom hole static temperature T_{bhs} and geothermal gradient:

Bottom Hole Static Temperature (°F):   166 – 414

Geothermal Gradient (°F/100 ft):   0.83 – 2.44

6.2.2   Input parameters needed for the prediction of downhole circulating temperatures:

- True Vertical Depth (D_{tvd})
- Surface temperature (T_s)
- Bottom Hole Static Temperature (T_{bhs})
- For offshore wells, water depth (D_w); for land wells, $D_w = 0$
- Geothermal gradient (t_g)
- Surface temperature (T_0) measured at a depth of 50 ft or approximated by the measured surface temperature

6.2.3 Temperature calculation methods for land and offshore wells

a) For land wells having a known T_{bhs}, the T_{bhc} can be calculated using the following method[11]:

1) Calculate geothermal gradient t_g (°F/100 ft):

$$t_g = 100 \frac{(T_{bbs} - T_0)}{D_{tvd}} \tag{31}$$

2) Calculate T_{bhc} (°F):

$$T_{bhc} = -102.1 + [3\,354 \times t_g] + [(1.342 - 22.28 \times t_g) \times T_{bhs}] \tag{32}$$

b) For land wells having a known geothermal gradient, T_{bhc} can be calculated by:

1) Calculate T_{bhs} (ºF):

$$T_{bbs} = T_0 + \left(\frac{t_g \times D_{tvd}}{100} \right) \tag{33}$$

2) Calculate T_{bhc} (°F):

$$T_{bhc} = -102.1 + [3\,354 \times t_g] + [(1.342 - 22.28 \times t_g) \times T_{bhs}] \tag{34}$$

c) For offshore wells having a known T_{bhs}, the above method can be used once the geothermal gradient has been adjusted for the presence of a water column t_{gw}:

1) Calculate the geothermal gradient adjusted for water depth t_{gw} (°F / 100 ft) by:

$$t_{gw} = \frac{(T_{bhs} - T_0)}{D_{tvd} - D_w} \tag{35}$$

2) Calculate T_{bhs} (ºF):

$$T_{bhc} = -102.1 + [3\,354 \times t_{gw}] + [(1.342 - 22.28 \times t_{gw}) \times T_{bhs}] \tag{36}$$

d) For offshore wells having a known geothermal gradient, the above equations can be used after adjusting for water depth:

1) Calculate T_{bhs} (°F):

$$T_{bhs} = T_0 + t_{gw} \cdot (D_{tvd} - D_w) \tag{37}$$

2) Calculate T_{bhc} :

$$T_{bhc} = -102.1 + [3\,354 \times t_{gw}] + [(1.342 - 22.28 \times t_{gw}) \times T_{bhs}] \tag{38}$$

6.2.4 Construction of a static temperature profile for a well

6.2.4.1 Temperatures for a static well are collected and predicted using the following data:

a) The measured surface temperature serves as the static temperature value at $D_{tvd} = 0$.
b) For offshore wells, adjustments in the geothermal gradients need to be made to account for the water depth.
c) Static temperatures in a seawater column can be predicted as a function of depth by:

For water depths <= 3000 ft:

$$T_{ml} \, (°F) = 154.43 - 14.214 \times \ln{(D_w)} \tag{39}$$

For water depths > 3000 ft,

$$T_{ml} \, (°F) = 41.714 - 0.0003714 \times D_w \tag{40}$$

6.2.4.2 While a well is being drilled, estimates for the T_{bhs} are made using a known geothermal gradient or the geothermal gradient is estimated using a known T_{bhs}. Several data points should be collected as functions of D_{tvd} while the well is being drilled.

6.2.4.3 A straight-line fit between the collected data points will give a predicted static temperature profile by depth. These values or averages of them over a desired depth interval can then be inserted into the models that predict the downhole static rheology and density of drilling fluids as outlined later in this subclause.

6.2.5 Construction of a dynamic temperature profile for a well

6.2.5.1 Dynamic circulating temperatures for a well can be predicted in a similar manner to those used above in predicting static temperatures.

6.2.5.2 Using the values for T_{bhs} and the geothermal gradients, the T_{bhc} for each of the points can be calculated using the equations in Subclause 6.2.3.

6.2.5.3 The flowline temperature T_{fl} is routinely measured and serves as the dynamic circulating temperature at depth $D_{tvd} = 0$. This value can be used to calibrate the circulating temperature predictions made from the equations in 6.2.3 above.

6.2.5.4 A straight-line fit between the collected data points will give a predicted dynamic temperature profile by depth. These values or averages of them over a desired depth interval can then be inserted into the models which predict the downhole dynamic rheology and density of drilling fluids as outlined later in this subclause.

6.3 Prediction of downhole rheology of oil-well drilling fluids

6.3.1 Accurate prediction of downhole rheology of drilling fluids is important for the optimization of hydraulic and hole-cleaning capabilities of oil-well drilling fluids. With enhanced prediction of downhole rheology, standard hydraulics calculations such as circulating pressure losses, surge and swab pressures, and hole-cleaning efficiencies can be more accurately determined. This increased accuracy can be of critical value in well sections where the differentials between pore pressures and formation fracture gradients are small. For certain drilling fluid types such as oil-based or synthetic-based fluids, downhole rheological properties can be significantly different from those measured at surface conditions. As a result, the usefulness of hydraulics calculations made with fluid rheological parameters derived solely from surface rheology measurements can be limited.

6.3.2 As with the prediction of downhole fluid density, the effects of temperature and pressure on rheology must be taken into account. When considered separately, the generalized effects of temperature and pressure on downhole rheological properties can be summarized as follows.

6.3.2.1   The effects of temperature usually serve to increase the viscosity of oil-well drilling fluids at low temperatures (< 70 °F, or 21 °C) and to decrease their viscosity at higher temperatures (<300 °F, or 150 °C). The temperature effects on fluid viscosity are generally non-linear.

6.3.2.2   The effects of pressure usually serve to increase the viscosity of drilling fluids. Pressure effects on fluid viscosity are generally non-linear.

6.3.3   The combined effects of temperature and pressure on drilling fluids. The magnitude of temperature and pressure effects on drilling fluids depends on the fluid type being used.

6.3.3.1   As with density modeling, the effects of temperature and pressure on water-based drilling fluids and brines are usually slight. Hence for most water-based drilling fluids and brines, the use of fluid rheology measured at surface will usually produce reasonable predictions of downhole circulating hydraulics. Special cases where downhole modeling of water-based drilling fluids and brines would enhance the accuracy of hydraulic calculations include High-Temperature / High-Pressure (HTHP) cases where bottomhole temperatures are very high, and deepwater cases where long risers are exposed to very cold water.

6.3.3.2   The effects of temperature and pressure on downhole fluid rheology are most pronounced for non-aqueous drilling fluids that are formulated using diesel, mineral oils, olefins, esters, etc. By way of example, the viscosity profiles of several non-aqueous based fluids as a function of temperature are presented in Figure 3. Here the non-linear reduction in fluid viscosity with increasing temperature is evident.
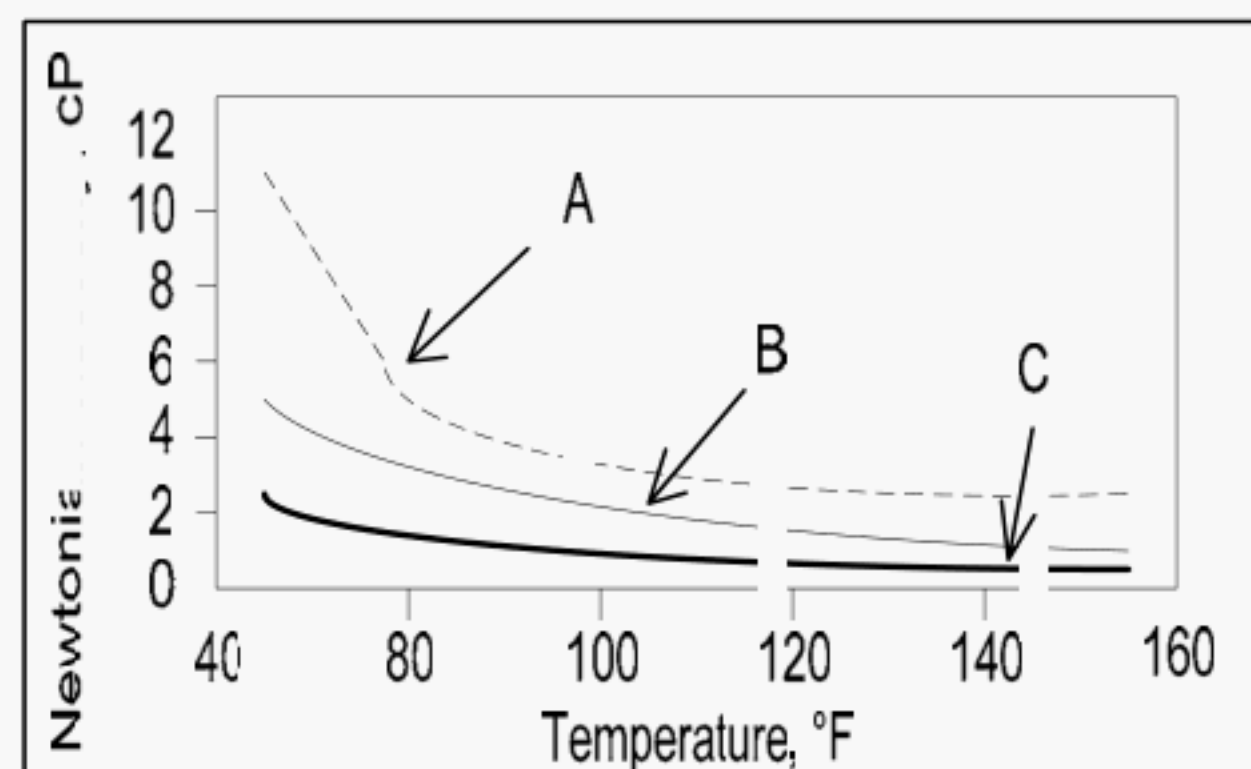
KEY

    A   is ester synthetic fluid

    B   is diesel oil

    C   is mineral oil

Figure 3- Viscosity of common base fluids as function of temperature

6.3.4   Testing is required to determine downhole rheological properties. The recommended procedure for predicting the downhole behavior of oil-based and synthetic-based drilling fluids and the aforementioned special cases involving water-based drilling fluids involves the testing of drilling fluids using HTHP viscometers. These viscometers are capable of testing at elevated temperatures and pressures and are described in Clause 5 of this Bulletin.

6.3.4.1   A comprehensive testing matrix should be planned and developed before any testing is undertaken. The development of a comprehensive testing matrix should include the following conditions:

6.3.4.2 The well schematic should be divided into individual sections, based on changes in hole angle, wellbore geometry, estimated circulating temperatures (see Clause 6), etc.

6.3.4.3 For each wellbore section, determine the average pressure and temperature conditions.

6.3.4.4 Construct a test matrix incorporating the temperature and pressure ranges from the wellbore plus add a buffer on each side of the temperature and pressure ranges so that slightly more severe conditions than the original conditions can be tested. For example, given a wellbore having temperature and pressure conditions ranging between 80 °F and 260 °F and 500 psia and 7,000 psia respectively, construct a testing matrix similar to that shown in Table 3.

Table 3—Example test matrix

Temp °F	Pressure reading, psia				
	0	2000	4000	6000	8000
70	data	Data	Data	data	data
120	data	Data	Data	data	data
170	data	Data	Data	data	data
220	data	Data	Data	data	data
270	data	Data	Data	data	data
NOTE: Alternatively, the number of laboratory measurements can be reduced by testing only at the average temperature and pressure conditions predicted for each of the wellbore sections. Consequently the reduced number of tests would be represented as a near diagonal in the test matrix above (see shaded cells).					

6.3.4.5 For each temperature/pressure combination in the test matrix, measure at the minimum the dial readings for the following rotational speeds: 600, 300, 200, 100, 6, and 3 rpm. Use of the standard R1B1 configuration for the rotor and bob on the viscometer is recommended.

6.3.4.6 Using the test data, calculate the drilling fluid rheological parameters (see Clause 5) using the Herschel-Bulkley rheological model for drilling fluids and the power law for water and brines.

6.3.4.7 Insert the fluid rheological parameters calculated above into the well sections determined as in Subclause 7.4 and run the hydraulics calculations (pressure losses, surge/swab, etc.) for each section.

6.4 Prediction of downhole density of oil-well drilling fluids

6.4.1 Principle - the need for prediction of downhole density

6.4.1.1 Accurate prediction of ECD is always important in drilling operations, especially in those drilling cases where there is a narrow window between pore pressure and fracture gradient. As with drilling fluid rheology, drilling fluid density is affected by downhole temperatures and pressures. In order to more accurately model ECD in oil wells, the drilling fluid density must be determined by taking account of downhole conditions.

6.4.1.2 For certain drilling fluid types such as oil-based or synthetic-based fluids, the drilling fluid density under downhole conditions can be significantly different from that measured at surface conditions.
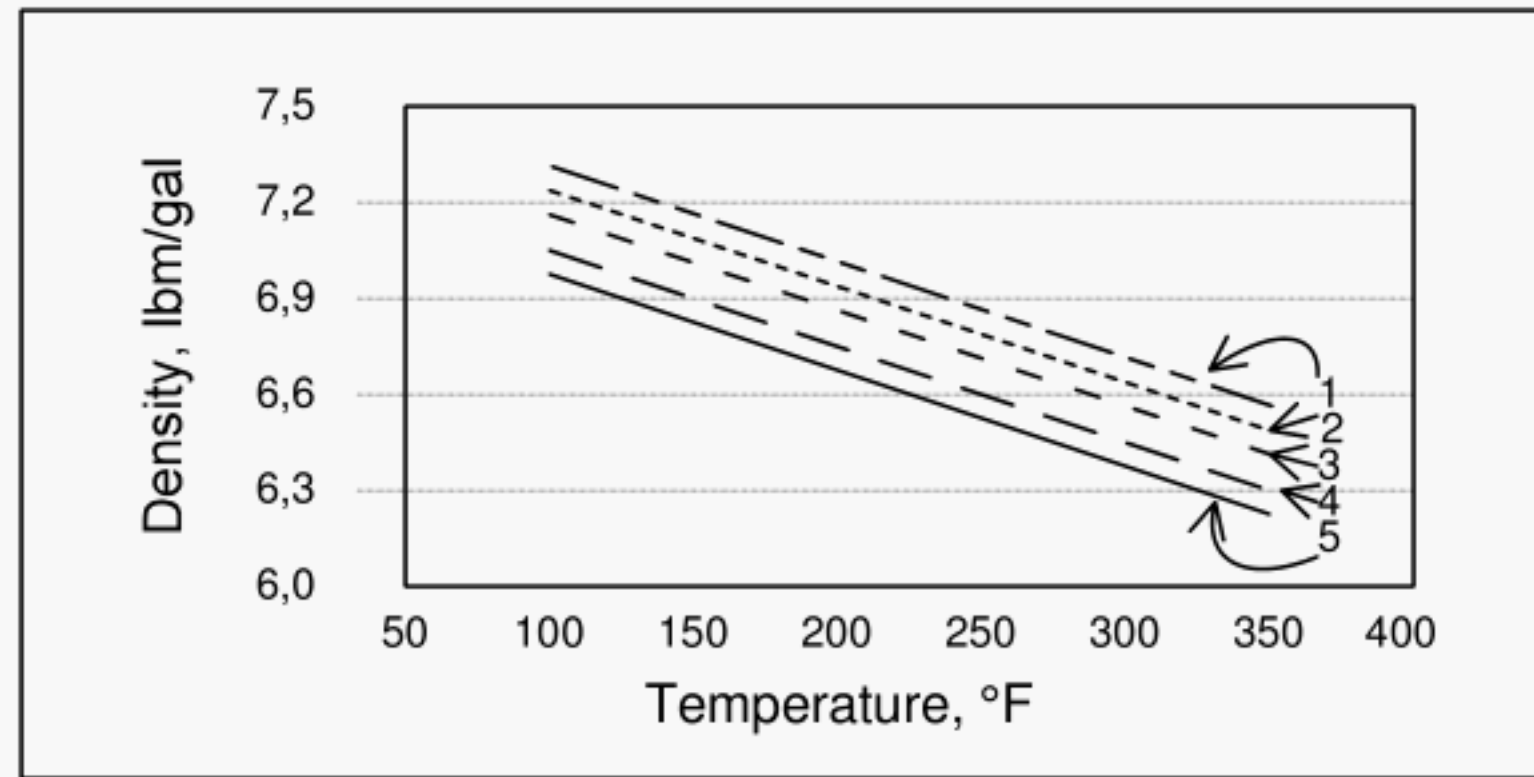
6.4.2 Effects of temperature and pressure on density

6.4.2.1 As with the prediction of downhole fluid rheology, the effects of temperature and pressure must be taken into account. When considered separately, the generalized effects of temperature and pressure on downhole drilling fluid density can be summarized as follows:

6.4.2.2 The effects of temperature usually serve to increase the density of oil-well drilling fluids at low temperatures and to decrease their density at higher temperatures. The temperature effects on fluid density are generally near-linear.

6.4.2.3 The effects of pressure usually serve to increase the density of drilling fluids in a generally non-linear fashion.

KEY

    1   Density at 12,500 psia

    2   Density at 10,000 psia

    3   Density at 7,000 psia

    4   Density at 3,000 psia

    5   Density at 15 psia

Figure 4— Density of diesel as a function of temperature and pressure

6.4.3 Effects of temperature and pressure on drilling fluids density

6.4.3.1 The magnitude of temperature and pressure effects on drilling fluids depends on the fluid type being used.

6.4.3.2 The effects of temperature and pressure on the density of water, water-based drilling fluids, and brines are usually slight. Monovalent brines are less affected by temperature and pressure than divalent brines are. Hence for most water-based drilling fluids and monovalent brines, the use of fluid density measured at surface may be acceptable for use in downhole simulations.

6.4.3.3 The effects of downhole temperature and pressure on the density of divalent brines such as calcium chloride warrant their being studied. In this subclause, a 19.3 wt% calcium chloride solution (ρ_{brine} = 9.764 lb$_m$/gal at ambient conditions) is used to model temperature and pressure effects of divalent brines.

6.4.3.4 The effects of temperature and pressure on downhole fluid density are most pronounced for invert emulsions and 100% non-aqueous fluids that are formulated using diesel, mineral oils, olefins, esters, etc. The effects of temperature and pressure on diesel are shown in Figure 4. The data clearly show the temperature and pressure effects. Because the data are well-ordered, a general mathematical model can describe these effects in a numerical fashion. Since different non-aqueous fluid behave differently with changes in temperature and pressure, individual correlations can be constructed to mathematically describe fluid behavior.

6.4.3.5 Special cases where downhole modeling of water-based drilling fluids and brines would enhance the accuracy of drilling fluid density calculations include HTHP cases where bottomhole temperatures are very high, and deepwater cases where long risers are exposed to very cold water temperatures.

6.4.4 Modeling the effects of temperature and pressure on drilling fluid rheology

6.4.4.1   The downhole density of drilling fluids can be accurately predicted with use of a compositional model that takes into account the liquid and solid phases in the drilling fluid.

6.4.4.2   From the drilling fluid retort analysis, the volumes of the individual components of the drilling fluid are measured. The appropriate value for ρ_{solids} is taken from the retort analysis and the brine wt% is determined by analysis of drilling fluid filtrate.

$$\text{Vol}_{total} = \text{Vol}_{base} + \text{Vol}_{brine} + \text{Vol}_{solids} \tag{41}$$

$$\text{Vol}_{brine} = \text{Vol}_{water} + \text{Vol}_{salt} \tag{41a}$$

Detailed calculations for determining the brine composition and corrected solids content can be found in the API Recommended Procedure 13B2, Subclauses 9.4 and 9.5. For 19.3 wt% $CaCl_2$ brine, Vol_{salt} can be approximated by:

$$\text{Vol}_{salt} \text{ (vol\%)} \quad = 0.0013091 * (\text{wt\% } CaCl_2) + 8.44\text{E-}05 * (\text{wt\% } CaCl_2)^2 \tag{42}$$

$$= 0.056704$$

The corrected volume of drilled solids in the fluid is then:

$$\text{Vol}_{ds}(\%) = \text{Vol}_{solids}(\%) - \left(\frac{0.056704 \times \text{Vol}_{water}(\%)}{100} \right) \tag{43}$$

Drilled solids are generally considered incompressible and the correction for Vol_{ds} (%) is the only correction needed.

The mass of the components are given by:

$$\text{Vol}_{total} \times \rho_{total} = \text{Vol}_{base} \times \rho_{base} + \text{Vol}_{brine} \times \rho_{brine} + \text{Vol}_{ds} \times \rho_{ds}. \tag{44}$$

6.4.4.3   Coefficients in Table 3 for five base fluid types can be used in the following general equation to determine the values of ρ_{base} and ρ_{brine} for combinations of temperature and pressure:

$$\rho_{base} \text{ or } \rho_{brine} = [(a_1 + b_1 \times P + c_1 \times P^2) + (a_2 + b_2 \times P + c_2 \times P^2) \times T] \tag{45}$$

6.4.4.4   Values for static temperature and pressure existing in each particular cell can be predicted using the method described in Subclause 6.2. The static drilling fluid density in the particular cell (Local Drilling fluid Density or ρ_i) of length L is then

$$\rho_i = \frac{\left(\text{Vol}_{base} \times \rho_{base} + \text{Vol}_{brine} \times \rho_{brine} + \text{Vol}_{ds} \times \rho_{ds} \right)}{\text{Vol}_{total}} \tag{46}$$

The static Equivalent Static Density at depth D+L ESD_{D+L} is then

$$ESD_{D+L} = ESD_D + \rho_i \times L. \tag{47}$$

Integration of the local static densities with the ESD_D lying immediately above them in a stepwise procedure down to well total depth produces the final ESD for the well ESD_f.

6.4.4.5   From the dynamic temperature prediction method discussed in Subclause 6.2, the appropriate dynamic circulating temperature for each cell of length L can be determined. The dynamic local drilling fluid density ρ_i and the Equivalent Dynamic Density EDD of the cell is calculated the same way as for static conditions.

$$\rho_i = \frac{\left(\text{Vol}_{base} \times \rho_{phase} + \text{Vol}_{brine} \times \rho_{brine} + \text{Vol}_{ds} \times \rho_{ds} \right)}{\text{Vol}_{total}} \tag{48}$$

$$EDD_{D+L} = EDD_D + \rho_l \times L. \tag{49}$$

Integration of the local dynamic densities with EDD_D lying immediately above them in a stepwise procedure down to well total depth produces the final EDD for the well EDD_f.

6.3.4.6 Sometimes the change in volume of a drilling fluid system with temperature and pressure is needed. For example, a prediction for volume change may be desired when circulation is stopped and the wellbore reverts to static temperature and pressure conditions. For cases such the relative volume change can be predicted by:

$$\Delta Vol\% = 100 \frac{EDD_f}{ESD_i} \tag{50}$$

The total volume change in a wellbore is given by:

$$\Delta Vol_{wb} = \Delta Vol\% \times Vol_{wb} \tag{51}$$

Table 3 – Temperature and pressure coefficients for determining fluid density

	Calcium Chloride 19.3 wt %	Diesel	Mineral Oil	Internal Olefin	Paraffin
Reference	22	23	22	24	25
Pressure Coefficients					
a_1 (lb$_m$/gal)	9.9952	7.3183	6.9912	6.8358	6.9692
b_1 (lb$_m$/gal/psi)	1.77 E-05	5.27 E-05	2.25 E-05	2.23 E-05	3.35 E-05
c_1 (lb$_m$/gal/psi^2)	6 E-11	-8 E-10	-1 E-10	-2 E-10	-5 E-10
Temperature Coefficients					
a_2 (lb$_m$/gal/ºF)	-2.75 E-03	-3.15 E-03	-3.28 E-03	-3.39 E-03	-3.46 E-03
b_2 (lb$_m$/gal/psi/ºF)	3.49 E-08	7.46 E-08	1.17 E-07	1.12 E-07	-1.64 E-08
c_2 (lb$_m$/gal/psi^2/ºF)	-9 E-13	-1 E-12	-3 E-12	-2 E-12	2 E-13
Fitting Statistics for Modeled Data					
Avg. Error %	0.135	0.237	0.166	0.194	0.214
r^2 coefficient	0.998	0.997	0.998	0.998	0.999
Range of Validity					
Max. Applied Pressure (psi)	20,300	20,000	20,300	24,000	14,500
Min. Temperature (ºF)	77	40	77	56.4	68
Max. Temperature (ºF)	392	400	392	392	302

7   Pressure-loss modeling

7.1   Principle

7.1.1   The purpose of this subclause is to provide methods and equations to calculate frictional pressure losses and hydrostatic pressures through the different elements of the circulating system of a drilling well. The information is suitable for hydraulics analyses, planning, and optimization.

7.1.2   It is also is useful for modeling special well-construction operations such as well control, cementing, tripping, and casing runs. Equations in this subclause are applicable to water, oil and synthetic-based fluids; they do not address air/gas, foam, and other aerated or highly compressible fluids.

7.2 Basic relationships

7.2.1 Pressures in the circulating system can be defined by fundamental relationships for standpipe (pump) pressure and bottomhole pressure that are valid under static and dynamic conditions.

7.2.2 Pump pressure P_p is equal to the sum of frictional pressure losses, surface back pressure, and hydrostatic-pressure difference between the annulus and drillstring.

$$P_p = P_{sc} + P_{ds} + P_{dt} + P_b + P_a + P_{cl} + P_c + P_{ha} - P_{hd} \tag{52}$$

7.2.3 Pressure at the bottom of the well P_{bh} is the sum of the annular frictional pressure losses, surface back pressure, and annular hydrostatic pressure.

$$P_{bh} = P_a + P_{cl} + P_c + P_{ha} \tag{53}$$

7.2.4 Hydrostatic pressure depends on true vertical depth D_v and the density profile of the drilling fluid column in the well. An effective annular hydrostatic pressure can be determined by including the volume percent of drilled cuttings. The process to estimate average cuttings concentration c and cuttings specific gravity ρ_c is presented in Clause 9.

7.2.4.1 Hydrostatic pressure in conventional wells

For conventional wells, average density in the drilling fluid column can be approximated by the drilling fluid density measured at the surface ρ_s.

Pipe
$$P_{hd} = 0.052 \ \rho_s D_v \tag{54}$$

Annulus without cuttings
$$P_{ha} = 0.052 \rho_s D_v \tag{55}$$

Annulus with cuttings
$$P_{ha} = 0.052 \big[(1 - c) \rho_s + 8.345 \, c \, \rho_c \big] D_v \tag{56}$$

7.2.4.2 Hydrostatic pressure in HTHP and deepwater wells

In high-pressure and extreme-temperature (hot and cold) wells, the density profile is significantly affected by temperature and pressure. The correct hydrostatic pressures in the drillstring and annulus (P_{hd} and P_{ha}, respectively) in these types of wells are calculated using equivalent static densities ESD_p and ESD_a (see Clause 6) defined at the true vertical depth of interest D_v.

Pipe
$$P_{hd} = 0.052 ESD_p D_v \tag{57}$$

Annulus without cuttings
$$P_{ha} = 0.052 ESD_a D_v \tag{58}$$

Annulus with cuttings
$$P_{ha} = 0.052 \big[(1 - c) ESD_a + 8.345 \, c \, \rho_c \big] D_v \tag{59}$$

7.3 Surface-connection pressure loss

Pressure loss in surface connections P_{sc} depends on pipe geometry, surface drilling fluid density ρ_s, and flow rate Q. Common practice is to categorize surface-connection piping into five general cases and use the appropriate proportionality constant C_{sc} from Table 4 to estimate the pressure loss [49].

$$P_{sc} = C_{sc}\ \rho_s \left(\frac{Q}{100}\right)^{1.86} \tag{60}$$

Table 4 – C_{sc} for surface-connection cases

Case	Standpipe	Hose	Swivel	Kelly	C_{sc}
1	40 ft x 3.0-in ID	45 ft x 2.0-in ID	4 ft x 2.0-in ID	40 ft x 2.25-in ID	1.00
2	40 ft x 3.5-in ID	55 ft x 2.5-in ID	5 ft x 2.5-in ID	40 ft x 3.25-in ID	0.36
3	45 ft x 4.0-in ID	55 ft x 3.0-in ID	5 ft x 2.5-in ID	40 ft x 3.25-in ID	0.22
4	45 ft x 4.0-in ID	55 ft x 3.0-in ID	6 ft x 3.0-in ID	40 ft x 4.00-in ID	0.15
5	100 ft x 5.0-in ID	85 ft x 3.5-in ID	22 ft x 3.5-in ID		0.15

7.4 Drillstring and annular frictional pressure loss

7.4.1 Principle

Flow rate, flow regime, rheological properties, and conduit geometry are among the key parameters that impact frictional pressure losses in the drillstring and annulus. The process to model these pressures, complex in its own right for Herschel-Bulkley fluids, is further complicated in HTHP and deepwater wells by the sensitivity of drilling fluid density and rheological properties to downhole temperatures and pressures.

7.4.2 Section lengths for pressure-loss calculations

An efficient method [32,57,58] to incorporate downhole conditions is to subdivide the drillstring and annulus into the short segments (or cells) of length L like those used to numerically integrate the density profile (see Clause 6). For the most part, equations and parameter values presented in this subclause apply to these individual cells. Geometric sections or casing intervals commonly used for conventional wells also can be used for critical wells; however, the various parameters must be properly averaged over each segment length.

7.4.3 Fluid velocity

7.4.3.1 Average (bulk) velocities V_p and V_a are inversely proportional to the cross-sectional area of the respective fluid conduit.

Pipe
$$V_p = \frac{24.51\ Q}{d_i^2} \tag{61}$$

Annulus
$$V_a = \frac{24.51\ Q}{d_h^2 - d_p^2} \tag{62}$$

7.4.3.2 Riser Booster Pumps

In deepwater drilling, booster pumps often are used to supplement flow in the riser to assist with hole cleaning. For these cases, flow rate in the riser/drillstring annulus should be the sum of the conventional and the booster flow rates.

7.4.4 Hydraulic diameter

The hydraulic-diameter concept is used to relate fluid behavior in an annulus to that in a circular pipe. There are several different expressions [1] used for the annular hydraulic diameter d_{hyd}, but the most widely used is based on the ratio of

the cross-sectional area to the wetted perimeter of the annular section. The hydraulic diameter for pipe flow is simply the internal diameter d_i.

Pipe
$$d_{hyd} = d_i \tag{63}$$

Annulus
$$d_{hyd} = d_h - d_p \tag{64}$$

7.4.5 Rheological parameters

Rheological parameters used for pressure-loss modeling are measured on field and HTHP laboratory viscometers (see Clause 5). Surface-measured values for *PV*, *YP*, and τ_y first must be adjusted for downhole temperatures and pressures in each well segment (Clause 6) before calculating the parameters *n* and *k* in that segment.

7.4.5.1 Herschel-Bulkley model parameters

The traditional oilfield rheological parameters *PV*, *YP* and τ_y should be used to determine Herschel-Bulkley parameters *n* and *k* in each downhole segment. The τ_y/YP ratio *R* is an additional parameter useful for defining rheological behavior (*R* = 0 for power-law, *R* = 1 for Bingham-plastic, and 0 < *R* < 1 for Herschel-Bulkley fluids).

$$n = 3.32 \log_{10}\left(\frac{2PV + YP - \tau_y}{PV + YP - \tau_y}\right) \tag{65}$$

$$k = \frac{PV + YP - \tau_y}{511^n} \tag{66}$$

$$R = \frac{\tau_y}{YP} \qquad \text{(for } YP > 0\text{)} \tag{67}$$

7.4.5.2 Power-law parameters

Several complex relationships for Herschel-Bulkley fluids are difficult and even impossible to evaluate analytically. Under some conditions, it is convenient to treat Herschel-Bulkley fluids as generalized power-law fluids characterized by n_p and k_p.[36] The assumption is that the log-log slope of the Herschel-Bulkley flow equation is numerically close to the power-law flow behavior index n_p at high shear rates.

$$n_p = 3.32 \log_{10}\left(\frac{2PV + YP}{PV + YP}\right) \tag{68}$$

$$k_p = \frac{PV + YP}{511^{n_p}} \tag{69}$$

7.4.6 Shear-rate geometry correction factors

The Newtonian (or "nominal") shear rate γ first must be converted to shear rate at the wall γ_w in order to calculate pressure loss. This is accomplished using correction factors that adjust for the geometry of the flow conduit (pipe or annulus) and oilfield viscometers used to measure rheological properties.[34] Appropriate corrections can be combined into a single factor *G*.

7.4.6.1 Well geometry shear-rate correction

Shear-rate correction for well geometry B_a is also dependent on the rheological parameter n. It is convenient to use a geometry factor α so that flow in pipes and annuli can be considered in a single expression. For simplicity without significant loss of accuracy, the annulus can be treated as an equivalent slot ($\alpha = 1$).

$$B_a = \left[\frac{(3-\alpha)n+1}{(4-\alpha)n}\right]\left[1+\frac{\alpha}{2}\right] \tag{70}$$

where

$\alpha = 0$ is the geometry factor in the pipe

$\alpha = 1$ is the geometry factor in the annulus

7.4.6.2 Field viscometer shear-rate correction

Unfortunately, closed analytical solutions do not exist for Herschel-Bulkley fluids, and complex numerical methods are inaccurate at very low shear rates. Practically speaking, it can be assumed that the viscometer correction $B_x \approx 1$. Alternatively, B_x for power-law fluids [38] can be used if it is important to preserve exact solutions for these fluids. For the standard bob/sleeve combination, B_x for power-law fluids varies from 1.0 (for $n_p = 1.0$) to 1.1569 (for $n_p = 0.3$).

$$B_x = \left[\frac{x^{2/n_p}}{n_p x^2}\right]\left[\frac{x^2-1}{x^{2/n_p}-1}\right] \approx 1 \tag{71}$$

where

$x = 1.0678$ in the standard bob/sleeve combination R1B1

7.4.6.3 Combined geometry shear-rate correction factor

The well geometry and viscometer shear-rate correction factors can be combined into a single factor G that can be used to convert nominal shear rate to wall shear rate. For many cases, it is acceptable to assume $B_x \approx 1$.

$$G = \frac{B_a}{B_x} \approx B_a \tag{72}$$

7.4.7 Shear rate at the wall

Shear rate at the wall γ_w required to determine the shear stress at the wall is calculated by multiplying nominal shear rate by the geometry factor G. This equation is applicable for pipes and annuli for appropriate values of fluid velocity V and hydraulic diameter d_{hyd}.

$$\gamma_w = \frac{1.6GV}{d_{hyd}} \tag{73}$$

7.4.8 Shear stress at the wall (flow equation)

Frictional pressure loss is directly proportional to the shear stress at the wall τ_w defined by the fluid-model-dependent flow equation. Flow equations for Bingham-plastic and Herschel-Bulkley fluids are complex and require iterative solutions; however, they can be approximated by an expression of the same recognizable form as the respective constitutive equations.[42] For $\tau_y = 0$, the flow equation reduces to the exact solution for power-law fluids. For $\tau_y = YP$, then $n = 1$ and the flow equation reduces to the simplified Bingham-plastic expression widely used in drilling.

$$\tau_f = \left(\frac{4-\alpha}{3-\alpha}\right)^n \tau_y + k\gamma_w^n \qquad \text{(viscometer units)} \qquad (74)$$

$$\tau_w = 1.066\tau_f \qquad \text{(engineering units)} \qquad (75)$$

7.4.9 Flow regime

Flow patterns and friction factors in fluid conduits are characterized by laminar, transitional, and turbulent flow regimes.

7.4.9.1 Reynolds number (generalized)

Generalized Reynolds number N_{ReG} applies to both pipes and annuli.[36] The most convenient form of the equation involves the shear stress at the wall τ_w (defined in 7.4.7).

$$N_{ReG} = \frac{\rho V^2}{19.36\tau_w} \qquad (76)$$

7.4.9.2 Critical Reynolds number (laminar to transitional regimes)

The critical Reynolds number N_{CRe} is the value of N_{ReG} where the regime changes from laminar to transitional flow.[59]

$$N_{CRe} = 3470 - 1370n \qquad (77)$$

7.4.9.3 Critical velocity

While not required to calculate pressure losses, critical velocity is still an important hydraulics parameter. Critical velocity V_c is the bulk velocity where the Reynolds number N_{ReG} from 7.4.9.1 equals the critical Reynolds number N_{CRe} from 7.4.9.2. Unfortunately, iterative methods are required to calculate V_c for Herschel-Bulkley fluids. A very close approximation, however, can be achieved by an empirical relationship based on critical velocity for power law fluids V_{cp}, critical velocity for Bingham-plastic fluids V_{cb}, and the τ_y/YP ratio R (from Subclause 7.4.5.1).

$$V_c = V_{cp} + (V_{cb} - V_{cp})R\sqrt{\frac{V_{cp}}{V_{cb}}} \qquad (78)$$

a) Critical velocity (power-law fluids)

$$V_{cp} = \left[\frac{28277(2.533 - n_p)k_p}{\rho}\left(\frac{1.6\,G_p}{d_{hyd}}\right)^{n_p}\right]^{\frac{1}{2-n_p}} \qquad (79)$$

where

$$G_p = \left[\frac{(3-\alpha)n_p + 1}{(4-\alpha)n_p}\right]\left[1 + \frac{\alpha}{2}\right] \qquad (80)$$

b) Critical velocity (Bingham-plastic fluids)

$$V_{cb} = \frac{67.86}{\rho}\left[B + \sqrt{B^2 + 9.42\,\rho\,YP\left(\frac{4-\alpha}{3-\alpha}\right)}\right] \qquad (81)$$

where

$$B = \frac{PV\left(1 + \dfrac{\alpha}{2}\right)}{d_{hyd}} \tag{82}$$

7.4.10 Critical flow rate

The critical flow rate Q_c is the flow rate at which the velocity equals the critical velocity V_c.

Pipe

$$Q_c = \frac{V_c d_i^2}{24.51} \tag{83}$$

Annulus

$$Q_c = \frac{V_c \left(d_h^2 - d_p^2\right)}{24.51} \tag{84}$$

7.4.11 Friction factor

Pressure loss in pipes and annuli is proportional to the Fanning friction factor f which is a function of generalized Reynolds number, flow regime, and fluid rheological properties.

7.4.11.1   Laminar-flow friction factor

Laminar-flow friction factors f_{lam} for pipes and concentric annuli are combined into a single relationship when using the generalized Reynolds number N_{ReG} defined in 7.4.9.1.

$$f_{lam} = \frac{16}{N_{ReG}} \tag{85}$$

7.4.11.2   Transitional-flow friction factor

An empirical equation consistent with critical Reynolds number N_{CRe} defined in 7.4.9.2 can be used to determine transitional-flow friction factor f_{trans}.

$$f_{trans} = \frac{16 N_{ReG}}{N_{CRe}^2} \tag{86}$$

7.4.11.3   Turbulent-flow friction factor

The Blasius form of the turbulent-flow friction factor f_{turb} for non-Newtonian fluids is a function of generalized Reynolds number N_{ReG} and rheological parameter n_p. Constants a and b are based on curve fits of data taken on power-law fluids. [59]

$$f_{turb} = \frac{a}{N_{ReG}^b} \tag{87}$$

where

$$a = \frac{\log_{10}(n_p) + 3.93}{50} \tag{88}$$

$$b = \frac{1.75 - \log_{10}(n_p)}{7} \quad (89)$$

a) Pipe roughness

Pipe roughness elevates the friction factor in fully developed turbulent flow; however, relative roughness for most wellbore geometries is low, and Reynolds numbers in pipes and annuli rarely reach the high values where effects of roughness are most significant.[1]

b) Drag Reduction

Viscoelastic fluids in turbulent flow exhibit lower frictional factors and pressure losses, and delayed onset of turbulence.[53] This drag-reduction phenomenon can be observed in the field as a greatly reduced pump pressure when circulating certain clean, polymer fluids. The reductions in pressure loss can be very significant and values of >70% reduction have been observed for dilute polymer systems. Various analytical and empirical techniques have been proposed to model this behavior, but none have been universally adapted for drilling fluids.

7.4.11.4   Friction factor (all flow regimes)

The following method[48] can be used to determine friction factor, f, for any Reynolds number and flow regime. This technique involves an intermediate term f_{int} (based on transitional and turbulent-flow friction factors f_{trans} and f_{turb}) and laminar-flow friction factor f_{lam}.

$$f = \left(f_{int}^{12} + f_{lam}^{12} \right)^{1/12} \quad (90)$$

where

$$f_{int} = \left(f_{trans}^{-8} + f_{turb}^{-8} \right)^{-1/8} \quad (91)$$

7.4.12 Frictional pressure loss

Frictional pressure losses in the drillstring and annulus are equal to the sum of the losses in the individual segments described in Subclause 7.4.1. The Fanning equation is used to calculate incremental pressure losses; however, the various parameters should be defined for each segment in the drillstring and annulus.[1]

Pipe

$$P_{ds} = \Sigma \frac{1.076 \rho_p V_p^2 f\ L}{10^5 d_i} \quad (92)$$

Annulus

$$P_a = \Sigma \frac{1.076 \rho_a V_a^2 f\ L}{10^5 d_{hyd}} \quad (93)$$

7.4.12.1   Eccentricity

Drillstring eccentricity e in directional wells reduces annular pressure loss in laminar and turbulent flow. A widely used industry method[45] to estimate this reduction involves multiplication of concentric-annulus pressure loss in each segment by an empirically derived ratio R_{lam} or R_{turb}, depending on flow regime. Eccentricity e is defined as the displacement of the radii divided by the difference in radii. The value of e is 0 for a concentric annulus and 1.0 for a fully eccentric annulus.

$$R_{lam} = 1.0 - 0.072\frac{e}{n}\left(\frac{d_p}{d_h}\right)^{0.8454} - \frac{3}{2}e^2\sqrt{n}\left(\frac{d_p}{d_h}\right)^{0.1852} + 0.96e^3\sqrt{n}\left(\frac{d_p}{d_h}\right)^{0.2527} \tag{94}$$

$$R_{turb} = 1.0 - 0.048\frac{e}{n}\left(\frac{d_p}{d_h}\right)^{0.8454} - \frac{2}{3}e^2\sqrt{n}\left(\frac{d_p}{d_h}\right)^{0.1852} + 0.285e^3\sqrt{n}\left(\frac{d_p}{d_h}\right)^{0.2527} \tag{95}$$

7.4.12.2   Laminar-flow pressure loss (special case)

Substitution of the laminar-flow friction factor f_{lam} (defined in Subclause 7.4.11.1) into the general equations (defined in Subclause 7.4.12) yields simplified relationships for laminar-flow pressure loss that also can be derived by force-balance analysis.[1] The individual parameters should be defined for each well segment.

Pipe

$$P_{ds} = \Sigma\frac{\tau_w L}{300d_i} \tag{96}$$

Annulus

$$P_a = \Sigma\frac{\tau_w L}{300d_{hyd}} \tag{97}$$

7.4.12.3   Breaking circulation (special case)

Laminar-flow pressure-loss equations in 7.4.12.2 can be used to estimate the pressure required to break circulation by substituting the fluid's 10-min gel strength G_{10m} for the yield stress τ_y under no-flow conditions. The G_{10m} value could represent an average for the entire well, or preferably could be adjusted for temperature and pressure if data are available.

Pipe

$$P_{ds} = \Sigma\frac{G_{10m}L}{300d_i} \tag{98}$$

Annulus

$$P_a = \Sigma\frac{G_{10m}L}{300d_{hyd}} \tag{99}$$

7.4.13 Special considerations

7.4.13.1   Tool joints

Tool joints can affect frictional pressure losses in the drillstring and annulus for several reasons, the most obvious of which is the diameter difference that can be included as a lumped parameter. For internally constricted tool joints, drillstring pressure loss can increase due to contraction and expansion effects as fluid enters and exits the tool joints.[50] Also, if full turbulence is achieved in the tool joint, the drillpipe joint may be too short to allow complete fluid recovery. Field data support that this can result in the elevation in the turbulent flow friction factor.[16]

7.4.13.2   Drillstring rotation

Drillstring rotation invariably increases annular pressure loss in the field, especially in directional and slimhole wells. Unfortunately, relationships are not readily available that consider combined effects of rotation, non-Newtonian fluid behavior, eccentricity, and hydrodynamic/drillstring instabilities. Part of the pressure increase in directional wells may be attributed to cuttings or sagged density material incorporated into the main flow stream. Most hydraulics studies on the subject have focused on slimhole geometry where narrow annular clearances can magnify the effects of rotation.[46]

7.4.13.3   Coiled tubing

Frictional pressure losses for coiled tubing on the reel are higher than for straight tubing due to imposed secondary flows.[51] A number of correlations have been published to compensate for this effect by adjusting friction factors in laminar and turbulent flow.[52] However, most of these modifications are empirically derived and are difficult to generalize due to their high sensitivity to drilling fluid characteristics.

7.5   Bit pressure loss

7.5.1   Pressure loss through bit nozzles P_b is based on a kinetic energy change. Drilling fluid density through the bit nozzles ρ_b can be replaced by surface drilling fluid density ρ_s for conventional wells. If downhole tools include provisions for fluid bypass, flow rate through the nozzles Q should be adjusted accordingly.

$$P_b = \frac{\rho_b \, Q^2}{120242 \, C_v^2 \, TFA^2} \tag{100}$$

7.5.2   Total fluid (nozzle) area

Total fluid area TFA is proportional to the sum of the squares of the various nozzle diameters. By convention, nozzle diameters d_n are defined in 1/32 in.

$$TFA = 0.00076699 \, (d_{n1}^2 + d_{n2}^2 + ...) \tag{101}$$

7.5.3   Jet nozzle discharge coefficient

The discharge coefficient C_v varies with the diametric ratio (output diameter/input diameter) and the fluid Reynolds numbers passing through the nozzles.[54] There is significant evidence to update the long-standing C_v value of 0.95 to 0.98, given the flow rates, drilling fluid densities, and nozzle ratios typical to oilfield operating conditions.

$$C_v = 0.98 \tag{102}$$

In field and laboratory test the flow not only through the nozzle but also the flow past the nozzle is considered when determining C_v. This results in a discharge coefficient of $C_v = 1.03$ for roller cone bits[55] The design of the bit has in this case an impact on the discharge coefficient. Especially for PDC bits a single C_v has not been determined yet. The reported C_v ranges between 0.89 and 0.97. Therefore, a final recommendation for the discharge coefficient considering the flow past the nozzle cannot be made. Further tests are necessary to resolve the issue.

7.6   Downhole-tools pressure loss

7.6.1   Bottomhole assemblies, logging-while-drilling tools, and other downhole tools invariably increase pressure losses inside the drillstring and annulus.

7.6.2   Miscellaneous downhole equipment

Pressure losses through turbines, thrusters, jars, and MWD tools depend strongly on the internal design of the individual tools. Vendor-published pressure losses are usually based on flow loop or rigsite tests run over a limited range of conditions. Pressure losses inside of these tools generally are in turbulent flow, so that data from suppliers can by adjusted to provide a closer fit to well conditions. These adjustments should include a drilling fluid-density correction determined by dividing the drilling fluid density at the bit ρ_b by the reference drilling fluid density provided by the tool manufacturer.

$$P_{dt} = \frac{\rho_b}{\rho_{dt}} C_{dt} Q^{1.86} \tag{103}$$

7.6.3 Positive-displacement motors (PDMs)

Pressure drop of PDMs consists of the no-load pressure drop (bit off-bottom) and the operating pressure drop (added to the no-load pressure drop when the bit is on bottom and cutting rock). No-load pressure drop is a function of flow rate, drilling fluid density, and PDM characteristics. Operating pressure drop of a PDM is not strongly dependent on flow rate. It is determined by bit torque which is the product of weight-on-bit and bit aggressiveness. Operating pressure drop is best obtained from the PDM manufacturer's data handbook.

7.7 Choke-line pressure loss

7.7.1 Single line

Circulating through the choke line on wells with subsea BOP stacks imposes additional pressure on the annulus. Pressure-loss calculations for the pipe in Subclause 7.4 can be used to model choke-line losses.

7.7.2 Multiple lines

Choke and kill lines sometimes are used simultaneously to reduce back pressure on the annulus during well-control operations. For two lines with identical diameters, return flow would be split equally, and the resulting net pressure loss would be roughly only one-fourth of that through a single line.

7.8 Casing pressure

7.8.1 Casing pressure is the surface back pressure applied on the annular side under both static and dynamic conditions.

7.8.2 Casing pressure while shut in

In a well-control situation, casing pressure is the shut-in casing pressure *SICP* and bottomhole pressure is the formation pressure P_f.

$$P_c = SICP = P_f - P_{ha} \qquad (104)$$

7.8.3 Casing pressure while circulating

Back pressure during circulation can be applied by a choke or by a rotating head. These pressures depend on drilling fluid density, flow rate and orifice or conduit geometry.

7.9 Equivalent circulating density (ECD)

The *ECD* at total depth is equivalent to the bottomhole pressure equation (from Subclause 7.2.3) expressed as a drilling fluid-density gradient. Equations presented here can be used to calculate *ECD* at any depth if ESD_a is defined at the depth of interest D_v and the annular pressure loss P_a is calculated from surface to D_v. For conventional wells, ρ_s can substitute for ESD_a. Cuttings concentration c and cuttings specific gravity ρ_c can be determined from equations presented in Clause 9.

Without drilled cuttings

$$ECD = ESD_a + \frac{P_a + P_{cl} + P_c}{0.052 D_v} \qquad (105)$$

With drilled cuttings

$$ECD = (1-c)ESD_a + 8.345\,\rho_c + \frac{P_a + P_{cl} + P_c}{0.052 D_v} \qquad (106)$$

8 Swab/surge pressures

8.1 Principle

8.1.1 The purpose of this subclause is to deliver the equations and procedures to calculate the changes in hydrostatic pressure which are created due to the movement of the pipe in a liquid filled wellbore.

8.1.2 The pressure changes can be induced due to several mechanisms.

a)   Frictional pressure loss due to the displacement of the fluid

b)   Pressure changes generated due to the inertia of the drilling fluid column

c)   Pressure loss due to breaking the drilling fluid gel

8.1.3 The pressure change due to the string movement is influenced by the following:

a)   Geometry of the well

b)   Speed of the string (drillstring or casing)

c)   Fluid properties as a function of pressure and temperature

8.1.4 Neglected in this subclause are the compressibility of the drilling fluid, the elasticity of the string, and the elasticity of the well.

8.2 Controlling parameters

8.2.1 String speed

The string speed should be the maximum speed of the string while tripping. Using the average string speed will underestimate the swab and surge effects.

8.2.2 Displaced fluid

8.2.2.1   The displaced fluid is a function of the geometry of the well and the string, and the tripping speed.

8.2.2.2   Distinction needs to be drawn between the situation when the string is open at the bottom-end or closed. In closed-mode all of the fluid has to be displaced into the annulus, while in open-mode some of the fluid will flow inside and some outside the string.

8.2.2.3   Closed pipe actually occurs only when drillpipe floats or conventional float collars are used during a casing run. Running a drillstring with a downhole motor can be considered as closed-mode tripping when no float valve is used on top of the motor.

8.2.3 Compressibility

The compressibility of the fluid leads to a reduction in the total volume of fluid to be displaced.

8.2.4 Clinging factor

The clinging factor is used to consider for the effect of relative motion between pipe and fluid. Tabulated and graphical values for various rheological models and laminar and turbulent flow are available in the literature.[61] A conservative estimate for the clinging factor C_g is a value of 0.45.

8.2.5 Effective velocity

8.2.5.1 The effective velocity is the combination of the velocity due to the displacement of the fluid and the relative motion between string and fluid. The resulting fluid velocity for closed-mode is:

$$V = \left(C_g + \frac{d_p^2}{d_h^2 - d_p^2} \right) V_p \tag{107}$$

8.2.5.2 The open-pipe case can be approximated with a simplified approach. It assumes that the fluid velocities in both string and annulus are equal. This can only be true if the pressures inside and outside the pipe are equal and if the cross sections are the same. The fluid velocity in this case is then:

$$V = \left(C_g + \frac{d_p^2 - d_i^2}{d_h^2 - d_p^2 + d_i^2} \right) V_p \tag{108}$$

8.2.5.3 The accurate approach to determine the tripping pressures in open-mode should consider the real pressure-loss characteristics of each flow conduit and calculate the flow rate in each path by equalizing the pressure losses inside and outside the string.

8.2.6 Pumps on

The general expression for the fluid velocity in the case of surge and swab is $V = V_a \pm V_d \pm V_p$, where V_a is the velocity in the section annulus resulting from pump flow, V_d is the velocity component due to the string displacement, and V_v is the velocity component due to the relative motion of the string. The positive sign is for surge; and the negative sign for swab.

8.2.7 Drilling fluid properties as a function of pressure and temperature

The drilling fluid properties can be considered for the swab and surge analysis following the procedures developed in Clause 6.

8.2.8 Frictional pressure loss

See Clause 7 for calculation details including laminar and turbulent flow, as well as the effect of drillstring eccentricity.

8.2.9 Acceleration pressure drop

The component of surge pressure due to the inertia of the drilling fluid is caused by the tendency of drilling fluid to resist change in motion. For closed pipes, the inertial pressure surge can be obtained from the following equation:

$$\Delta p = \frac{L\rho\left(d_p^2\right)a_p}{g\left(d_h^2 - d_p^2\right)} \tag{109}$$

For open pipes the tripping pressure is

$$\Delta p = \frac{L\rho\left(d_p^2 - d_i^2\right)a_p}{g\left(d_h^2 - d_p^2 + d_i^2\right)} \cdot \qquad (110)$$

These equations assume that the fluid is incompressible and will therefore over-predict the inertia effect. A suggested estimate for pipe acceleration is 4.5 ft/s².

Allowing for drilling fluid compressibility, pipe elasticity and rock compressibility will lead to more realistic estimates. An estimate for the inertial pressure drop considering a completely rigid (inelastic) string and borehole, but considering the drilling fluid compressibility:

$$\Delta p = \frac{\rho V_{wave}\Delta V}{g} \qquad (111)$$

with

$$V_{wave} = \sqrt{\frac{619}{c_e\rho}} \cdot \qquad (112)$$

A general expression for the velocity of propagation is:

$$V_{wave} = \sqrt{\frac{g}{\rho(C_f + B)}} \qquad (113)$$

with C_f (3×10^{-6} 1/psi or 0.435×10^{-9} 1/Pa) the fluid compressibility and B the expansibility of the conduit.

8.2.10 Breaking the gel

The surge pressure required to break the gel strength may be estimated using the definition of shear stress as a function of pressure.

$$P_a = \Sigma \frac{G_{10m}L}{300d_{hyd}} \qquad (99)$$

The pressures required to break the gel are normally lower than the surge pressures at peak velocities.

8.3   Closed-string procedure

8.3.1   The procedure to be followed when calculating the pressure change due to tripping and their effect on the overall hydrostatic pressure is outlined below. To maintain the equivalent drilling fluid density beyond the limit for pore or fracture pressure gradient, it is necessary to determine a safe trip speed. A safety margin can be used to ensure the maximum trip speed is still within the allowable limit.

8.3.2   Define the point of interest

The point of interest (POI) is the position in the well which is most critical with respect to the pressures while tripping. It can be the casing shoe, TD or a known weak zone along the open hole.

8.3.3   Divide well in sections

The well needs to be divided into short sections to account for the pressure loss due to the geometry and the downhole fluid properties (see Subclause 6.3.4.2).

8.3.4 Determine the drilling fluid properties

The drilling fluid properties can be determined using the procedures described in Clauses 5 and 6.

8.3.5 Loop around speed

Select a range of speeds to be evaluated.

8.3.6 Choose a trip speed

8.3.7 Loop around bit depth

Set a bit depth.

8.3.8 Calculate pressures

Determine the fluid to be displaced.
Assume laminar flow.
Determine the clinging factor.
Determine the effective velocity.
Calculate the frictional pressure loss.
Repeat the calculation in 8.3.5, 8.3.6 and 8.3.7, if the flow is not laminar.
Calculate the total pressure at the point of interest.
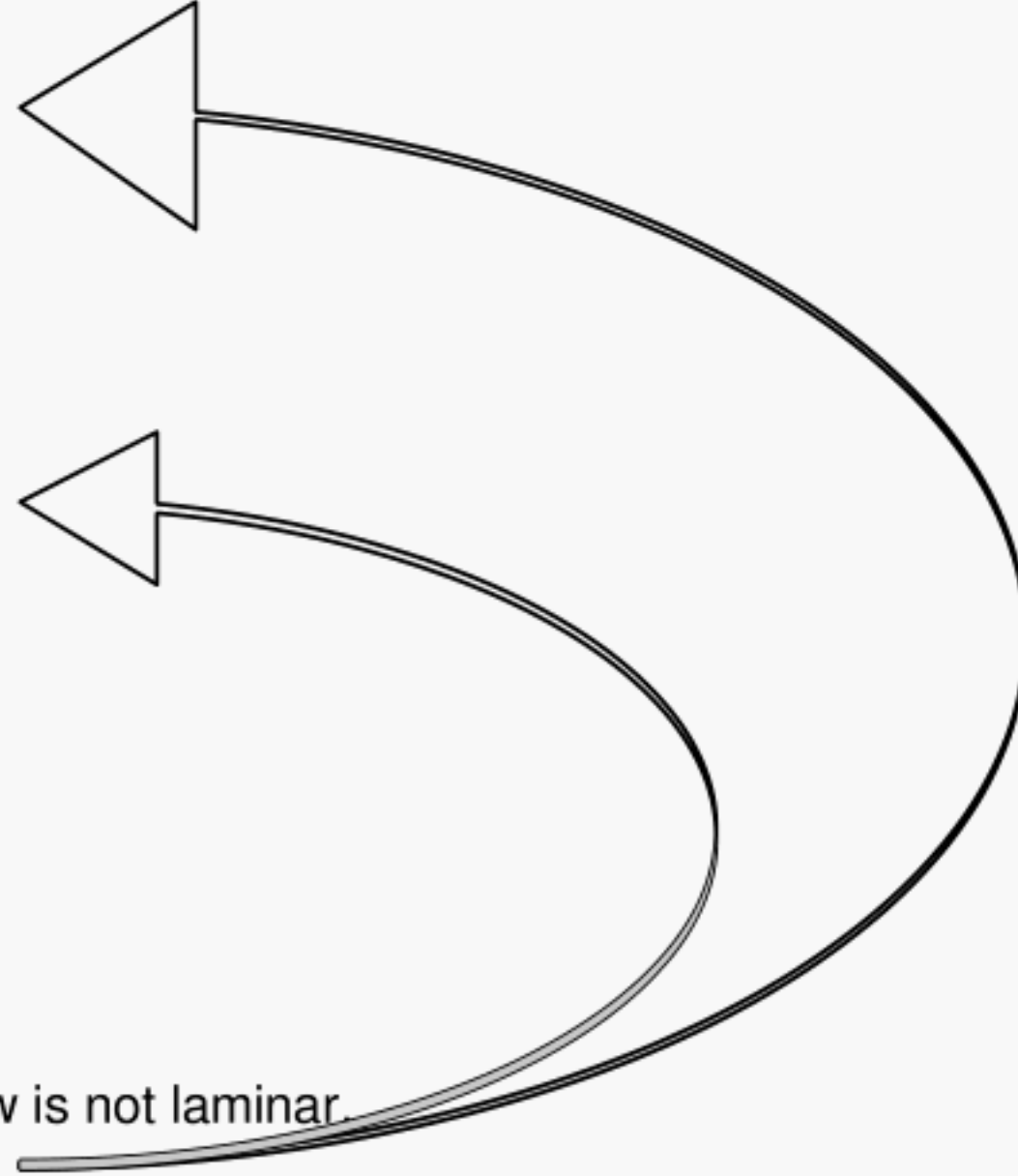
8.3.9 Transform the pressure to EMW

Calculate *EMW*.

8.3.10 Compare EMW with fracture gradient

The direct calculation of the maximum allowable speed based on the known maximum *EMW* is only possible for very simple well geometries. This is due to the iterative procedures needed to conduct the calculation.

8.4 Open-string procedure

The analysis for an open-string configuration requires the determination of the flow distribution between the annulus and the string. After an initial guess is made for the flow distribution, the pressure due to tripping can be calculated for each flow conduit. The flow distribution needs to be adjusted till the pressure loss in each path is equal.

8.5 Transient swab/surge analysis

Tripping pressures are not steady-state for the several reasons. The pipe is set in motion and then brought to a stop as soon as a complete joint of casing or a stand of pipe is run-in or pulled from the hole. Further, the fluid is compressible, and so are the various conduits through which it flows under pressure. The unsteady flow causes pressure transients or surges that propagate in the fluid at the speed of sound. Fully dynamic surge models are more complex and require more computer resources than steady-state surge models.

9   Hole cleaning

9.1   Description of the challenge

9.1.1   Removal of cuttings from the wellbore is essential to the drilling operation. Failure to effectively transport the cuttings can result in a number of drilling problems including: excessive overpull on trips; high rotary torque; stuck pipe; hole pack-off; excessive ECD's and cuttings accumulation; formation break-down; slow rates of penetration; and difficulty running casing and logs.

9.1.2   The key to optimizing hole cleaning is integrating a good well plan with good drilling fluid properties and good drilling practices. These all need to be supported by careful monitoring and observation at the rig site.

9.1.3   Successful hole cleaning relies upon integrating optimum drilling fluid properties with best drilling practices. When difficulties are encountered, it is essential to understand the nature and causes of the problem. This allows options to be focused to determine the most appropriate actions. Poor hole cleaning will result in high cuttings loading the annulus. This can be detected using downhole annular pressure measurement. When circulation stops these cuttings can fall back and pack-off the bottomhole assembly (BHA). When packing-off occurs, the flow rate is too low or the well has not been circulated for sufficient time.

9.2   How cuttings are transported

9.2.1   Vertical versus high angle

9.2.1.1 In deviated wells, cuttings tend to settle on the low side wall and form cuttings beds. These cuttings are often transported along the low side of the hole either as a continuous moving bed or in separated beds/dunes. Figure 5 is a schematic representation of the transport mechanisms for a range of well inclinations.
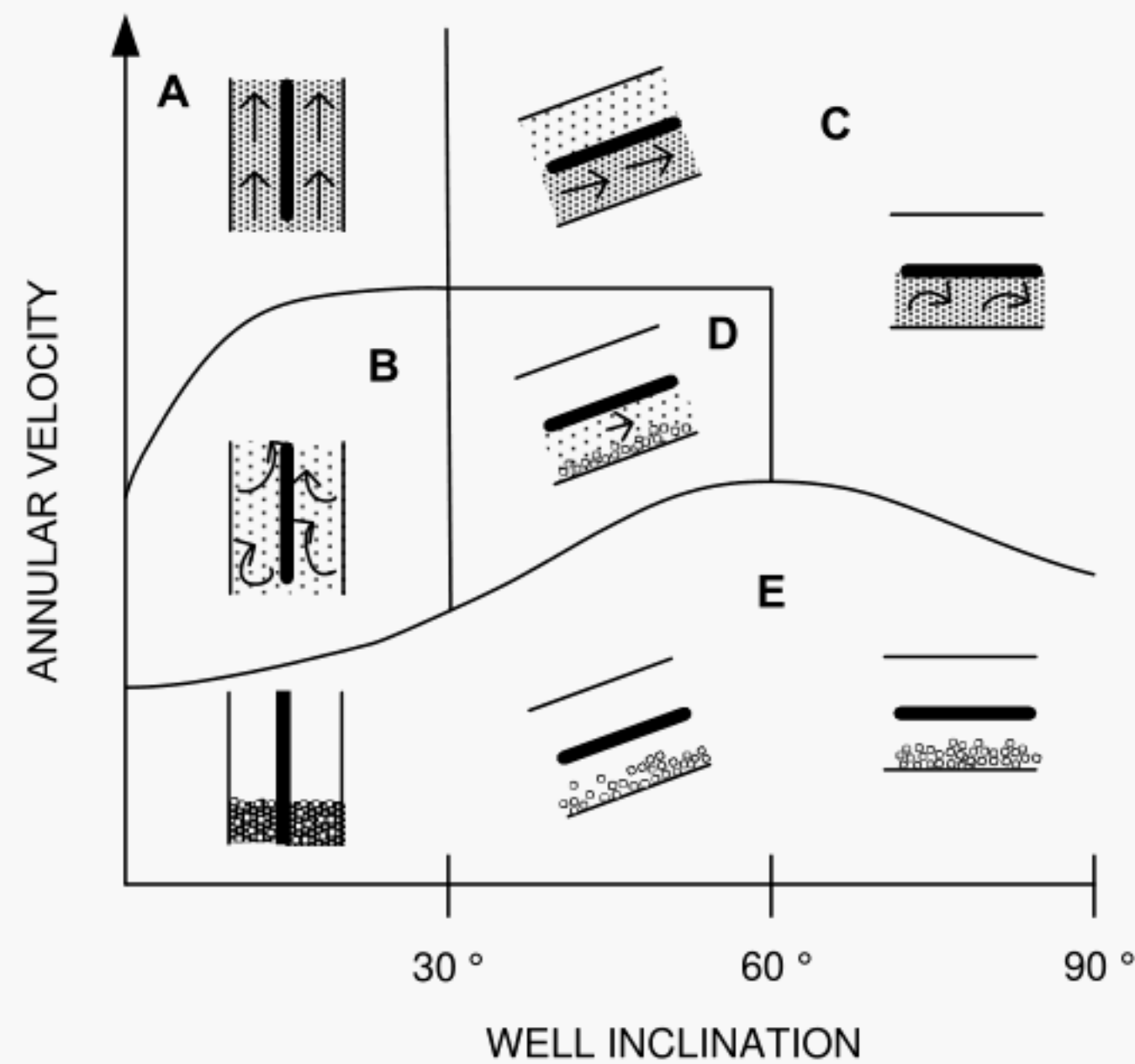
KEY

A   Zone 1 - Efficient hole cleaning

B   Zone 2 - Slow cuttings removal

C   Zone 3 - Good hole cleaning with moving cuttings bed

D   Zone 4 - Some hole cleaning – cuttings bed formed

E   Zone 5 - No hole cleaning

Figure 5—Cuttings transport mechanisms in vertical and deviated wells

9.2.1.2   In holes inclined less than 30°, the cuttings are effectively suspended by the fluid shear and beds do not form (Zones 1 and 3). For such cases conventional transport calculations based on vertical slip velocities are applicable. For these shallow angles, annular velocity requirements are typically 20-30% in excess of vertical wells. Beyond 30°, the cuttings form beds on the low side of the hole which can slide back down the well, causing the annulus to pack-off. Cuttings which form on the low side of the hole can either move en-masse as a sliding bed (Zone 4), or alternatively may be transported at the bed/drilling fluid interface as ripples or dunes (Zone 2). Drillpipe movement (rotation and reciprocation) can help mechanically disturb the cuttings beds and distribute them in the faster flowing drilling fluid towards the high side of the hole. Flow patterns in the annulus depend strongly upon flow rate and drilling fluid rheology. Low viscosity fluids with low yield points tend to promote turbulence and cuttings saltation. High-viscosity fluids with high yield points increase the fluid drag force and cause the cuttings beds to slide.

9.2.1.3   The ideal zones for good cuttings transport are Zones 1 and 2. Zone 5 is virtually a guarantee of tight hole problems.

9.2.2 Forces acting on cuttings

In vertical and near vertical section the cuttings are effectively carried in suspension. The annular fluid velocity acts to overcome the cuttings settling force and there is a net upward movement of the cuttings. In a high-angle well, the gravitation force acting on the cuttings tends to cause the formation of a cuttings bed on the low side of the hole. The annular fluid velocity creates a drag force which tends to move the cuttings bed along the wellbore and a fluid lift force that tend to move the cuttings away from the wellbore and towards the higher velocity flow stream.

9.3 Review of modeling approaches

9.3.1 Vertical and low-inclination wells

Hole cleaning in vertical and near-vertical wells is generally modeled by comparing the annular fluid velocity with the slip velocity of the cuttings. Providing the annular velocity of the fluid is higher than the cuttings slip velocity, there will be a net upward velocity of the cuttings. The rate at which cuttings accumulate in the annulus will be a function of this net upward velocity of the cuttings and the rate at which cuttings are produced (a function of bit size and penetration rate).

The in-situ cuttings concentration C_a is given by:

$$\text{Ca} = \frac{(D_b)^2 ROP}{448.4 \ Q \ R_t}$$

(114)

The Transport Ratio R_t is defined by:

$$R_t = \frac{V_u}{V_a}$$

(115)

where

V_u is the net upward velocity of the cutting defined by:

$$V_u = V_a - V_s$$

(116)

The slip velocity of the cutting V_s can be estimated by a number of empirical calculations. A simple method is recommended here[62]. For particle Reynolds number > 100, the flow is assumed turbulent and the cuttings slip velocity V_s is given by:

$$V_s = 2.19\left[\frac{h(\rho_c - \rho)}{\rho}\right]^{\frac{1}{2}}$$

(117)

where

h is the thickness of cutting in in.

ρ_c is the density of cutting in g/cm^3

ρ is the drilling fluid density in lb$_m$/gal

The particle Reynolds number is calculated using an empirical relation for shear stress due to particle slip:

$$\tau_s = 7.9[h(8.345\rho_c - \rho)]^{\frac{1}{2}}$$

(118)

43

The shear rate corresponding to the shear stress is determined from the fluid rheogram. The apparent viscosity is then calculated at this shear rate:

$$\mu_e = \frac{479\tau_s}{\gamma} \tag{119}$$

If the particle Reynolds number is < 100, the following correlation is used to calculate the cutting slip velocity:

$$V_s = 0.0203\tau_s \left[\left(\frac{d_c\gamma}{(\rho)^{\frac{1}{2}}} \right) \right]^{\frac{1}{2}} \tag{120}$$

A final check is then conducted on the particle Reynolds number. If $N_{Rep} > 100$, then the slip velocity is calculated using Equation (117). If the particle Reynolds number < 100, then the slip velocity is calculated using Equation (120). The particle Reynolds number is given by:

$$N_{Rep} = \frac{928\,\rho\,V_s\,d_c}{\mu_e} \tag{121}$$

9.3.2 High-angle wells

Analytical and numerical methods have been used successfully to model fluid flow in eccentric annuli. In practice, the complexity of cuttings transport in deviated wells rules out the use of pure analytical approaches to modeling heterogeneous cuttings/drilling fluid mixtures. Most modeling attempts to date are based on purely empirical methods of using laboratory data to fit physically-based models. The transition from low angle to high angle is typically considered to be 30°. At angles above 30°, the cuttings tend to move as beds rather than discrete cuttings.

9.4 Recommended calculation methods

9.4.1 Vertical and low-angle wells

9.4.1.1 At the drilling rig there are three drilling fluids-related "hole-cleaning" variables can be controlled: drilling fluid density, viscosity of the drilling fluid, and annular velocity. Increasing any one of these variables improves hole cleaning. An empirical equation has been developed from field observations to predict good hole cleaning.

9.4.1.2 The Carrying Capacity Index (CCI) has been developed to describe hole cleaning[64]:

$$CCI = \frac{\rho\,k\,V_a}{400,000} \tag{122}$$

9.4.1.3 Good hole cleaning is expected when *CCI* is equal to or greater then 1. The cuttings are sharp-edged and generally large. When *CCI* has a value of 0.5, the cuttings are rounded and generally very small. When *CCI* has a value of less than 0.3, the cuttings can be grain-sized.

9.4.1.4 The viscosity value used in this equation is the consistency value k_1 calculated at 1 s^{-1} using the power law:

$$\tau = k\,\gamma^n \tag{123}$$

where

   τ is the shear stress,

γ is the shear rate, and

$$k_1 = [511]^{(1-n_p)}[PV + YP]$$

(124)

and,

$$n = 3.32\log_{10}\frac{2PV + YP}{PV + YP}$$

(125)

9.4.1.5 A summary of evaluating carrying capacity in vertical and near wells:

a)   Use Equation (124) to determine value of k_1 from *PV* and *YP*.

b)   Use flow rate and maximum hole diameter to determine annular velocity.

c)   Determine CCI using Equation (122)

d)   If CCI is less than 1.0, or the cuttings discharged by the main shale shaker have rounded edges, calculate the yield point needed to increase the carrying capacity

$$k_1 = \frac{400,000}{\rho V_a}$$

(126)

e)   Use solids removal system to attempt to lower *PV*. This will have the effect of raising k_1.

9.4.2   High-angle wells

9.4.2.1   The model is based on the fluid forces acting on cuttings within a settled bed and is applicable to hole angles >30°. The model takes into account both lift and drag forces to predict the minimum flow rate required to prevent formation of stationary cuttings beds. The model was originally developed from flow loop data and has been validated in the field against numerous high-angle and horizontal wells[65]. Here the primary measure of good hole cleaning has been the absence of operational problems associated with poor hole cleaning.

9.4.2.2 The main features of the model are:

a)   allows for rheology and flow regime

b)   models washed-out hole

c)   assumes the drillpipe is rotated at 100 rpm

d)   predicts flow-rate requirements with changing ROP

9.4.2.3   The model demonstrates that either thick or thin fluids can be used to clean high-angle sections. Intermediate viscosity drilling fluids provide the worst conditions and should be avoided. In situations where ECD is not a limiting factor, high-viscosity fluids with high *YP/PV* ratios are preferred.
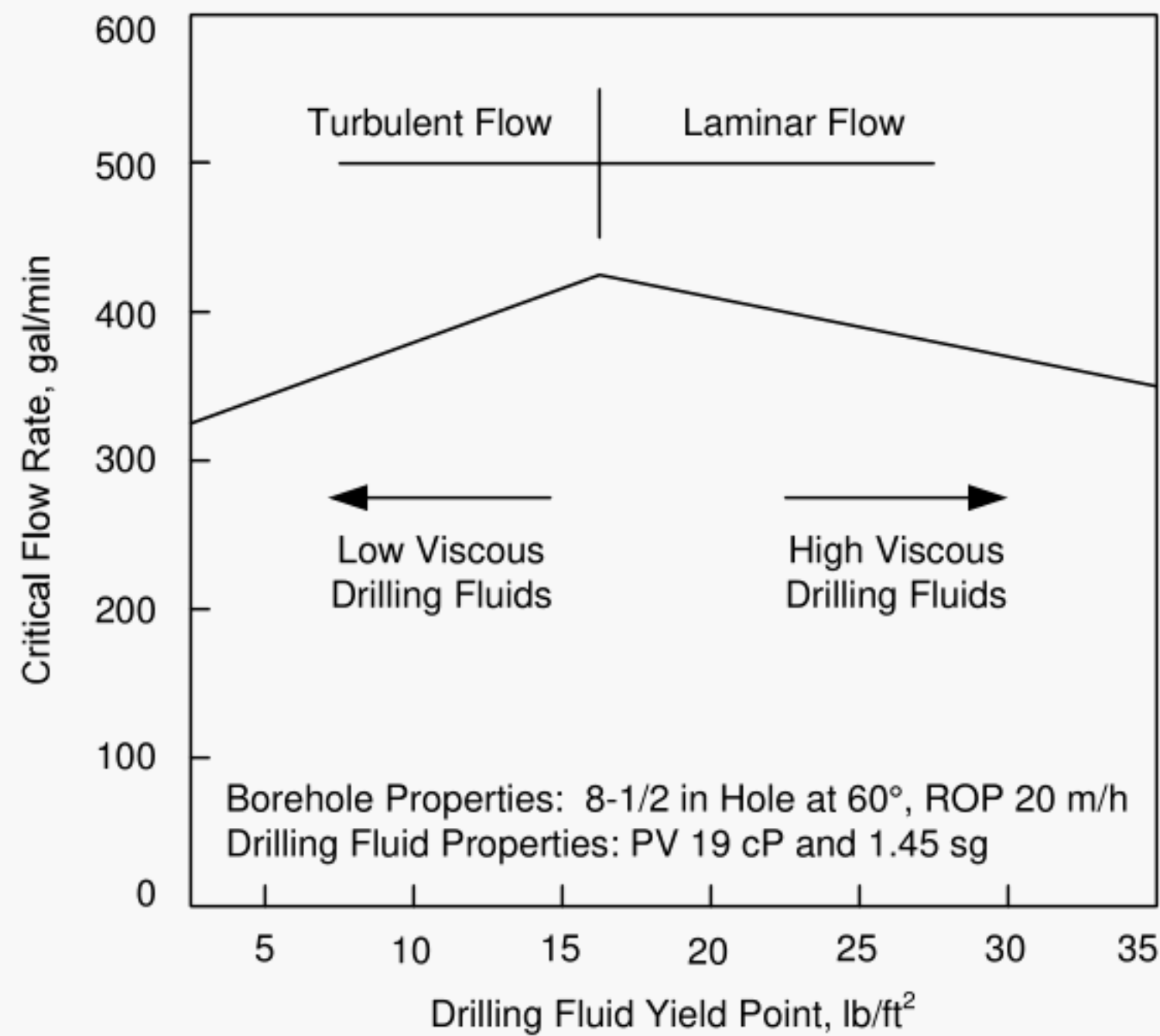
Figure 6— Effect of yield point on critical flow rate

9.4.2.4   Figure 6 shows how increasing the drilling fluid yield point causes the flow mechanism to change from turbulent to laminar. Intermediate values of *YP* should be avoided since they produce the worst conditions for cuttings transport. In general the higher *YP* (and hence laminar flow) regime is preferred because the higher viscosity drilling fluid provides better cuttings suspension and improved transport in the near vertical regions of the well.

9.4.2.5   Under conditions where ECD is a limiting factor, the use of thin fluids in turbulent flow should be considered. Thin fluids reduce annular frictional pressure losses, and hence result in lower ECD's. Turbulent flow in the annulus should be avoided with weakly consolidated formations due to the increased risk of hole erosion (see Clause 10). Extra care is also required with low viscosity drilling fluids due to the increased risk of barite sag.

9.4.2.6   A simple graphical method is recommended for estimating the optimum flow properties and flow rate to achieve adequate hole cleaning in high-angle wells. The charts below apply to 8 ½" hole sections. Similar charts for other 17 ½" and 12 ¼" hole sizes are available.[66]
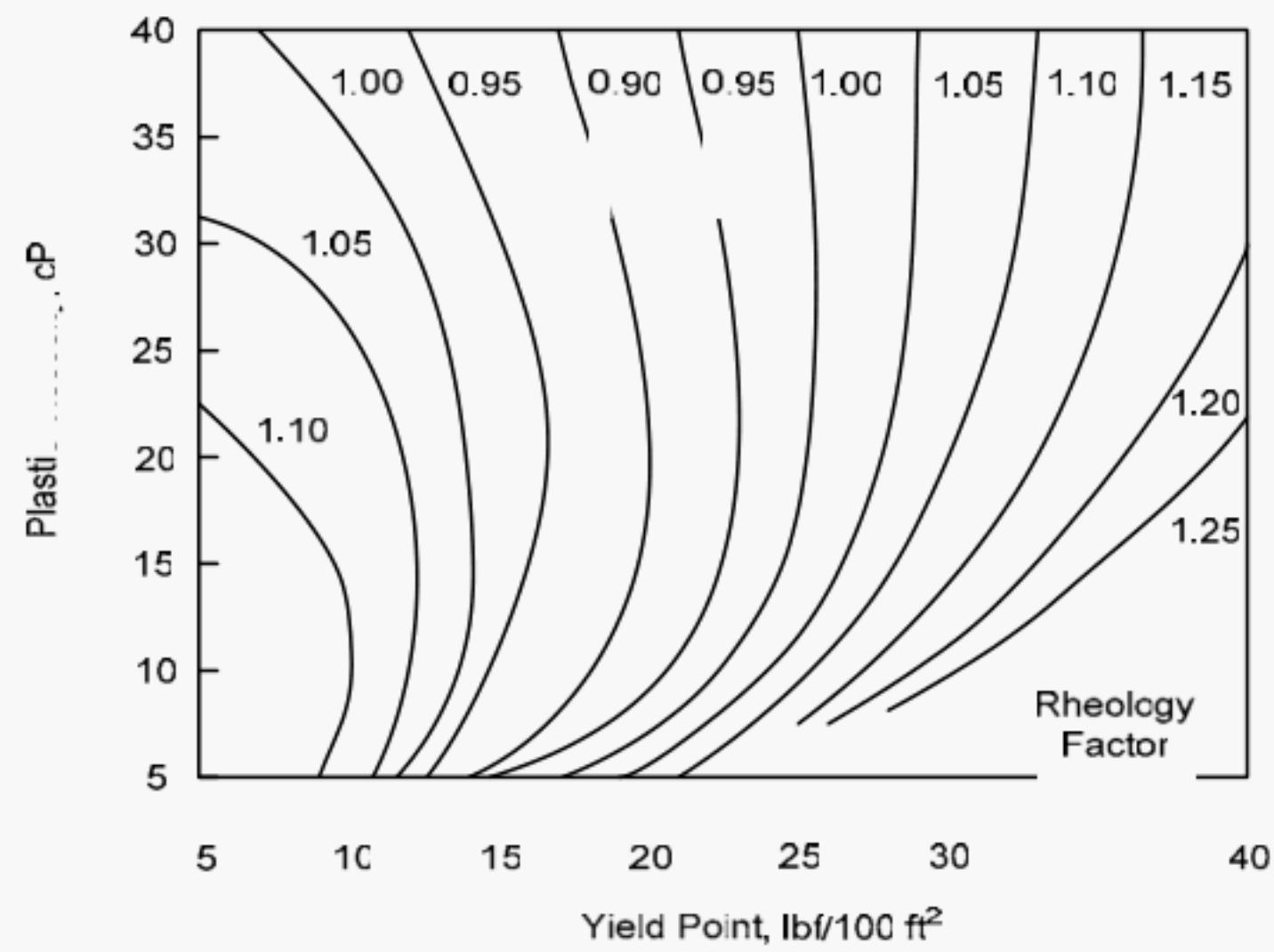
Figure 7— Rheology factor chart for 8-1/2 in. holes
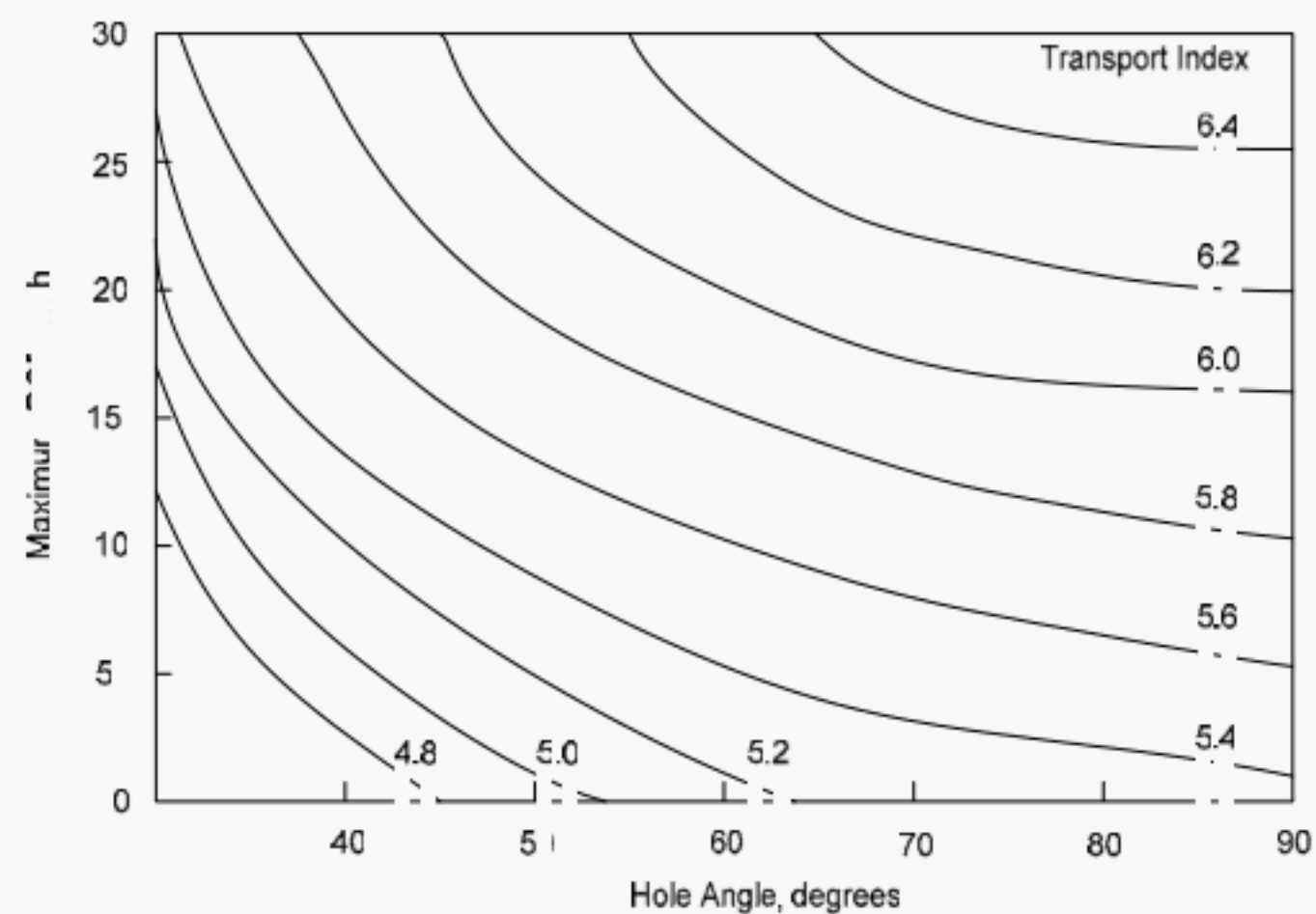
Figure 8— Hole-Cleaning Chart for 8-1/2 in. Holes

9.4.2.7   Recommended procedure:

a)   Enter the Rheology Factor chart with the appropriate values of *PV* and *YP* values at 120 °F and atmospheric pressure. Read the value of the Rheology Factor *RF*.

b)   Calculate the Transport Index *TI* based on the drilling fluid flow rate and drilling fluid density given by:

$$TI = \frac{Q \; \rho \; RF}{834.5}$$

(127)

c)   Enter the maximum Rate of Penetration *ROP* chart. With the value of Transport Index *TI* calculated from Equation (127) and the maximum hole angle, read the maximum *ROP* that can be sustained while still maintaining adequate hole cleaning.

9.4.3 Impact of drillpipe rotation

9.4.3.1 Movement of the drillpipe (rotation and/or reciprocation) will mechanically disturb cuttings beds and assist hole cleaning. Rotation is more effective since this helps equalize fluid velocities on the low and high side of the hole. The influence of drillpipe rotation is more pronounced in viscous drilling fluids and in smaller holes (<17-1/2 in.). In cases where the pipe is not rotated (*e.g.*, slide drilling), cuttings beds are more difficult to remove. Under these special circumstances, increased flow rate or changes in operation practices (*e.g.*, rotary wiper trips) will be necessary to improve hole cleaning. Rotary Steerable Systems (RSS) have proven very beneficial for improving hole cleaning in high-angle wells by eliminating the requirement for sliding.

9.4.3.2 The normal range of drillpipe rotational speeds is typically 90 to180 rpm (up to 120 rpm on-bottom, up to 180 rpm off-bottom). In practice, there needs to be a balance between good effects for hole cleaning versus possible detrimental effects (*e.g.*, vibration causing premature failures of downhole equipment). High rpm values should also be avoided in unstable formations since the string action can knock off loose sections of the wellbore. Limitations on downhole tool components (*e.g.*, downhole motors) can also restrict the maximum allowable rpm.

9.4.3.3 The above graphical method assumes that the drillpipe is rotated at 100 rpm. If the drillpipe is not rotated the significantly higher flow rate will be required to clean the hole. Alternatively, it may prove necessary to use remedial drilling practices to clean the hole after an extended period of slide drilling.

9.5 Recommended hole cleaning practices

9.5.1 Guidelines on viscous / dense pills

The properties for the drilling fluid in circulation should always be optimized to provide adequate hole cleaning. Under certain conditions, it may be necessary to supplement hole cleaning with limited use of viscous or weighted pills. Excessive use of pills should be avoided since they can contaminate the drilling fluid system. Generally a high-viscosity (and preferably high density) pill is effective at removing accumulated cuttings in shallow angle wells <30°. For wells above 30°, weighted pills are more effective. Generally, the pills will be formulated at 3 to 4 lb_m/gal above baseline drilling fluid density. The volume of the pills will be dictated by hydrostatic considerations, but typically the pill volume should be sized to give 400 ft annular height.

9.5.2 Circulation prior to tripping

9.5.2.1 No simple predictions are available for the rate at which cuttings are removed. Because the cuttings move more slowly than the circulating drilling fluid, it is essential that sufficient bottoms-up are circulated prior to tripping. A single bottoms-up is seldom sufficient to clean the hole of cuttings.

9.5.2.2 The minimum on-bottom circulation time prior to tripping will be influenced by hole size, inclination and flow history (*i.e.*, drilling fluid properties and flow rate). These factors will affect the height of any residual cuttings beds.

9.5.2.3 Before tripping, monitor the shakers to ensure the cuttings return rate is reduced to an acceptable background level. If available, use downhole annular pressure data to determine whether the ECD has leveled out to a minimum value.

9.5.3 Recommended drilling practices

It is important to recognize that the overall success of any hole-cleaning campaign is a combination of good planning and good execution. It is recommended that a set of appropriate drilling practices is developed to assist with execution and implementation. Table 5 provides guidance on the type of parameters and controls which may be used to provide assurance on best practices. Table 5 is not meant to be prescriptive nor fully exhaustive. It has been provided merely to acknowledge the importance of appropriate drilling practices and provide a suitable starting framework for an engineer planning an operation.

Table 5 —Example hole sections operational practices

Downhole Annular Pressure Monitoring	Real-time downhole annular pressure measurement will be the main focus for the effective hydraulic management throughout this hole section. It will indicate when preventative action or extra hole cleaning measures should be taken. Alarm point is when ECD reaches 0.2 lb_m/gal over the actual ECD prediction with cuttings loading. This ECD prediction should be derived from fingerprinting data for clean hole conditions and form following trends throughout the hole section. Hole conditions will have to be improved if the ECD rises above this 0.2 lb_m/gal indicating cuttings loading.
Flow rate	Numbers to be calculated using API RP13D or other chosen method.
Rotation	Maximum rpm based on drilling experience and hole conditions.
Connections	No backreaming as a standard procedure. Perform 2 surveys per stand (every 60 ft). Once stand down circulate for 5 min (so cuttings are above BHA), shut pumps off / pumps on, perform survey, make connection. Start rotation and pumps slowly to break gels.
ROP	Maintain steady ROP and control instantaneous drill rate to avoid overloading annulus with cuttings. Maximum instantaneous ROP is 150 ft/h. Be aware of overloading the annulus. Use downhole pressure measurements to detect increases in ECD.
Monitor Trends	Watch trends between surface versus downhole parameters (Weight on Bit, Temperature and Torque). Record pick-up, slack-off and rotating weights
Cuttings Monitoring	Monitor the amount, shape and size of cuttings over the shakers. Small rounded cuttings indicate that cuttings have been spending extended periods downhole being reground by the drillstring. Quantitatively measure the cuttings return rate at the shakers compared with the volume predicted from ROP. Have all data visible on a board in shaker house and report any major changes immediately to the Driller. Watch for any sign of cavings over the Shakers. Report immediately.
Critical Drilling fluid Properties	The drilling fluid properties are critical to the hydraulics and ECD control needed to drill this section. Trend graphs of the critical properties (for all tests) to be reviewed daily. If necessary, stop and condition the drilling fluid before continuing to drill. Record any seepage losses they often indicate the start of a differential sticking problem. Record Drilling fluid Density in and out of the hole every 15 min and logged. Perform a minimum two drilling fluid checks per day. Condition drilling fluid properties prior to running casing and cementing.
Hole Cleaning Viscous / LCM Pills	Pills will only be pumped on an indication from annular pressure measurement or a mechanical downhole problem. Stop and circulate, 3 times bottoms-up with slow pipe movement. Pill and sweep information requires to be recorded. High density pills (~3 lb_m/gal over baseline drilling fluid density) will be used. The resulting increase in drilling fluid density from these pills should be monitored with the projected weight up schedule. These pills will give 400 ft of annular length which equates to a total volume of approximately 50 bbl. Only pump a pill after the hole has been conventionally cleaned with circulation and rotation, do not overload the annulus with cuttings. Use annular pressure measurement for ECD control while pumping. Monitor the benefits of the pills using downhole annular pressure measurement. Pills should be pumped at the beginning of a stand. Only allow one pill in the hole at any one time. Check shakers and numbers of bottoms up required to circulate pills out. Pump the pill all the way round the system without any stoppages or connections. All pills at discretion of Company Drilling Supervisor.
Wiper Trips	Only perform wiper trips as a means of monitoring hole condition. If the hole dictates, short trip at TD to make sure we have enough drilling fluid density margin to come out of the hole. Use annular pressure measurement and trend analysis to indicate that a cleaning trip is needed.
Hole Pack-off	Stop pumping, work pipe slowly until circulation is established. Review Company Stuck Pipe Policy and Manual

9.6   Impact of cuttings loading on ECD

9.6.1   Vertical and low-angle Wells

Because cuttings have a higher density than the drilling fluid, any cuttings which are suspended by the drilling fluid in the annulus will add to the effective drilling fluid density and hence increase ECD. The equation describing this increase in ECD can be found in Clause 7.

9.6.2   High-angle wells

Cuttings held in suspension will contribute to an increase in effective drilling fluid density in the same manner as for a vertical well. Cuttings which settle on the low side of the hole are supported by the wellbore and do not add to the effective hydrostatic pressure.

9.6.3   Calculation methods

9.6.3.1 It is possible to estimate the cuttings contribution to drilling fluid density for a simple vertical well. This is based on the cuttings feed rate, the drilling fluid flow rate and the Transport Ratio defined in Equation (127). The Transport Ratio is a measure of how fast the cuttings are carried in the drilling fluid compared with the annular fluid velocity. If no slip occurs then the Transport Ratio is unity. The Transport Ratio can be regarded as the reciprocal of the number of bottoms-up that are required to bring cuttings to the surface.

9.6.3.2 In the case of a deviated well no simple method exists to calculate the cuttings contribution to ECD. It is, however, possible to use results from downhole annular pressure measurements and estimate the cuttings contribution to static drilling fluid density. These data are normally only available from the memory data since the pumps must be off to record the static drilling fluid density.

9.7   Barite sag

9.7.1   In weighted drilling fluids the separation of weighting material can lead to local fluctuations in fluid density. This is referred to as barite sag. It can be particularly pronounced in high-angle wells and lead to significant variations in return drilling fluid density as drilling fluid is circulated to surface. In the field, barite sag is defined as the change in drilling fluid density observed when circulating bottoms-up. Barite sag is almost always characterized by drilling fluid having a density below nominal, being followed by drilling fluid densities above nominal, being circulated out of the annulus. The use of a pressurized balance is recommended, to eliminate aeration effects on density, whenever barite sag is suspected.

9.7.2   Problems such as lost circulation, well control and stuck pipe have resulted from the occurrence of barite sag. Historically barite sag has been associated with a static well environment; consequently test devices and rheological measurements were originally based on static conditions. Often the conditions under which barite sag is measured in laboratory tests are unrelated to the field conditions under which barite sag occurs. Work in the early 1990's found that barite sag is most problematic under dynamic, not static, conditions[78]. An important conclusion from this work was that barite sag generally observed in the field is primarily due to barite deposition occurring under dynamic conditions.

9.7.3   Dynamic sag is best measured and studied with a flow loop designed to mirror field conditions such as annular flow rates, angle, eccentricity, pipe rotation and, to a degree, temperature. There are two prominent variables conducive to creating dynamic sag; 1) low shear rate conditions (drilling process-related) and 2) insufficient ultra-low shear rate viscosity (drilling fluid-related).

9.7.4   Sag is not entirely a drilling fluid-related problem, and that certain conditions in the drilling operation are conducive to creating dynamic sag. The potential for dynamic sag is promoted by an eccentric pipe such as when sliding in deviated wells and by low annular velocities (< 100 ft/min).

9.7.5   Barite sag cannot be totally eliminated; however, it can be managed to within levels that do not adversely affect the drilling operation.

9.7.6   A common theme in the published literature is that low shear rate viscosity is a rheological parameter of importance in determining the capacity of a drilling fluid to manage dynamic barite sag. Most refer to "low shear rate" as that corresponding to 3 rpm dial reading (~5.1 s^{-1}) obtained from the oilfield 6-speed viscometer. Another study recently demonstrated that viscosity measurements taken at ultra-low shear rates (< 2 s^{-1}) can predict the onset of dynamic barite sag. There is ongoing discussion among industry experts in this field on the most appropriate measurement technique to manage the problem of barite sag; however, these experts generally agree that: barite sag cannot be totally eliminated and modern industry standards are needed for measurement and management; the severity of barite sag is highest under dynamic conditions and measurement and management techniques should focus on dynamic sag.

10 Hydraulics optimization

10.1 Optimization objectives

10.1.1 Principle of hydraulic optimization

10.1.1.1 Optimized hydraulic design is defined here as the determination of the jet nozzle sizes and flow rates to satisfy an optimization criterion. Criteria used are the maximization of the bit hydraulic power per square inch (HSI) or of the impact force (IF).

10.1.1.2 Constraints in this optimization process include rig capability limitations - maximum available standpipe pressure P_{max}, maximum horsepower of the rig pumps, minimum required and maximum available flow rate, and downhole-tool limitations.

10.1.1.3 The goal of the optimization is to determine the total flow area TFA, the nozzle sizes and the flow rate to deliver maximum bit hydraulic horsepower (HSI) or impact force (IF) within the limitation of maximum pump pressure and hydraulic power available from the drilling fluid pumps.

10.1.1.4 If a cutting is removed before the next tooth reaches the cutting, the bottom of the borehole is being cleaned. The drilling rate for a roller cone drill bit will increase as a function of the square of the weight on a roller cone drill bit until cuttings generation is too rapid for the drilling fluid to remove all of the cuttings. At this point, the founder point, the drilling rate will not increase as rapidly when the weight on the bit is increased. Increasing hydraulic parameters very far below the founder point will not significantly increase drilling rate. In fact under these circumstances, increased flow rate may increase the bottom hole pressure and decrease drilling rate. With high pressure differentials, cuttings are more difficult to remove after they are formed and the founder point will decrease.[64,84,87-89]

10.1.1.5 Including drilling rate as a mathematical parameter in the optimization process is beyond the scope of this document.

10.1.2 Maximizing HSI and impact force

10.1.2.1 Hydraulic horsepower per square inch and specific impact force are maximized, because it is believed that the cuttings and the debris underneath the drill bit will be moved away from the bottom of the hole before being reground. This raises the founder point.

10.1.2.2 Hydraulic power can be expressed as $\rho Q V^2$ and hydraulic impact force can be expressed as $\rho Q V$. The optimum flow rate for the maximum hydraulic power will be lower than the optimum flow rate for the maximum hydraulic force. Since hydraulic power is related to the square of the velocity, jet velocity is more important than flow rate. No comparison studies have been reported in the literature comparing drilling rates for these two optimum techniques with the identical conditions at the rig. Note also, that drilling rate is not included in the optimization derivation.

10.1.2.3 The theory for the optimization has been developed for roller cone bits. PDC bits experience shows that the ROP is best for a certain value of HSI. In this case, the nozzle size needs to be determined to achieve a specified HSI value instead of the maximum HSI.

10.1.3 Maximizing jet velocity

Some drilling programs select flow rates by using the maximum possible jet velocity for a particular selected annular velocity. Jet velocity increases as the pressure across a nozzle increases. The flow rate in the circulating system is selected to be as low as possible to provide the maximum pressure available for the drill bit. Some rule-of-thumb guidelines recommend that the nozzle velocity be maintained above 230 ft/s to reduce the possibility of plugged jet nozzles.

10.1.4 Annular velocity

10.1.4.1 Annular velocity is used to move cuttings from the bottom of the hole to the surface. Increasing annular velocity will increase the annular pressure loss and ECD, and therefore, will have an adverse affect on drilling rate. For hole cleaning guidelines, see Clause 9.

10.1.4.2 With PDC bits, the HSI is more important than the nozzle velocity. The HSI required increases as the shale reactivity of the formation increases.

10.2 Calculation

10.2.1 The parasitic pressure loss, which includes all pressure losses in the system except the bit pressure drop, is calculated using the equation:

$$P_{Parasitic} = KQ^u \tag{128}$$

10.2.2 The optimization is applied using the following procedure.[64]

a) Caliper the individual nozzles. Since the bit pressure drop is inversely proportional to d^4, slight changes in the diameter will have a big impact.

b) Calibrate the rig pumps to achieve accurate flow rate measurements.

c) Determine the parasitic pressure loss characteristics of the wellbore.

   1) On the rig: measure the standpipe pressure *SPP* of the wellbore for the range of flow rates of interest. Then calculate the bit pressure drop from the measured *SPP*. Subtract the bit pressure drop (see Clause 7) from the *SPP* to achieve the parasitic pressure loss.

   2) In the office: calculate the parasitic pressure loss of the wellbore system (see Clause 7) for the range of flow rates of interest.

d) Determine the slope *u* and the coefficient *K* of the parasitic pressure loss equation.

   1) Plot the parasitic pressure loss on log-log scaled paper and measure the slope u with a ruler. Calculate K for a known set of pressure loss and flow rate by rearranging Equation (128).

   2) Use a spreadsheet program to plot the sets of parasitic pressure loss and flow rate in a graph. Fit the data points to a power function (like y = k x^u). Extract the slope *u* and the coefficient *K* from the line fit function of the spreadsheet.

e) Apply the optimization

Table 6 — Optimization equations

Criterion	Maximum impact force		Maximum hydraulic power
Limiting factor	Hydraulic power	Maximum SPP	Maximum SPP
Optimum Bit pressure drop	$P_{opt} = \left(\dfrac{u+1}{u+2}\right)P_{max}$ Equation (129)	$P_{opt} = \left(\dfrac{u}{u+2}\right)P_{max}$ Equation (130)	$P_{opt} = \left(\dfrac{u}{u+1}\right)P_{max}$ Equation (131)
Optimum flow rate	$Q_{opt} = \left(\dfrac{P_{max}}{K(u+2)}\right)^{\frac{1}{u}}$ Equation (132)	$Q_{opt} = \left(\dfrac{2P_{max}}{K(u+2)}\right)^{\frac{1}{u}}$ Equation (133)	$Q_{opt} = \left(\dfrac{P_{max}}{K(u+1)}\right)^{\frac{1}{u}}$ Equation (134)

NOTE: Equation numbers are included in the cell with the formula.

f)   For maximum power at the drill bit nozzles, the maximum SPP must be used, so the optimum flow rate is equal to or less than Q_{crit}.

g)   For maximum hydraulic impact, the optimum flow rate may be above, equal to, or less than Q_{crit}.[1] Q_{crit} is the flow rate at the intersection of SPP_{max} and available hydraulic horsepower.

$$Q_{crit} = \frac{HHP_{max}}{SPP_{max}} \qquad (135)$$

h)   In the log-log scaled diagram three regions can be identified when optimizing for maximum impact force.

1)   Region 1 - limited by SPP_{max}. Region 1 reaches from zero flow rate to Q_{crit}. For flow rates below Q_{crit}, the maximum horsepower of the pumps cannot be reached because of the pump pressure limitation.

2)   Region 3 - limited by HHP_{max}. Region 3 reaches from Q_{crit} to the maximum flow rate provided by the pumps. For flow rates larger than Q_{crit}, the maximum pump pressure cannot be reached because of the horsepower limitation.

3)   Region 2 – is the intersection between Region 1 and Region 3. It is coupled to Q_{crit} where both the maximum pump pressure and the maximum horsepower can be used as limiting criteria for the optimization. See Figure 9 for illustration.
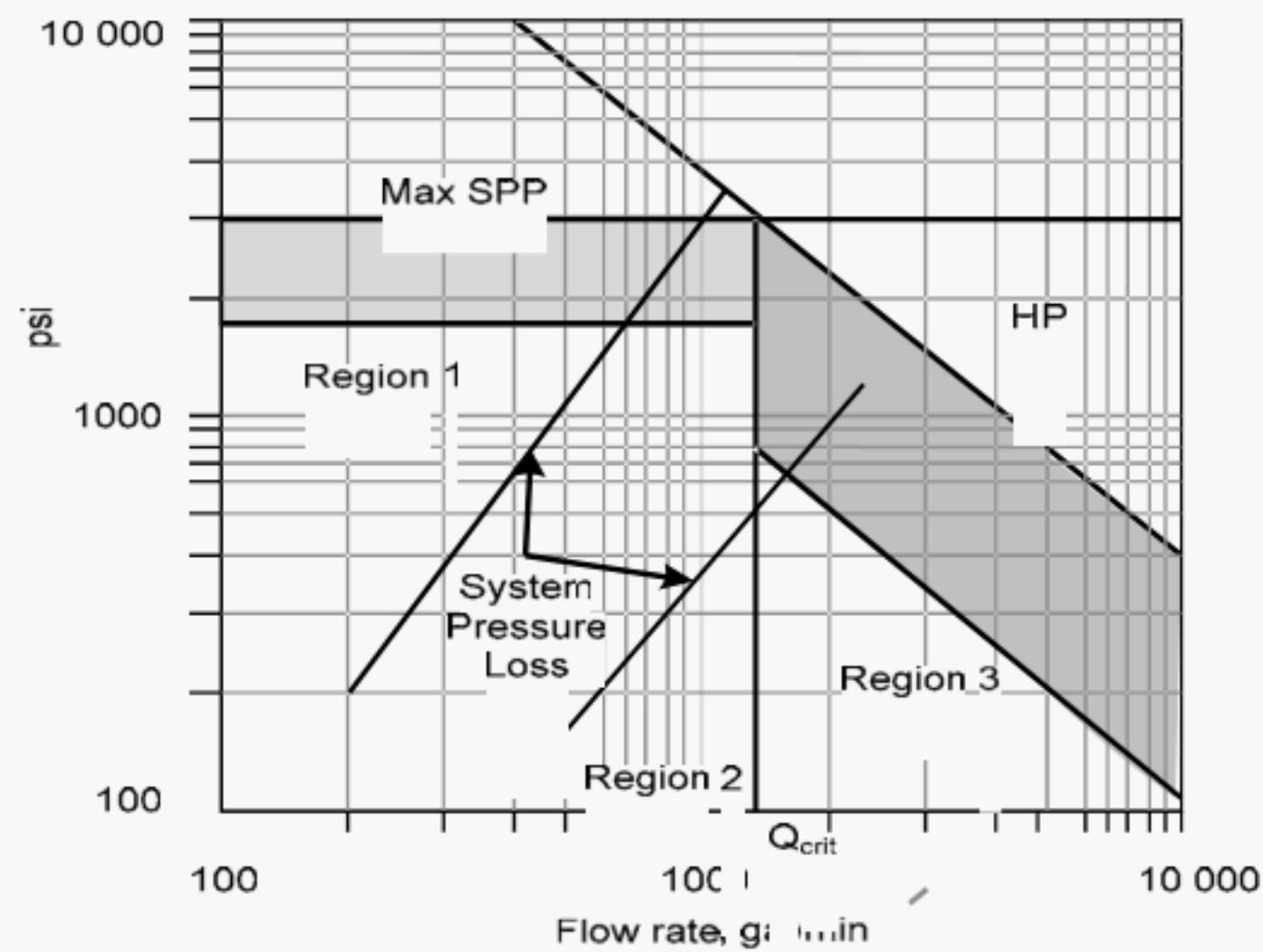
Figure 9 – Optimizing maximum impact force

i) Check whether the resulting optimum flow rate is covered by the flow rate range used to determine the slope u.

j) Determine the optimum *TFA* by rearranging the bit pressure drop equation.

$$P_{bopt} = \frac{\rho\, Q^2}{12042\, C_v^2 TFA^2} \tag{136}$$

$$TFA = \frac{Q}{C_v} \sqrt{\frac{\rho}{12042\, P_{bopt}}} \tag{137}$$

k) Divide the optimum TFA in individual nozzles to achieve the real TFA.

l) Calculate SPP based on the optimum flow rate and using the real TFA. Adjust the flow rate, if *SPP* exceeds the maximum allowable SPP.

10.3 Reaming while drilling with a pilot-bit configuration

10.3.1 There are two distinct cases where the hole being drilled is opened to a larger diameter with the same drilling assembly. In these cases, it will be necessary to optimize the flow distribution between the two drilling tools to maintain proper hydraulic balance.

10.3.2 Bicenter Bits - specifications identify both a "pilot-section" diameter and a "reamer-section" diameter, *i.e.*, the objective full hole diameter being drilled. The bit must rotate concentrically around the pilot section in order to maintain the objective full hole diameter. If the pilot section were allowed to wash out (larger than the pilot diameter), the bit would not be able to drill to full hole diameter. To avoid this problem, the optimized flow distribution from field experience, is 40% flow on the pilot section, 60% flow on the reamer wing. The ratio of the TFAs between the pilot and the reamer sections should be adjusted to this 40/60 ratio.

10.3.3 Underreamers / ream-while-drilling (RWD) tools - In most cases, the underreamer or RWD tools are run with a conventional drill bit leading the assembly. In this case, the flow distribution between the pilot and the reamer hole sections should follow the ratio of the areas of the hole diameters being drilled (flow-split ratio = (Area of the Bit)/(Area of the RWD Gauge)).

10.4 Bit-nozzle selection

10.4.1   The bit TFA needs eventually be divided in individual nozzles following the hydraulics configuration of the bit.

10.4.2   The nozzles size for roller cone bits can be determined such that the flow underneath the bit is asymmetric. This is achieved by either blocking a nozzle or by using unequal nozzle diameters.

10.4.3   Modern PDC bits with bladed designs contain one or more nozzles per blade. A symmetrical nozzle arrangement is desirable for optimum cleaning. The available optimized *TFA* should be divided equally among the number of nozzles required. Following this rule can sacrifice the optimum *TFA*.

10.5   Pump-off pressure/force

Pump-off pressure and force are of interest when using PDC bits with shallow rib designs, impregnated bits and face-set natural diamond bits with shallow water courses. Due to the generally small flow path or junk slot area under the bit, the pump-off force acts to push the bit up off-bottom, and will significantly reduce the effective WOB. The best practice is to determine the pump-off force in a drill-off test, or estimate it by:

$$HPO = [0.942 \times P_{bit} \times (d_s - 1.0) \times 0.001] \tag{138}$$

where

   HPO is the negative weight on bit, 1000 lb

11 Rigsite monitoring

11.1 Introduction

11.1.1 Most drilling hole problems occur when the downhole safe operating pressure limits are exceeded. These limits are defined by the pore, collapse, and fracture pressures. Additional hole problems can occur if the conditions are insufficient to remove the drilled cuttings from the hole. Poor cuttings removal (hole cleaning) often results in excessive reaming times, packing-off, and stuck pipe.

11.1.2 Careful monitoring of real-time annular pressure losses can reveal important information about hole cleaning, barite sag, and swab and surge pressures.

11.2 Measurement of annular pressure loss

11.2.1 Equivalent circulating density

11.2.1.1 Successful drilling requires that the drilling fluid pressure to stay within a tight drilling fluid-density window defined by the pressure limits for well control and wellbore integrity. The lower pressure limit is either the pore pressure in the formation (where formation fluid can enter the wellbore in permeable zones), or the limit for avoiding wellbore collapse (Figure 10). If the drilling fluid pressure is less than the pore pressure, then formation fluid or gas could flow into the borehole, with the subsequent risk of a blowout at surface or underground.
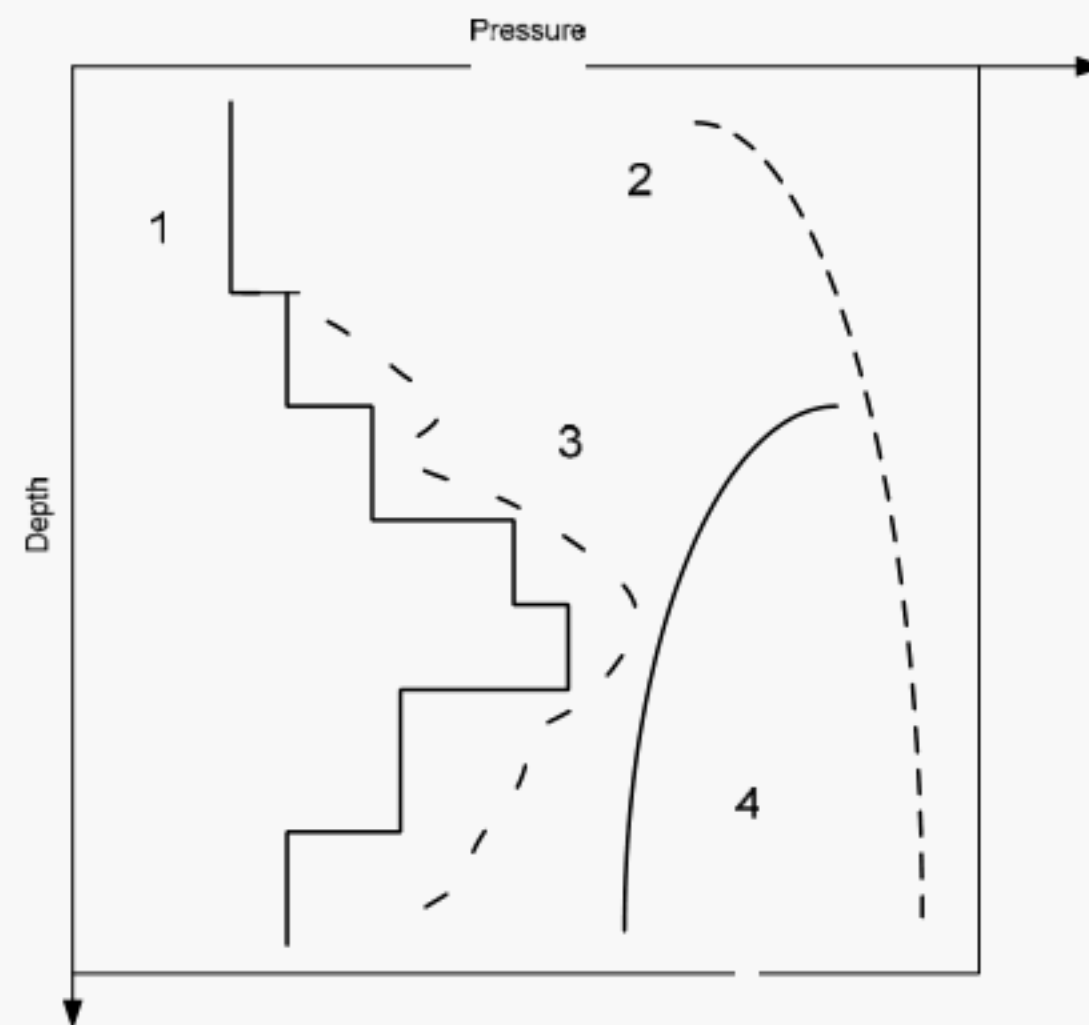
KEY

1   Pore pressure

2   Fracture gradient

3   Annular pressure

4   Kick tolerance

Figure 10- The drilling pressure window

11.2.1.2 The downhole annular pressure has three components:

a)   The first is a static pressure due to the density gradients of the fluids in the borehole annulus: the weight of the fluid vertically above the pressure sensor. The density of the drilling fluid column including solids (such as drilled cuttings) is called the Equivalent Static Density *ESD*, and the fluid densities are pressure-dependent and temperature-dependent.

b)   The second is a dynamic pressure related to the pipe velocity (swab, surge and drillpipe rotation), inertial pressures from the drillstring acceleration or deceleration while tripping, excess pressure to break drilling fluid gels, and the cumulative pressure losses required to move drilling fluids up the annulus. Flow past constrictions, such as cuttings beds or swelling formations, changes in hole geometry, and influxes and effluxes of liquids, gases and solids all contribute to the dynamic pressure. The ECD is defined as the effective drilling fluid weight at a given depth created by the total hydrostatic (including the cuttings pressure) and dynamic pressures (see Clause 7).

c)   The third component is related to restrictions in the hydraulic system. When the annulus becomes blocked due to excessive cutting, cavings and poor hole cleaning, the hole may pack-off resulting in excessively high or low pressures below the restriction. In addition, there may be times when the annulus is shut-in at surface (*e.g.*, during a leak-off tests, well control incident, or managed pressure drilling) that can lead to higher or lower pressures than an open system.

11.2.2 Pumps-off measurements

The pressure tools are capable of continuous recording during times of no-flow with data pulsed to surface once flow is resumed, which enables real-time dynamic testing during pumps-off periods, such as during leak-off tests, connections, or well-control incidents.

11.2.3 Data formats

11.2.3.1 There are three modes that pressure-while-drilling data are recorded and displayed in:

a) *Memory mode* (also known as recorded mode): in this mode the downhole tool is continually recording data into the tool memory. This data can then be retrieved when the tool is brought back to surface. Recoded-mode data tend to be sampled at a higher frequency than real-time data and as such are richer in detail. Recording gauges are programmable, and can store data at required intervals from one second upwards. Typical settings are from five to twenty seconds. It is important to realize that some short time scale phenomena could be missed by an incorrect setting of the memory mode recording interval. For example, fast transients due to swab/surge pressures could be missed, or their peak pressure amplitudes distorted.

b) *Real-time mode*: In this format, the downhole pressure data are interfaced with a downhole MWD (measurement – while-drilling) system. This can be a drilling fluid-pulse, an electromagnetic system, or a hard-wired system to the surface and the real-time data should be sent to surface every thirty seconds or so. With a drilling fluid-pulse MWD system, the data can only be sent to surface when the pump flow rate is above a certain threshold. Below this flow rate, no information can be sent to surface. There is no limitation with electromagnetic or hard-wired systems

c) *Pumps-off mode*: In this mode, recorded-mode data are processed in the downhole tool and a limited amount of information is sent to surface when pump circulation resumes for pulser-type MWD systems. This mode is of use during connections or LOTs. Either a continuous pumps-off recorded pressure can be transmitted or a limited set.

11.2.3.2 Typical information from the limited set that is processed and transmitted to surface includes:

- Maximum annular pressure (expressed in terms of ECD)

- Minimum annular pressure (expressed in terms of ECD)

- Average annular pressure during the connection

- Static drilling fluid density, or equilibrated pressure (expressed as the ESD) if all transient fluid motion has ceased during the connection.

11.2.4 Drillers logs

11.2.4.1 Typically, there are two distinct modes of display for drilling logs - time-based logs and depth-based logs. Depth-based logs are more associated with wireline and formation evaluation measurements, where the characterization of the reservoir is of importance. For real-time drilling information, and post-event interpretation of memory mode data, a time-based format is more appropriate.

11.2.4.2 Pressure data should be presented in the context of many other drilling variables for an interpretation to be useful. For example, an annular pressure trace on its own tells nothing more than the minimum and maximum pressures that occured during that time or depth interval. Other key measurements that are important to have are as follows: pump flow rate, standpipe pressure, drillstring rpm, surface and downhole weight, surface and downhole torque, block velocity (ROP), drilling fluid properties (drilling fluid density in, viscometer readings, gel strength, and temperature and pressure dependence if available), total gas, cuttings volume rate, pit level, and rig heave.

11.2.4.3 It is also important that the measurements are made in the context of the previous drilling history in the region.

11.2.5 Time-based log format

Figure 11 shows a typical time-based log format, with the pressure-while-drilling measurement placed in the context of the other downhole and surface measurements. It is important to note that for real-time applications the scales for the various parameters must be chosen with care to maximize the visibility of the expected signatures, particular for that of the annular pressure (or ECD). For example, if the ESD is 12 lb_m/gal and the ECD is 14 lb_m/gal, and the expected swab and surge pressures are approximately equivalent to $\pm$ 1 lb_m/gal, then the ECD should probably be plotted on a scale from 11 lb_m/gal to 15 lb_m/gal so that the detailed pressure trace has a high sensitivity, and drilling anomalies can be easily visualized.
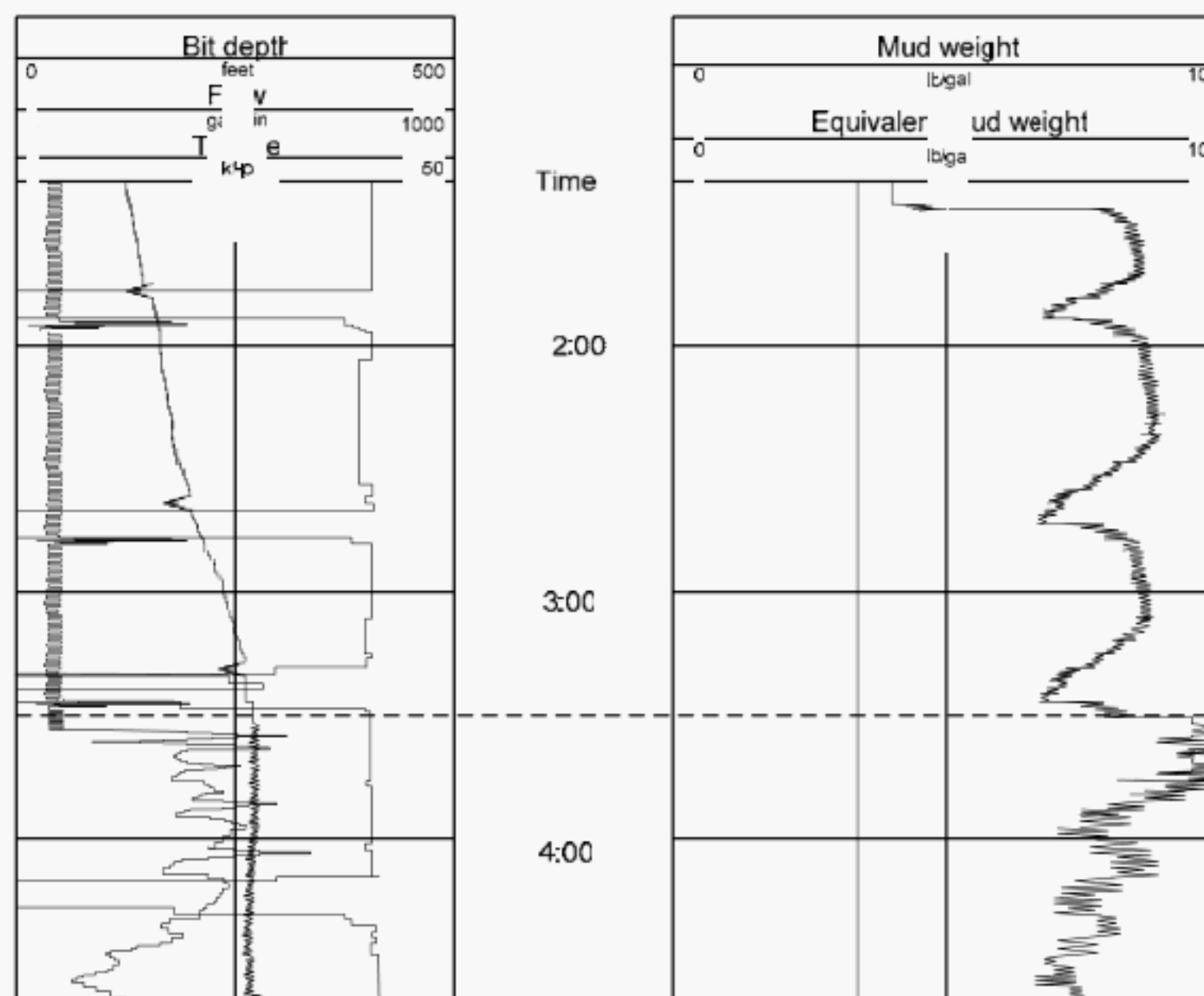
Figure 11-Time-based log format

11.2.6   Sensor calibration

Master calibrations of the pressure sensors are performed over a range of temperatures using a dead-weight tester. At the location or wellsite, hydraulic tests using a hand pump are performed on the gauges before and after use in each well to verify calibrations.

11.3 Validation of hydraulics models

11.3.1 Principle

The value of real-time downhole pressure measurement lies in its ability to monitor pressures wherever the sensors are placed. They can also be used to validate predictive hydraulics models, and to refine the calculations from those models by enabling some of the unknown parameters to be refined or determined. Downhole pressure measurements can also be used to understand the limitations of hydraulics models, particularly in allowing for the complex distributions of cuttings that can occur along the annulus, the effects of which are typically poorly handled by conventional hydraulics models.

11.3.2 Rigsite calibration

11.3.2.1 Many of the hydrodynamic responses of a pressure sensor to drilling parameters are not easily predicted, as illustrated above with the example of the cuttings. In the absence of prediction models for these effects, field procedures need to be developed which calibrate the response of the pressure sensor to each of the drilling control variables. In this way it is then possible to discriminate the contribution that cuttings make to the ECD and determine whether the hole is being cleaned effectively.

11.3.2.2 For absolute validation of hydraulics models, it is critical that all the rig sensors are correctly calibrated. This includes pressure gauges, flow meters, density meters, and viscometers. Where direct measurement flow meters are not used, it is important that the discharge characteristics and mechanical efficiencies of the pumps are determined under representative pressure conditions. It is also important that the dimensions of the drillpipe and bit nozzles are accurately determined. For example a 10% error in nozzle diameter will lead to approximately 40% error in pressure loss determination.

11.3.3 Drillpipe rotation

11.3.3.1 Another example demonstrates the effect of drillpipe rotation on hole cleaning. Figure 12 shows the ECD on the right-hand graph, rotary speed (left-hand trace on middle graph), and a rough approximation of produced cuttings seen at the surface (left-hand trace on the left-hand graph). While sliding, cuttings fall out of suspension, causing a gradual drop in the effective drilling fluid density and ECD.

11.3.3.2 At approximately 19:20, pipe rotation resumes to around 100 rpm, resulting in an instantaneous increase in bottomhole pressure of roughly 50 psi and a corresponding increase in ECD. This instantaneous pressure increase is due to flow redistribution in the eccentric annulus. The pressure then continues to increase gradually as the cuttings are stirred up and become entrained in the flow, contributing to the effective density of the drilling fluid.

11.3.3.3 Once the cuttings are fully mobilized, a pressure maximum is reached (with a corresponding maximum in the cuttings seen at surface after a delay). The pressure then drops back to normal, with the corresponding decrease in cuttings seen at the surface.
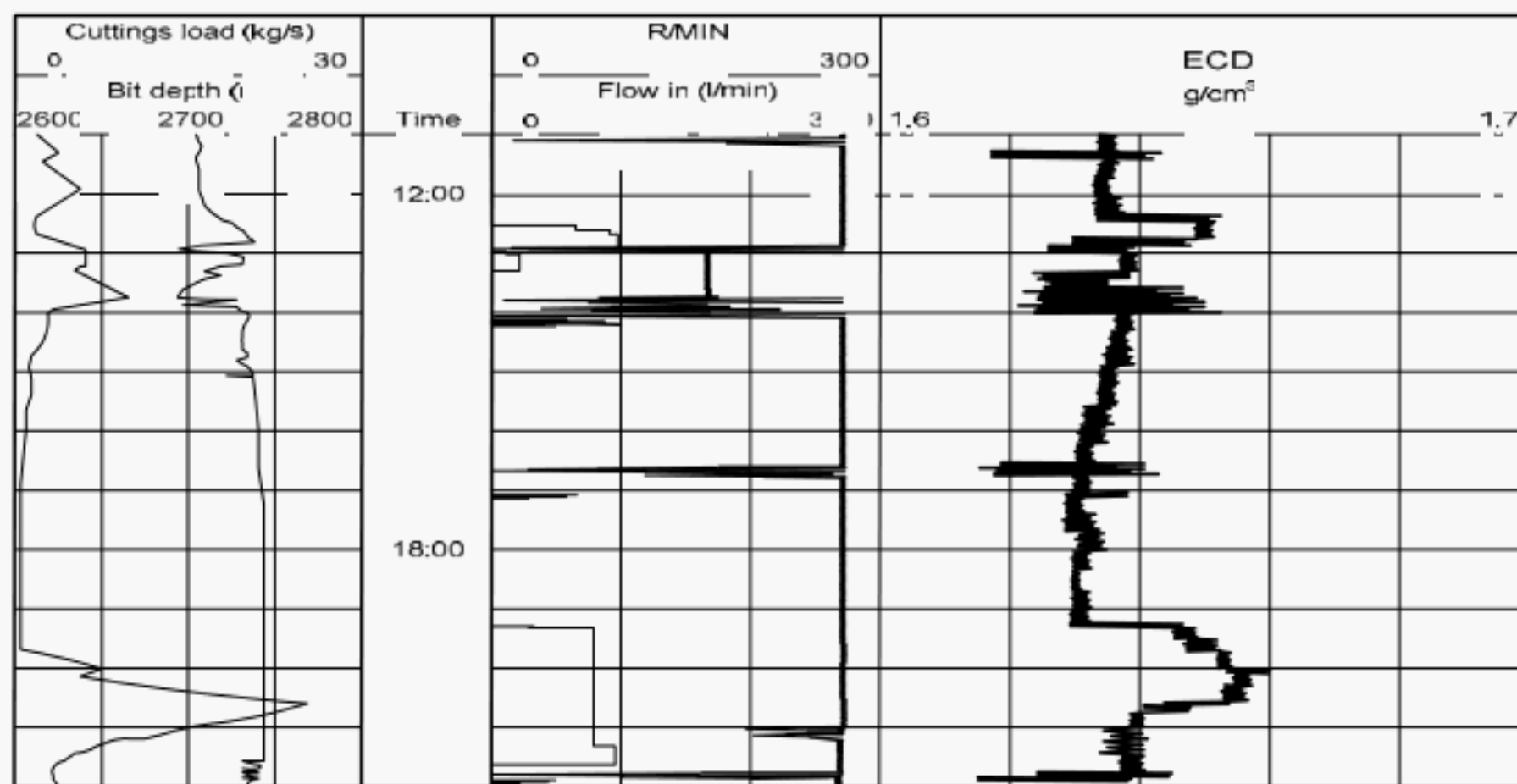
Figure 12- Cuttings mobilization

11.3.3.4 It is important to recognize that the increase in ECD caused by drillpipe rotation will be related to the size of the cuttings bed. In the case of slide drilling, hole cleaning is less efficient and cuttings tend to accumulate on the low side of the hole. Following long periods of slide drilling, it is recommended to circulate the hole clean while rotating the drillpipe at normal rotary drilling rpm.

11.4 Interpretation table for downhole pressure measurements

11.4.1 Principle

Downhole annular pressure interpretation is still an evolving technique. All possible downhole events have not yet been observed. Sometimes the data are enigmatic. Nonetheless, certain clearly identifiable and repeatable signatures can be used to help diagnose problems. Combining the information gleaned from downhole annular pressure logs with other drilling parameters creates an overall assessment. This global view helps decipher the individual measurements used to detect drilling problems downhole.

11.4.2 The following interpretation guide, as shown in Table 7, can be used as a simple wellsite diagnostic tool. Monitoring the ECD along with other drilling parameters can help determine what is happening downhole in the wellbore. Some of the known, clearly repeatable signatures of ECD changes are shown along with secondary or confirming indications, such as those in complimentary surface measurements.

Table 7- Interpretation guide

Event or procedure	ECD change	Other indications	Comments
Drilling fluid gelation / pump startup	Sudden increase possible	Increase in pump pressure	Avoid surge by slow pumps and break rotation (rotation first)
Cuttings pick-up	Increase then leveling as steady-stated reached	Cuttings at surface	Increase may be more noticeable with rotations
Plugging annulus	Intermittent surge increases	• Standpipe pressure • Surge increase • Torque / rpm fluctuations • High overpulls	Packoff may "blow-through" before formation breakdown
Cuttings bed formation	Gradual increase	• Total cuttings expected not seen at surface • Increased torque • ROP decreases	If near plugging, may get pressure surge spikes
Plugging below sensor	Sudden increase as packoff passes sensor – none if packoff remains below sensor	• High overpulls • "Steady" increase in standpipe pressure	Monitor both standpipe pressure and ECD
Gas migration	Increase if well is shut-in	Shut-in surface pressures increase linearly (approx.)	Take care if estimating gas migration rate
Running in hole	Increase – magnitude dependent on gap, rheology, speed, etc.	Monitor trip tank	Effect enhanced if nozzles plugged
Pulling out of hole	Decrease – magnitude dependent on gap, rheology, speed, etc.	Monitor trip tank	Effect enhanced if nozzles plugged
Making a connection	Decrease to static drilling fluid density	Pumps on/off indicator Pump flow rate lag	Watch for significant changes in static drilling fluid density
Barite sag	Decrease in static drilling fluid density or unexplained density fluctuations	High torque and overpulls	While sliding periodically or rotating wiper trip to stir up deposited beds, use correct drilling fluid rheology
Gas influx	Decreases in typical size hole	Increases in pit level and differential pressure	Initial increase in pit gain may be masked
Liquid influx	Decreases if lighter than drilling fluid Increases if influx accompanied by solids	Leak for flow at drilling mudline if relevant	Plan response if shallow water flow expected

Annex A
(informative)

Worked example input parameters

A.1 Well information

a)   Flow rate, Q = 420 gal/min
b)   Drillpipe
- Length = 21,500 ft
- Outside diameter = 5 in.
- Inside diameter = 4.276 in.

c)   Drill collars
- Length = 200 ft
- Outside diameter = 6.75 in.
- Inside diameter = 3.0 in.

d)   Marine riser
- Length = 3,000 ft
- Outside diameter = 20.0 in.
- Inside diameter = 19.0 in.

e)   Casing
- Length = 16,700 ft
- Outside diameter = 9.625 in.
- Inside diameter = 8.535 in.

f)   Bit
- Diameter = 8.5 in.
- Nozzles = 12, 12, 12, 12 (1/32 in.)

g)   Open hole
- Length = 2,000 ft
- Diameter = 8.5 in.

A.2 Drilling fluid information

a)   Surface drilling fluid density
- Density = 12.5 lb_m/gal
- Measured at 60°F

b)   Fluid properties
- Organic phase fluid
- Internal olefin base
- Oil content = 63% (by volume)

c)   Brine properties
- Calcium chloride
- Weight concentration = 20%
- Water content = 15% (by volume)

d)   Solids properties
- Corrected solids content = 21.9% (by volume)
- Average solids density = 3,730 kg/m^3

A.3 Wellbore temperature and profile

a)   Temperature conditions

- Surface temperature = 65 °F
- Flowline temperature = 55 °F
- Geothermal gradient = 1.235 °F / 100 ft.

b)   Well trajectory

Table A.1- Well trajectory

MD ft	TVD ft	MD ft	TVD Ft	MD ft	TVD ft
0	0	4725	4500	13690	9000
500	500	5690	5000	14690	9500
1000	1000	6690	5500	15690	10000
1500	1500	7690	6000	16690	10500
2000	2000	8690	6500	17690	11000
2500	2500	9690	7000	18690	11500
3000	3000	10690	7500	19690	12000
3506	3500	11690	8000	20690	12500
4052	4000	12690	8500	21690	13000

A.4 Wellbore schematic
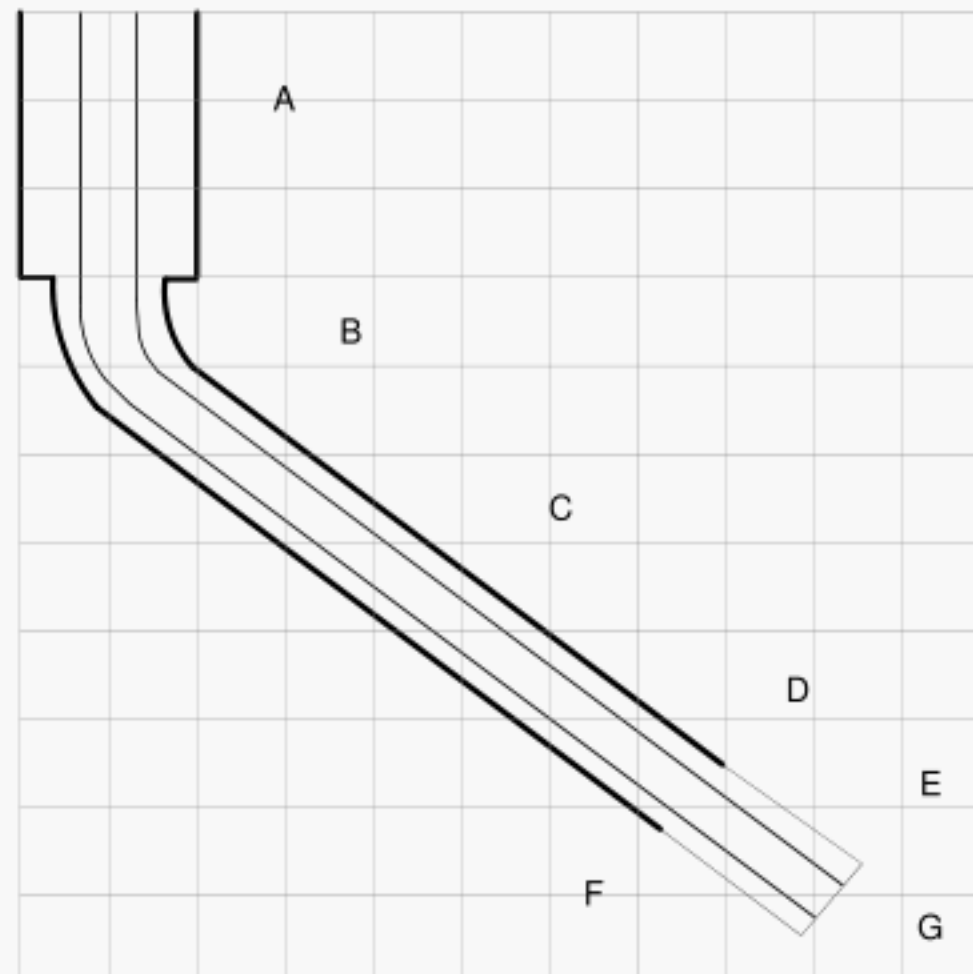
KEY

A   Riser with 19 in. ID

B   Water depth = 3,000 ft

C   Tangent angle = 60°

D   21,500 ft of 5 in. DP (ID = 4.276 in.) and 2,000 ft of 6-3/4 in. DC (ID = 3.0 in.)

E   2,000 ft of 8-1/2 in. open hole

F   9-5/8 in. casing = 19,700 ft MD (12,000 ft TVD)

G   8-1/2 in. TD = 21,700 ft MD (13,000 ft TVD)

Figure A.1- Wellbore dimensions

Annex B
(informative)

Modeling of downhole properties

B.1 Downhole density modeling

Table B.1 – Hydraulic sections data

	MD	TVD	OD	ID	L	Static Temperature	Dynamic Temperature
	ft	ft	In.	In.	ft	°F	°F
	0	0	19	5	0	65	55
1	3000	3000	19	5	3000	40.6	66.55
2	4298	4200	8.535	5	1600	55.4	71.17
3	11690	8000	8.535	5	7600	102	85.8
4	19690	12000	8.535	5	7500	151.7	101.2
5	21490	12900	8.5	5	1800	162.9	113.1
6	21690	13000	8.5	6.75	200	164	114.4

Table B.2 – Downhole density calculated

MD	TVD	Static Temperature	Applied Static Pressure	Static Drilling Fluid Density	Dynamic Temperature	Applied Dynamic Pressure	Dynamic Drilling Fluid Density
ft	ft	°F	psi	lbm/gal	°F	psi	lb$_m$/gal
0	0	65.0	0.0	12.47	55.0	0.0	12.49
500	500	60.9	324.2	12.48	56.9	324.9	12.49
1000	1000	56.9	649.3	12.50	58.9	649.8	12.50
1500	1500	52.8	975.3	12.52	60.8	974.9	12.50
2000	2000	48.7	1302.2	12.53	62.7	1300.1	12.50
2500	2500	44.7	1629.9	12.55	64.6	1625.4	12.50
3000	3000	40.6	1958.4	12.57	66.6	1950.9	12.50
3506	3500	46.8	2287.8	12.56	68.5	2276.4	12.51
4052	4000	52.9	2612.9	12.55	70.4	2602.1	12.51
4725	4500	59.1	2937.6	12.54	72.3	2927.9	12.51
5690	5000	65.2	3261.9	12.53	74.3	3253.8	12.51
6690	5500	71.3	3585.9	12.53	76.2	3579.9	12.52
7690	6000	77.5	3909.6	12.52	78.1	3906.1	12.52
8690	6500	83.6	4232.9	12.51	80.0	4232.4	12.52
9690	7000	89.7	4555.9	12.51	82.0	4558.8	12.52
10690	7500	95.9	4878.6	12.50	83.9	4885.4	12.53
11690	8000	102.0	5201.0	12.49	85.8	5212.2	12.53
12690	8500	108.2	5523.2	12.49	87.7	5539.0	12.53
13690	9000	114.4	5845.0	12.48	89.7	5866.0	12.53
14690	9500	120.6	6166.5	12.47	91.6	6193.1	12.54
15690	10000	126.9	6487.8	12.47	93.5	6520.4	12.54
16690	10500	133.1	6808.8	12.46	95.4	6847.8	12.54
17690	11000	139.3	7129.5	12.46	97.4	7175.4	12.54
18690	11500	145.5	7450.1	12.45	99.3	7503.0	12.55
19690	12000	151.7	7770.4	12.45	101.2	7830.8	12.55
20690	12500	157.9	8090.4	12.44	107.8	8158.8	12.54
21690	13000	164.0	8410.3	12.44	114.4	8480.4	12.54

B.2 Downhole rheology modeling

B.2.1 Rheological profiles

Table B.3 – Test matrix for HTHP viscometer data

Test #	Temp F	Pressure psi
1	61	975
2	69	2350
3	78	3970
4	94	6520
5	107	8120
6	114	8440

B.2.2 Results for rheological models

Table B.4 – Example of HTHP viscometer results

Test #	Surface	Well hydraulic sections					
		1	2	3	4	5	6
600 rpm	63	80	102	105	117	119	124
300 rpm	38	48	63	65	70	74	79
200 rpm	28	35	47	48	51	55	60
100 rpm	18	23	30	30	33	36	39
6 rpm	8	9.2	10	11	12	13	14
3 rpm	7	8.2	9	10	11	12	13

Table B.5 – Calculation of Herschel-Bulkley parameters (numerical method)

	Surface	Well hydraulic sections					
		1	2	3	4	5	6
N	0.876	0.87	0.79	0.81	0.87	0.80	0.76
K, $lb_f/100$ ft^2 s^n	0.138	0.196	0.42	0.368	0.303	0.457	0.602
K, eq cP	66.2	93.8	201.1	176.2	145.1	218.8	288.2
τ_y, $lb_f/100$ ft^2	7.1	7.9	7.9	9.1	10.5	10.9	11.5

Table B.6 – Calculation of Herschel-Bulkley parameters (measurement method)

	Well hydraulic sections						
	Surface	1	2	3	4	5	6
N	0.833	0.84	0.77	0.78	0.83	0.78	0.74
K, lb_f/100 sq ft s^n	0.177	0.223	0.443	0.439	0.329	0.493	0.658
K, eq cP	85	106.7	212.0	210.0	157.7	236.2	315.2
τ_y, lb_f/100 ft^2	6	7.2	8	9	10	11	12

Table B.7 – Calculation of Bingham plastic parameters

	Well hydraulic section						
	Surface	1	2	3	4	5	6
PV, cP	25	32	39	40	47	45	45
YP, lb_f/100 ft^2	13	16	24	25	23	29	34

Annex C
(informative)

Modeling of pressure loss

C.1 Input parameters

a) Flow rate = 420 gal/min
b) Surface drilling fluid density = 12.5 lb_m/gal
c) Drillpipe eccentricity = 0 (concentric)
d) Surface connection pressure loss = Case 1

C.2 Pressure loss in drillstring

Table C.1 – Spreadsheet data of pressure loss in drillstring

												Drillstring			
Measured Depth	TVD	Hole/Csg Diameter	Pipe OD	Pipe ID	ρ	Hydro Press (complex wells)	Surface Conn	R_{600}	R_{300}	R_6	R_3	Velocity	Friction Factor	Pressure Loss	
ft	ft	in.	in.	in.	lb_m/gal	w/o Cut	psig					ft/min	f	cell	cum
0	0	19.000	5.000	4.276	12.49	0	180	80	48	9.2	8.2	563	0.00715	0	0
3000	3000	19.000	5.000	4.276	12.51	1952		80	48	9.2	8.2	563	0.00715	214	214
4298	4200	8.535	5.000	4.276	12.55	2741		102	63	10	9	563	0.00743	97	311
11690	8000	8.535	5.000	4.276	12.53	5212		105	65	11	10	563	0.00749	553	864
19690	12000	8.535	5.000	4.276	12.55	7831		117	70	12	11	563	0.00790	633	1497
21490	12900	8.500	5.00	4.276	12.54	8412		119	74	13	12	563	0.00770	139	1636
21690	13000	8.500	6.75	3.000	12.54	8477		124	79	14	13	1144	0.00617	73	1708
						8477	180								1708
						Phd	Psc								Pds

C.3 Pressure loss in annulus

Table C.2 – Spreadsheet data of pressure loss in annulus

												Annulus				
Measured Depth	TVD	Hole/Csg. Diameter	Pipe OD	Pipe ID	ρ	Hydro Press (complex wells)	Surface Conn	R600	R300	R6	R3	Velocity	Friction Factor	Pressure Loss		ECD
ft	ft	in.	in.	in.	lb$_m$/gal	w/o Cut	psig					ft/min	f	cell	cum	lb$_m$/gal
0	0	19.000	5.000	4.276	12.40	0	180	80	48	9.2	8.2	31	0.31101	0	0	12.49
3000	3000	19.000	5.000	4.276	12.51	1962		80	48	9.2	8.2	70	0.31052	8	8	12.56
4296	4200	8.535	5.000	4.276	12.55	2741		102	63	10	9	215	0.01889	44	52	12.79
11690	8000	8.535	5.000	4.276	12.53	5212		105	65	11	10	215	0.01995	260	312	13.28
19600	12000	8.535	5.000	4.276	12.55	7831		117	70	12	11	215	0.02063	292	604	13.52
21480	12900	8.500	5.000	4.276	12.54	8412		119	74	13	12	218	0.02279	75	679	13.55
21690	13000	8.535	6.750	3.000	12.54	8477		124	79	14	13	386	0.01607	37	716	13.60
						8477	180								716	
						Phs	Psc								Pa	

C.4 Pressure loss versus flow rate

Table C.3 – Data for pressure loss versus flow rate

Flow Rate gal/min	Pressure Loss in Drillstring psig	Pressure Loss in Annulus psig
300	887	609
350	1248	655
400	1576	699
450	1912	742
500	2268	784

Annex D

(informative)

Modeling of swab/surge pressures

D.1 Input parameters

a) Operation = Tripping in hole

b) Trip speed = 93 ft/min

c) Stand length = 93 ft

d) Bit depth = 19,690 ft (measured depth); 12,000 ft (TVD)

e) Drilling fluid clinging factor = 0.45

D.2 Closed-ended case

D.2.1 Assuming the string is closed while tripping in, all fluid will be displaced in the annulus.

D.2.2 With the bit is at the casing shoe the annulus consists of three sections. For each section the effective velocity including the constant clinging factor of 0.45 and the pressure loss need to be calculated.

Table D.1 – Example of three sections of wellbore (closed-ended pipe)

Hole ID in	Pipe OD in	Length ft	Effective Velocity ft/min	Pressure Loss psi
19	5	3000	48.8	10
8.535	5	16500	90.5	308.
8.535	6.75	200	197.4	15

D.2.3 The total pressure loss is 332 psi. Together with the hydrostatic pressure at the casing shoe is the pressure while tripping 8133 psi. This calculates in an EMW of 13.03 lb_m/gal at a drilling fluid density of 12.5 lb_m/gal.

D.3 Open-ended case

D.3.1 When the bit is open to flow, the flow split between the string and the annulus needs to be calculated such that the pressure loss is identical in both conduits. This requires iterative procedures.

D.3.2 The annulus sections remain the same as before. The string has two different IDs and the bit TFA.

Table D.2 – Example of three sections of wellbore (open ended pipe)

	Annulus				String		
d_s, in.	19	8.535	8.535				
OD, in.	5	5	6.75				
ID, in.					4.276	3	
Length, ft	3000	16500	200		19500	200	
TFA, in²							0.4418
							$(4*{}^{12}/_{32})$"
First Guess	80% flow in the annulus and 20 % in the string						
Effective Velocity, ft/min	46.8	76.5	173		46	94	
Pressure Loss, psi	9.72	292.5	13.5		206.9	3.8	6
Pressure Difference, psi				98			
Second Guess	60% flow in the annulus and 40 % in the string						
Effective Velocity, ft	44.8	62.6	148.5		92.7	188.5	
Pressure Loss, psi	9.7	276.4	12.38		237.8	5	23.85
Pressure Difference, psi				31			
Final Flow split	51.44% flow in the annulus and 48.55 % in the string						
Effective Velocity, ft	44	56.65	138.1		112.6	228.7	
Pressure Loss, psi	9.67	269.4	11.9		250.4	5.4	35.15
Pressure Difference, psi				0			

D.3.3   The total pressure loss is 291 psi. Together with the hydrostatic pressure at the casing shoe is the pressure while tripping 8091 psi. This calculates in an EMW of 12.96 lb_m/gal at a drilling fluid density of 12.5 lb_m/gal.

Annex E
(informative)

Modeling of hole cleaning

E.1 Input parameters

a)   PV = 25 cP

b)   YP = 13 lb_f /100 ft^2

c)   Drilling fluid density = 12.5 lb_m/gal

d)   ROP = 60 ft/h

e)   Flow rate = 420 gal/min

f)   Tangent angle = 60°

E.2 Hole cleaning in marine riser

$$CCI = \frac{(MW)(K)(V_a)}{400,000} = 0.20 \qquad\qquad (E.1)$$

where:

   K = 206 cP

   V_a = 30.6 ft/min

The ideal value of *CCI* for good hole cleaning is >1. In practice the hole cleaning in the marine riser can be improved by additional flow rate from a riser booster pump together with increasing the *YP* of the drilling fluid. Increasing *YP* will increase the *K* factor and hence increase the value of *CCI*.

E.3 Hole cleaning in vertical casing

The annular velocity inside 9 5/8 in. casing at 420 gal/min is 215 ft/min
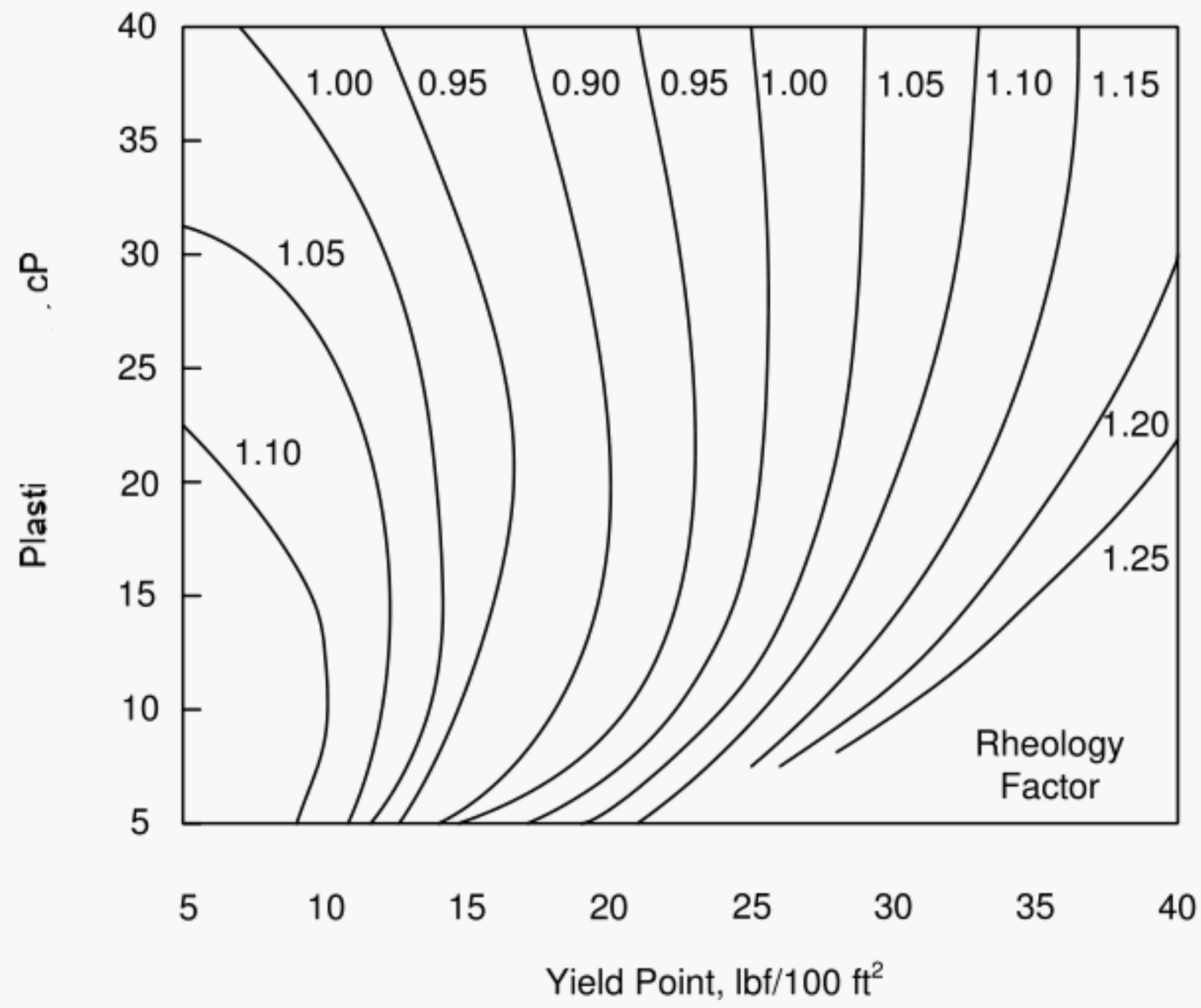
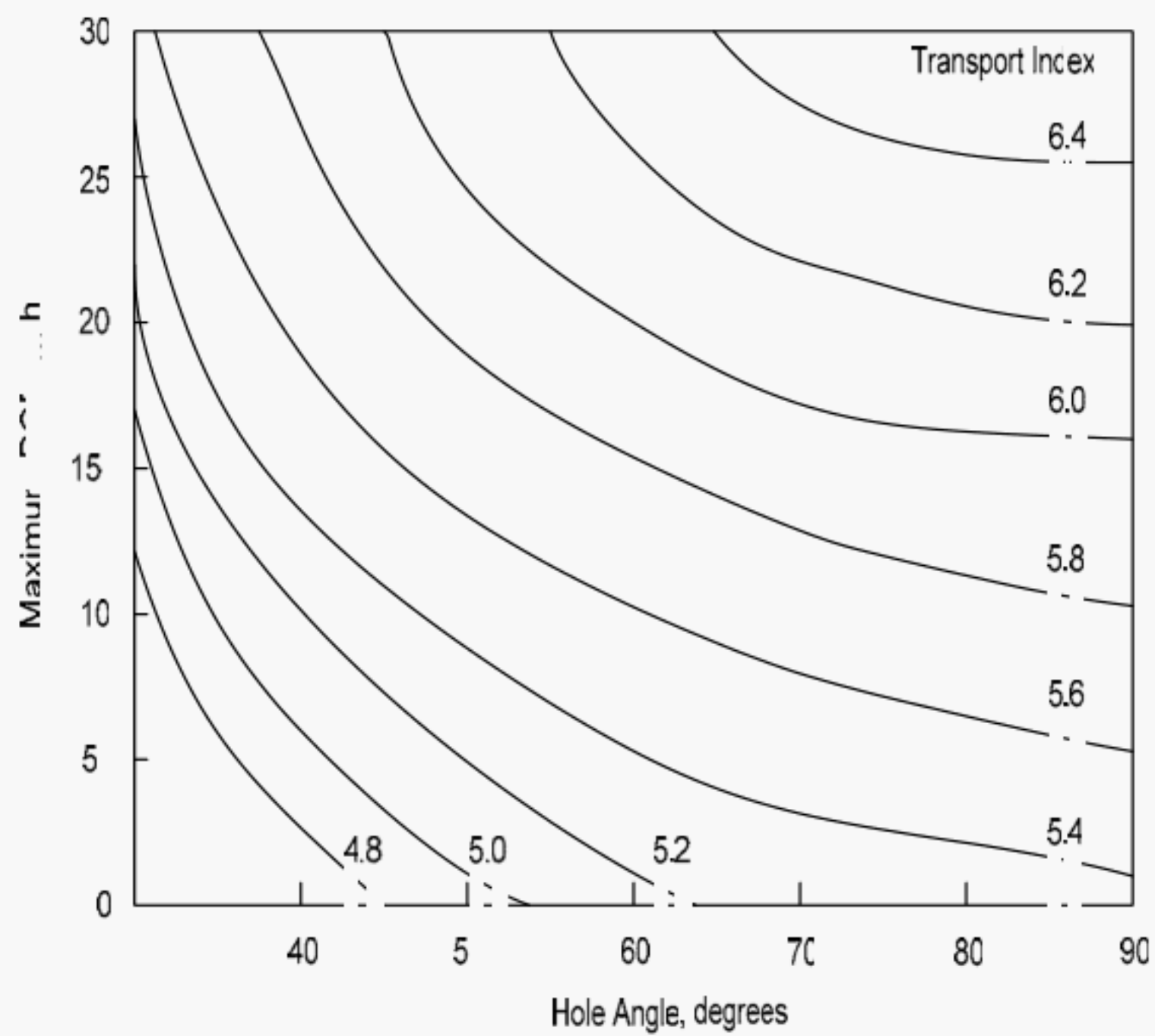$$CCI = \frac{(MW)(K)(AV)}{400,000} = 1.38$$

where
   K = 206 cP

   V_a = 215 ft/min

This implies that hole cleaning in the vertical casing below the marine riser will be good.

E.4 Hole cleaning in open hole section

Figure E.1- Rheology factor chart for 8-1/2 in. holes

Figure E.2- Hole cleaning chart for 8-1/2" holes

a) Enter the Rheology Factor chart with the appropriate values of *PV* and *YP* values at 120 °F and atmospheric pressure. Read the value of the Rheology Factor *RF*

$$RF = 0.97$$

b) Calculate the Transport Index based on the drilling fluid flow rate and drilling fluid density given by:

$$TI = \frac{Q \rho\, RF}{834.5} \qquad\qquad (E.2)$$

where

$$TI = 6.1$$

c) Enter the maximum ROP chart. With the value of Transport Index calculated at 6.1 and the maximum hole angle, read the maximum ROP that can be sustained while still maintaining adequate hole cleaning.

$$ROP_{max} = 25 \text{ m/h (82 ft/h)}$$

d) The actual penetration rate is below this value and hence hole cleaning will be adequate.

Annex F
(informative)

Modeling of optimization

F.1 Input parameters

a) The rig is pumping 450 gal/min at a standpipe pressure of 5,000 psi through four 12/32 in. nozzles.

b) While drilling the last 1,000 ft of hole with a four 12/32 in. nozzles in an 8-½ in. PDC bit, a new 537 drill bit was programmed to drill the last 1,000 ft. Before tripping out of the hole, while circulating bottoms-up before the trip out, the standpipe pressure was measured for several pump stroke rates. The data are presented below:

Table F.1- Rig data for flow rate and standpipe pressure

Flow rate gal/min	Standpipe pressure Psi
450	5000
422	4465
388	3852
342	3086
300	2451
287	2268

c) The pressure loss through the drill bit was calculated from the equation:

$$P_{Bit} = \frac{MW\,(Q)^2}{12042\,(1.03)^2\,(Area)^2} \qquad (F.1)$$

The area of four 12/32 in. nozzles* is 0.4418 in^2, and the drilling fluid density is 12.5 lb$_m$/gal.

d) The pressure loss through the drill bit was calculated for each flow rate and subtracted from the standpipe pressure. This is the parasitic pressure loss through the system.

Table F.2- Calculated parasitic pressure loss

Flow Rate gal/min	Standpipe Pressure, psi	Calculated	
		Pbit psi	Psystem psi
450	5000	1015	3985
422	4465	893	3573
388	3852	755	3097
342	3086	586	2499
300	2451	410	2000
287	2268	413	1855

e)   The boundary condition imposed by the drilling fluid pumps is plotted on a log-log plot as pressure versus flow rate. The drilling fluid pump is powered with a 2,700 HP motor. Assuming an 85 % mechanical efficiency and a 90% volumetric efficiency, 2,066 HHP can be delivered to the drilling fluid. The maximum standpipe pressure is 5,000 psi, so the flow rate (called Q_{crit}) where the maximum pressure is delivered at the available horsepower is 706 gal/min. These lines are shown on the chart below.
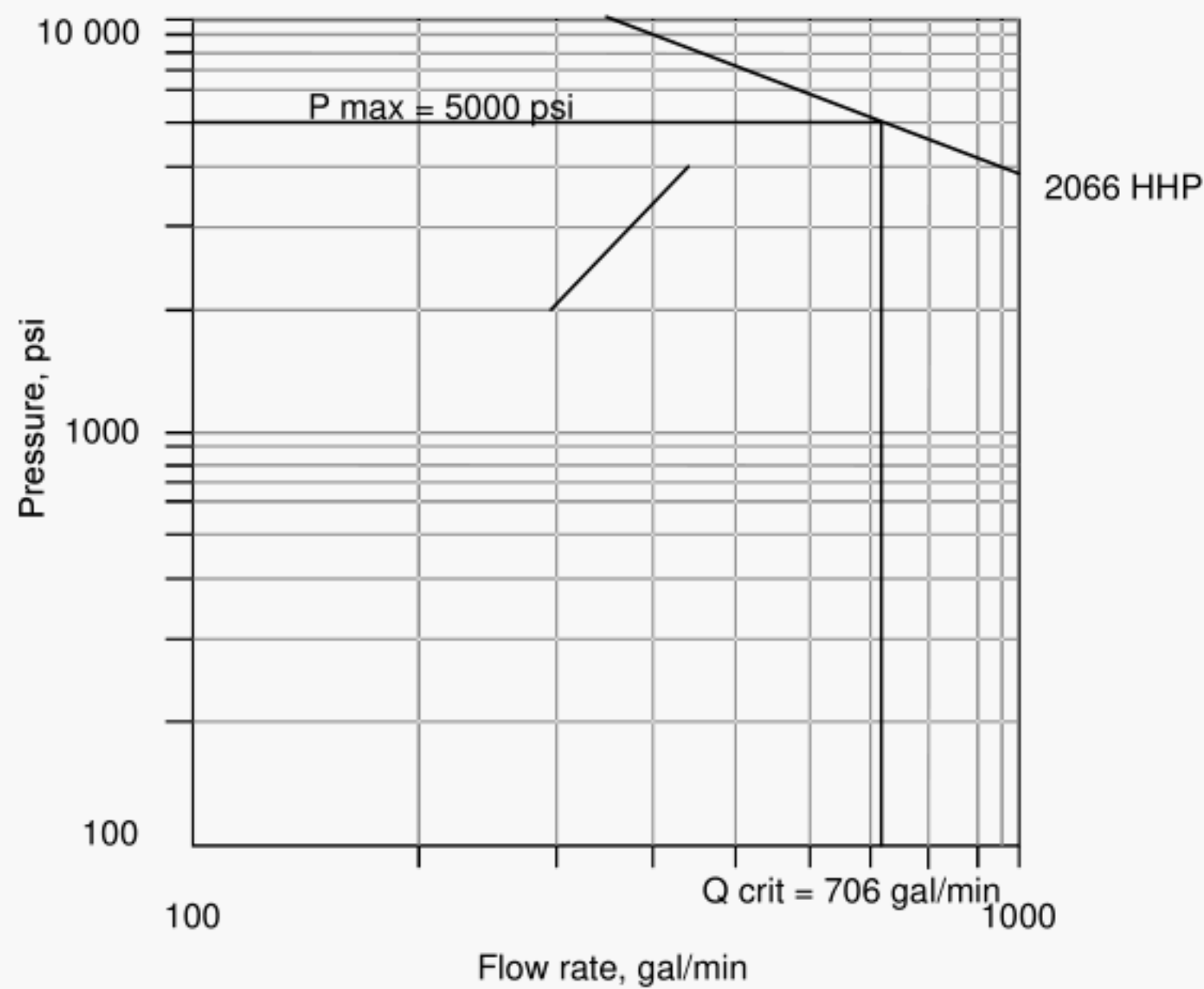
Figure F.1- On-site nozzle test

The slope of the P_{system} line is measured by measuring the linear distances horizontally and vertically with a ruler. In this case the slope u is 1.7. Since the P_{circ}/Q line falls well below the Q_{crit} line, the limiting condition will be the maximum pressure.
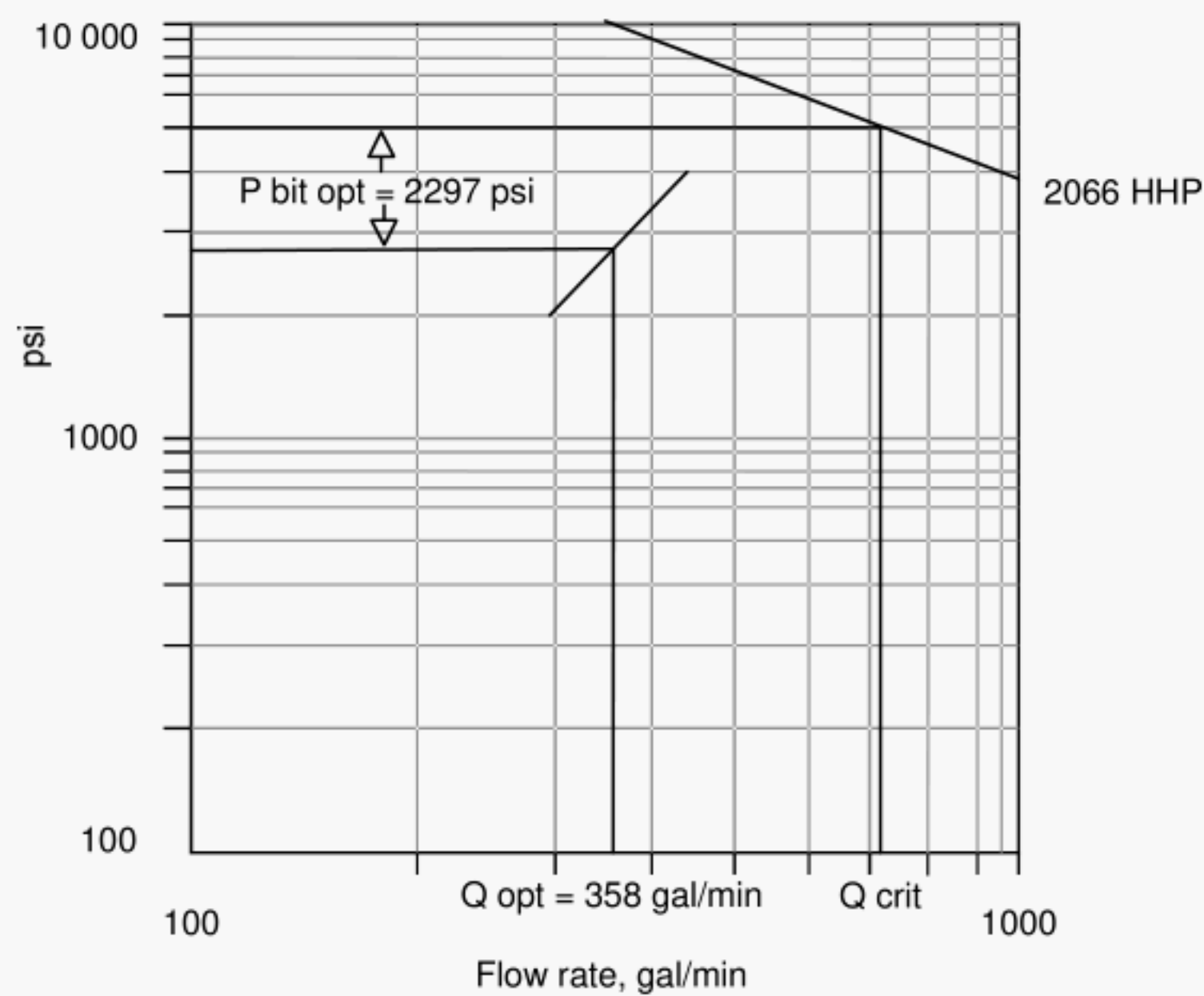
F.2 Maximum hydraulic impact

F.2.1 Maximum hydraulic impact method

The optimum bit pressure loss for maximum hydraulic impact would be calculated from the equation:

$$P_{bit\,opt} = \frac{u}{u+2}\ P_{max} = \frac{1.7}{3.7}\,(5000\,psi) = 2297\,psi \qquad\qquad (F.2)$$

The optimum circulating pressure loss in the system is 5,000 psi − 2,297 psi = 2,703 psi. The intersection of the 2,703 psi and the parasitic pressure losses on the graph indicates that the new optimum flow rate should be 358 gal/min as shown in the graph below.

Figure F.2- On-site nozzle test for maximum hydraulic impact

From the equation for pressure loss through bit nozzles, the area of 0.23365 in^2 can be created by three 10/32 in. nozzles. They actually have an area of 0.2301 in^2. A 12/32 in. nozzle and a 13/32 in. nozzle have an area of 0.2301 in^2.

So for a maximum hydraulic impact force, the next bit will be dressed with two nozzles, a 12/32 in. and a 13/32 in. The nozzle velocity will be 478 ft/s, compared with the 327 ft/s. The maximum nozzle shear rate will be in the range of 122,000 s^{-1}, which may result in hole erosion. (The shear rate should be less than 100,000 s^{-1} to decrease the possibility of hole erosion.)

F.2.2 Maximum hydraulic power method

If the preferred optimization procedure is to maximize the hydraulic power at the drill bit, the pressure loss across the nozzles should be calculated from the equation:

$$P_{bitOpt} = \frac{u}{u+1}P_{max} = \frac{1.7}{2.7}\,(5000) = 3148\,psi \qquad\qquad (F.3)$$

The pressure loss through the circulating system should be (5,000 psi − 3,148 psi) or 1,851 psi.

The circulating pressure loss through the system intersects the optimum pressure at a value of 287 gal/min. The nozzles will be selected to provide a pressure loss through the nozzles of 3,148 psi at a flow rate of 287 gal/min.

$$\Delta P_{Bit\ Opt} = \frac{(12.5)(287)^2}{12042(1.03)^2(Area)^2} = 3,148 psi \tag{F.4}$$

The area of the nozzles should be 0.1600 in^2. This would require three nozzles (8/32 in., 8/32 in., and 9/32 in.) or two nozzles (10/32 in. and 11/32 in). The nozzle velocity would be 575 ft/s. The nozzle shear rate would be 220,000 s^{-1}. This would result in rapid hole erosion. (The shear rate should be less than 100,000 s^{-1}.)

F.3 Comparison of optimization methods

A comparison of the impact forces for the three cases indicates that the hydraulic impact forces were 953 lb, 1,167 lb, and 1,069 lb, in the order presented above. The impact force for the four nozzle bit was 953 lb. Calculating the force for the Impact Force optimization procedure indicates a force of 1,167 lb would be applied to the bottom of the hole. A force of 1,069 lb would be applied for hydraulic power optimization procedure.

A comparison of hydraulic power losses through the nozzles for the three cases indicates that the hydraulic power was 567 HP, 1,050 HP, and 1,117 HP, in the order presented above. The hydraulic power for the four nozzle bit was 567 HP. The impact force optimization procedure results in 1,050 HP being lost through the nozzles. The hydraulic power optimization procedure results in 1,117 HP being applied through the nozzles.

Table F.3- Impact force methods comparison

Stand Pipe Pressure psi	Flow Rate gal/min	Nozzle Velocity ft/s	Impact Force lb	Hydraulic Power HP	Nozzle Shear Rate 10^6 s^{-1}	Va In Riser ft/min
5000	450	327	953	567	0.8	33
5000	358	499	1167	1050	1.3	26
5000	287	575	1069	1117	1.5	21

Bibliography

TEXT BOOKS

[1] BOURGOYNE A.T., *et al. Applied drilling engineering.* SPE, Richardson, Texas, 1991.

[2] DARLEY H.C.H. and GRAY G.R. *Composition and properties of oil well drilling fluids.* Gulf Publ., Houston, Texas, 5th edn., 1988, pp. 184-281.

[3] MOORE P. *Drilling practices manual.* Petroleum Publ., 2nd edn., 1986.

[4] SKELLAND A.H.P. *Non-Newtonian flow and heat transfer.* John Wiley & Sons, New York, 1967.

[5] GOVIER G.W. and AZIZ K. *The flow of complex mixtures in pipes.* Litton Education Publishing, New York, 1972.

REFERENCES – Rheological models

[6] SAVINS J.G. and ROPER W.F. A direct-indicating viscometer for drilling fluids. *API Drilling and production practices.* API, 1954, pp. 7-22.

[7] HEMPHILL T., PILEHARVI A. and CAMPOS W. Yield power law model more accurately predicts drilling fluid rheology. *Oil & Gas J.* August 23, 1993, pp. 45-50.

[8] BOURGOYNE A.T., CHENEVERT M., MILHEIM K., and YOUNG F.S. *Applied drilling engineering*, SPE, Richardson, Texas, 1991, p. 136.

[9] ZAMORA M. and POWER D. *Making* a case for AADE hydraulics and the unified rheological model. AADE-02-DFWH-HO-13. AADE 2002 Technology Conf., Houston, TX, Apr. 2-3.

[10] API RP 13D:1995. *Recommended practice on the rheology and hydraulics of oil-well drilling fluids.* American Petroleum Institute, 1220 L Street NW, Washington, DC 20005

REFERENCES - Downhole fluid behavior

[11] KUTASOV I. and TARGHI A. Better deep-hole BHCT estimations possible. *Oil & Gas J.* May 25, 1987.

[12] KUTASOV I. Method corrects API borehole circulating-temperature correlations. *Oil & Gas J.* Jul. 15, 2002, pp. 47-51.

[13] EBELTOFT H., YOUSIF M. and SOERGARD E. Hydrate control during deepwater drilling: overview and new drilling fluids formulations. *SPE Drilling & Completion*, **16** (1), 2001, pp. 19-26.

[14] KENNY P. and HEMPHILL T. Hole cleaning capabilities of an ester-based drilling fluid system. *SPE Drilling & Completion*, **11** (1), 1996, pp. 3-9.

[15] McMORDIE W.C., BENNETT, R.B., and BLAND R.G. The effect of temperature and pressure on the viscosity of oil base drilling fluids, SPE 4974. SPE 1975 Annual Technical Conf. and Exhibit, Houston, TX, Sep. 28-Oct. 1.

[16] WHITE W.W., ZAMORA M. and SVOBODA C.F. Downhole measurements of synthetic-based drilling fluid in offshore well quantify dynamic pressure and temperature distributions. *SPE Drilling & Completion,* **12** (3), p. 149.

[17] BARTLETT L.E. Effect of temperature on the flow properties of drilling fluids, SPE 1861. SPE 1967 Annual Technical Conf. and Exhibit, Denver, CO, Sep. 28-Oct.1.

[18] SORELL R., JARDIOLIN R., BUCKLEY P., and BARRIOS J. Mathematical field model predicts downhole density changes in static drilling fluids, SPE 11118. SPE 1982 ATCE, New Orleans, LA, Sep. 26-29.

[19] ISAMBOURG P., ANFINSEN B., and MARKEN C. Volumetric behavior of drilling fluids at high pressure and high temperature, SPE 36830. SPE 1996 European Petroleum Conf., Milan, Italy, Oct. 22-24.

[20] PETERS E., CHENEVERT M., AND ZHANG C. A model for predicting the density of oil-based drilling fluids at high pressures and temperatures. *SPE Drilling Engineering*, **5** (2), pp. 141-148.

[21] Data courtesy of Chevron Phillips Chemical Company.

[22] Data courtesy of Total.

[23] API RP 13B-2 (Feb. 1998), *Recommended practice standard procedure for field testing oil-based drilling fluids – third edition*.

[24] Section D - Concentrative properties of aqueous solutions, *Handbook of chemistry and physics*, CRC Press, LLC, division of Taylor & Francis Group, LLC, 6000 NW Broken Sound Parkway, Suite 300, Boca Raton, FL, 33487.

[25] WARD M., *et al.* A joint industry project to assess circulating temperatures in deepwater wells, SPE 71364. SPE 2001 Annual Technical Conf. and Exhibit, New Orleans, LA, Sep 30 – Oct 3.

[26] HOLMES C.S. and SWIFT S.C. Calculation of circulating drilling fluid temperatures. *J of Petroleum Technology*, Jun. 1970, pp. 670-674.

[27] RAYMOND L.R. Temperature distribution in a circulating drilling fluid. *J of Petroleum Technology*, Mar. 1969, pp. 333-341.

[28] SAGAR R., *et al..* Predicting temperature profiles in a flowing well. *SPE Production Engineering*, Nov. 1991, pp. 441-448.

[29] KABIR C.S., *et al.* Determining circulating fluid temperature in drilling, workover and well-control operations. *SPE Drilling & Completion*, **11** (2), pp. 74-79.

[30] ZAMORA M., *et al.* The top 10 drilling fluid-related concerns in deepwater drilling operations, SPE 59019. SPE 2001 International Petroleum Conf. and Exhibit, Villahermosa, Tabasco, Mexico, Feb. 1-3.

[31] ANNIS M.R. High temperature flow properties of drilling fluids. *J of Petroleum Technology*, August 1967, pp 1074-1080.

[32] ZAMORA M. Virtual rheology and hydraulics improve use of oil and synthetic-based drilling fluids. *Oil & Gas J*, March 3, 1997, pp. 43-55.

[33] HEMPHILL T. and ISAMBOURG P. New model predicts oil, synthetic drilling fluid densities. *Oil & Gas J*, **103** (16), pp. 56-58.

[34] ZAMORA, M. and LORD, D.L. Practical analysis of drilling mud flow in pipes and annuli, SPE 4976. SPE 1974 Annual Technical Conference, Houston, Texas, Oct. 6-9.

REFERENCES - Pressure-loss modeling

[35] DODGE D.W. and METZNER A.B. Turbulent flow of non-Newtonian systems. *American Institute of Chemical Engineering J*, **5** (2), pp. 189-204.

[36] METZNER A.B. and REED J.C. Flow of non-Newtonian fluids – correlation of laminar, transition and turbulent flow regions. *American Institute of Chemical Engineers J*, **1**, pp. 434-440.

[37] REED T.D. and PILEHVARI A.A. A new model for laminar, transitional and turbulent flow, SPE 25456. SPE 1993 Production Operations Symposium, Oklahoma City, OK, Mar. 21-23.

[38] SAVINS J.G. Generalized Newtonian (pseudoplastic) flow in stationary pipes and annuli. *Petroleum Transactions of AIME*, **218**, pp. 332.

[39] KLOTZ J.A. and BRIGHAM W.E. To determine Herschel-Bulkley coefficients. *J of Petroleum Technology*, Nov. 1998, pp. 80-81.

[40] Power law model more accurately predicts drilling fluid rheology. O*il & Gas J*, August 23, 1993, p. 45.

[41] ZAMORA M. and BLEIER R. Prediction of drilling mud rheology using a simplified Herschel-Bulkley Model. ASME Intl. Joint Petroleum Mechanical Engineering and Pressure Vessels and Piping Conf., Mexico City, Sep. 19-24. 1976.

[42] ZAMORA M. and POWER D. Making a case for AADE hydraulics and the unified rheological model, AADE-02-DFWM-HO-13. AADE 2002 Technology Conf., Apr. 2-3, 2002

[43] DAVISON J.M., *et al.* Rheology of various drilling fluid systems under deepwater drilling conditions and the importance of accurate predictions of downhole fluid hydraulics, SPE 56632. SPE 1999 Annual Technical Conf. and Exhibit, Houston, TX, Oct. 3-6, 1999.

[44] HACIISLAMOGLU M. and LANGLINAIS J. Non-Newtonian flow in eccentric annuli. Annual Energy Sources Conf., ASME Drilling Technology Symposium, New Orleans LA, Jan. 14-18, 1990.

[45] HACIISLAMOGLU M. and CARTALOS U. Practical pressure loss predictions in realistic annular geometries, SPE 28304. SPE 1994 Annual Technical Conf. and Exhibit, New Orleans, LA, Sep. 25-28.

[46] McCANN R.C., *et al.* Effects of high-speed rotation on pressure losses in narrow annuli, SPE 26343. SPE 1993 Annual Technical Conf. and Exhibit., Houston, TX, Oct. 3-6.

[47] MINTON R.C. and BERN P.A. Field measurement and analysis of circulating system pressure drops with low-toxicity oil-based drilling fluids, SPE 17242. IADC/SPE 1988 Drilling Conf., Dallas, TX, Feb. 28-Mar. 2.

[48] CHURCHILL S.W. Friction factor equation spans all fluid-flow regimes. *Chemical Engineering*, Nov. 7, 1977, pp. 91-92.

[49] *Yield Point*, Smith International. (computer software)

[50] JEONG Y-T and SHAH S.N. Analysis of tool joint effects for accurate friction pressure loss calculations, IADC/SPE 87182. IADC/SPE 2004 Drilling Conf., Dallas, TX, Mar. 2-4.

[51] SAS-JAWORSKY II A. and REED T.D. Predicting pressure losses in coiled tubing operations, *World Oil*, Sep. 99, pp. 141-146.

[52] ZHOU Y. and SHAH S.N. New friction factor correlations for non-Newtonian fluid flow in coiled tubing, SPE 77960. SPE 2002 Asia Pacific Oil and Gas Conf. and Exhibit, Melbourne, Australia, Oct. 8-10.

[53] SHAH S.N. and ZHOU Y. An experimental study of drag reduction of polymeric solutions in coiled tubing. *SPE Production & Facilities,* Nov. 3, pp. 20-287.

[54] EN ISO 5167-3:2003. Measurement of fluid flow by means of pressure differential devices inserted in circular cross-section conduits running full -- Part 3: Nozzles and venturi nozzles

[55] WARREN T.M. Evaluation of jet-bit pressure losses, SPE 17916. *SPE Drilling & Completion Engineering,* **4** (4), pp. 335-340.

[56] ZAMORA M., *et al.* Comparing a basic set of drilling fluid pressure-loss relationships to flow-loop and field data, AADE-05-NTCE-27. AADE 2005 National Technical Conf. and Exhibit, Houston, TX, Apr. 5-6.

[57] BARANTHOL, C., ALFENOR, J. COTTERILL, M.D. and POUX-GUILLAUME, G. Determination of hydrostatic pressure and dynamic ECD by computer models and field measurements on the directional HPHT well 22130C-13, SPE 29430. SPE/IADC 1995 Drilling Conference, Amsterdam, Netherlands, Feb. 28-Mar. 2.

REFERENCES – Swab/surge pressures

[58] FONTENOT J.E. and CLARK R.K. An improved method for calculating swab/surge and circulation pressures in a drilling well. *SPE J*, Oct. 1974, pp 451-461.

[59] SCHUH F.J. Computer makes surge-pressure calculations useful. *Oil & Gas J*, Aug. 3, 1965, pp. 96-104.

[60] RUDOLF R.L. and SURYANARAYANA P.V.R. Field validation of swab effects while tripping-in the hole on deep, high temperature wells, IADC/SPE 39395. IADC/SPE 1998 Drilling Conf. Dallas, TX, Mar. 3-6.

[61] BROOKS, A.G. Swab and surge pressures in non-Newtonian fluids. 1982. Unsolicited manuscript, archived in SPE eLibrary.

REFERENCES - Hole cleaning

[62] WALKER R.E. and MAYES T.M. Design of drilling fluids for carrying capacity. *J of Petroleum Technology*, Jul. 1967, pp. 893-900.

[63] WILLIAMS C.E. and BRUCE G.H. Carrying capacity of drilling muds. *Trans. AIME*, **192**, 1951, pp. 111-120.

[64] ROBINSON L.H. and RAMSEY M.S. Onsite continuous hydraulics optimization (OCHO), AADE 01-NC-HO-30, 2001.

[65] LUO Y., *et al.* Flow rate predictions for cleaning deviated wells, SPE 23884. IADC/SPE 1992 Drilling Conf., New Orleans, LA, Feb. 18-21.

[66] LUO Y., *et al.* Simple charts to determine hole cleaning requirements, IADC/SPE 27486. IADC/SPE 1994 Drilling Conf., Dallas, TX, Feb. 15-18.

[67] SIFFERMAN, T.R., *et al.* Drilling-cutting transport in full-scale vertical annuli. *J of Petroleum Technology*, Nov. 1974, pp. 1295-1302.

[68] KENNY P. and HEMPHILL T. Hole Cleaning capabilities of an ester-based drilling fluid system. *SPE Drilling & Completion,* **11** (1), pp. 3-10.

[69] HEMPHILL T. and LARSEN T.I. Hole-cleaning capabilities of water- and oil-based drilling fluids: a comparative experimental study. *SPE Drilling & Completion*, **11** (4), pp, 201-207.

[70] MARTINS A.L., *et al.*Evaluating the transport of solids generated by shale instabilities in ERW drilling, SPE 59729. *SPE Drilling & Completion*, **14** (4), December 1999, pp. 254-259.

[71] GAVIGNET A.A. and SOBEY, I.J. Model aids cuttings transport prediction, *J of Petroleum Technology*, Sep. 1989, p. 916. *Trans. of AIME*, p 287.

[72] SANCHEZ R.A., *et al.* The effect of drillpipe rotation on hole cleaning during directional well drilling, SPE 37626. IADC/SPE 1997 Drilling Conf., Amsterdam, The Netherlands, Mar 4-6.

[73] ZEIDLER H.U. An experimental analysis of the transport of drilled particles. *SPE J,* Feb. 1972, pp. 39-8. *Trans. AIME*, p. 23.

[74] CLARK R.K. and BICKMAN K.L. A mechanistic model for cuttings transport, SPE 28301. SPE 1994 Annual Technical Conf. and Exhibit, New Orleans, LA, Sep 25-28.

[75] SAASEN A. and LOKLINHOLM G. The effect of drilling fluid rheological properties on hole cleaning, IADC/SPE 74558. IADC/SPE 2002 Drilling Conf., Dallas TX, Feb. 26-28.

[76] KENNY P., *et al.* Hole cleaning modelling: what's "n" got to do with it?, IADC/SPE 35099. IADC/SPE 1996 Drilling Conf., New Orleans, LA, Mar. 12-15.

[77] RASI M. Hole cleaning in large, high-angle wellbores, IADC/SPE 27464. IADC/SPE 1994 Drilling Conf. Dallas, TX, Feb. 15-18.

[78] HANSON P.M., *et al.* Investigation of barite sag in weighted drilling fluids in highly deviated wells, SPE 20423. SPE 1990 Annual Technical Conf. and Exhibit, New Orleans, La, Sep. 23-26.

[79] BERN P.A., *et al.* Barite sag: measurement, modeling and management, IADC SPE 47784. IADC 1998 Asia Pacific Drilling Technology, Jakarta, Indonesia, Sep 7-9.

[80] ZAMORA M and JEFFERSON D.T. Controlling barite sag can reduce drilling problems. *Oil & Gas J*, Feb. 14, 1994.

[81] DYE W., *et al.* Correlation of ultra-low shear rate viscosity and dynamic barite sag. *SPE Drilling & Completion*, **16** (1), pp. 27-34.

REFERENCES - Bit hydraulics optimization

[82] SCOTT, K.F. A new practical approach to rotary drilling hydraulics, SPE 3530. SPE 1971 Annual Technical Conf. and Exhibit, Oct. 3-6.

[83] KENDALL H.A. and GOINS W.C. Design and operation of jet-bit programs for maximum hydraulic horsepower, impact force, or jet velocity. *Petroleum Transactions Reprint Series, no.6 (Drilling).*

[84] RANDALL B.V. Optimum hydraulics in the oil patch. *Petroleum Engineering*, Sep. 1975, pp. 36-52.

[85] BUCKLEY P. and JARDIOLIN R.A. How to simplify rig hydraulics. *Petroleum Engineering International,* Mar. 1982, pp. 154-178.

[86] DORION H.H. and DEANE J.D. A new approach for optimizing bit hydraulics, SPE 11677. SPE 1983 California Regional Meeting, Ventura, CA, Mar. 23-25.

[87] ROBINSON, L.H. On-site nozzle selection increases drilling performance. *Petroleum Engineering International,* Dec. 1981, pp. 7-82.

[88] ROBINSON, L.H. Optimizing bit hydraulics increases penetration rates. *World Oil,* Jul. 1982, pp. 167-179.

[89] RAMSEY, M.S. Are you drilling optimized or spinning your wheels?, AADE 01-NC-HO-31. AADE 2001 National Drilling Conf. Houston, TX, Mar. 27-29.

REFERENCES - Rigsite monitoring

[90] HUTCHINSON M. and REZMER-COOPER I. Using downhole annular pressure measurements to anticipate drilling problems, SPE 49114. SPE 1998 Annual Technical Conf. and Exhibit, New Orleans, LA.

[91] ZAMORA M., *et al.* Major advancements in true real-time hydraulics, SPE 62960. SPE 2000 Annual Technical Conf. and Exhibit, Dallas, TX, Oct. 1-4.

[92] ROY S. and ZAMORA M. Advancements in true real-time wellsite hydraulics. AADE 2000 Technical Conf., Houston, TX, Feb. 9-10.

[93] WARD C. and CLARK R. Anatomy of a ballooning borehole using PWD. Workshop on Overpressures in Petroleum Exploration, Pau, France, Apr 7-8, 1998.

[94] WARD C. and ANDREASSEN E. Pressure-while-drilling data improve reservoir drilling performance. *SPE Drilling & Completions*, **13** (1), pp. 19-24.

[95] MALLARY C.R., *et al.* Using pressure-while-drilling measurements to solve extended-reach drilling problems on Alaska's North Slope, SPE 54592. SPE 1999 Western Regional Meeting, Anchorage, AK, May 22-28.